

Titre: Development of Poly(N-isopropylacrylamide) Based Hydrogel
Platform and its Applications

Auteur: Yinghao Xu
Author:

Date: 2021

Type: Mémoire ou thèse / Dissertation or Thesis

Référence: Xu, Y. (2021). Development of Poly(N-isopropylacrylamide) Based Hydrogel
Platform and its Applications [Thèse de doctorat, Polytechnique Montréal].
Citation: PolyPublie. <https://publications.polymtl.ca/5610/>

 **Document en libre accès dans PolyPublie**
Open Access document in PolyPublie

URL de PolyPublie: <https://publications.polymtl.ca/5610/>
PolyPublie URL:

**Directeurs de
recherche:** Abdellah Ajji, & Marie-Claude Heuzey
Advisors:

Programme: Génie chimique
Program:

POLYTECHNIQUE MONTRÉAL

affiliée à l'Université de Montréal

**Development of Poly(N-isopropylacrylamide) based hydrogel platform and its
applications**

YINGHAO XU

Département de génie chimique

Thèse présentée en vue de l'obtention du diplôme de *Philosophiæ Doctor*

Génie chimique

Janvier 2021

POLYTECHNIQUE MONTRÉAL

affiliée à l'Université de Montréal

Cette thèse intitulée :

Développement of Poly(N-isopropylacrylamide) based hydrogel platform and its applications

présentée par **Yinghao XU**

en vue de l'obtention du diplôme de *Philosophiæ Doctor*

a été dûment acceptée par le jury d'examen constitué de :

Charles DUBOIS, président

Abdellah AJJI, membre et directeur de recherche

Marie-Claude HEUZEY, membre et codirectrice de recherche

Fabio CICOIRA, membre

Hani NAGUIB, membre externe

DEDICATION

The meaning of life is to experience, as much as you can.

ACKNOWLEDGEMENTS

I wish to thank all those who have been a part of my wonderful experience in Montreal and helped me in completion of this project. I would like to express the deepest appreciation to my supervisors Prof. Abdellah Ajji and Prof. Marie-Claude. Heuzey for accepting me as their Ph.D student. I am very grateful for their continued support and encouragement throughout my project. The way they supervise my project gives me as many opportunities as I can expect to learn to manage a research project. The research attitude, skills to make a research plan and execute it, and mindset adjustment when facing challenges, all these I learned from both of my supervisors would become a priceless treasure and benefit me for the rest of my life.

I would also like to send a heartfelt acknowledgement to my colleagues, especially Hanan Abdali and Charles Bruel, for their valuable suggestions on my project. I would express my thanks to Claire Cerclé and Matthieu Gauthier for their technical assistance to my experimental work. I would also give credits to Farhad Farnia from Sherbrooke University for his help and suggestions on the work of organic synthesis in my project. I would also like to acknowledge the financial support from China Scholarship Council (CSC).

There are also too many names of my friends in my mind that I cannot thank one by one. Thank you all for making my life colorful and meaningful. My special thanks would be reserved for my family, it is your unconditional love and support have made me today.

RÉSUMÉ

Le poly (N-isopropylacrylamide) (PNIPAM) est un polymère thermosensible qui subit une transformation conformationnelle réversible à la température de 32 °C, proche de la température corporelle. Cette caractéristique attrayante, combinée à sa structure définie pouvant être adaptée facilement, fait de lui un candidat idéal pour l'administration de médicaments. De plus, l'hydrogel correspondant est ainsi utilisé à grande échelle dans la culture des cellules et le domaine de l'ingénierie tissulaire. Pour utiliser son grand degré de gonflement et de contraction, des efforts ont été réalisés afin de développer des hydrogels à base de PNIPAM et les utiliser comme capteurs et actionneurs. Cependant, sa faible capacité de réaction à la température et sa résistance mécanique ont entravé ses potentielles applications dans ces domaines. Pour améliorer ces deux aspects, certaines technologies ont été utilisées séparément. Plus précisément, il a été rapporté qu'un réseau de polymères interpénétrés et des additifs réticulants permettent de renforcer les hydrogels de PNIPAM, tandis qu'un rapport de volume/surface élevé est le meilleur moyen d'accélérer sa vitesse de réaction à la température. En effet, le réseau de polymères interpénétrés comme le réseau réticulé servent de cadre pour limiter le mouvement des chaînes de PNIPAM face aux variations de températures. Ainsi, un rapport de volume/surface plus élevé, fabriqué par une technologie de formage poreux ou par structure fibreuse en électrofilage est important pour compenser l'effet secondaire résultant d'une résistance mécanique plus élevée. Compte tenu de la polyvalence, de la flexibilité et de la facilité de production de fibres, l'utilisation de l'électrofilage serait idéale pour fabriquer des hydrogels à base de PNIPAM présentant un rapport de volume/surface élevé.

Par ailleurs, la performance de l'hydrogel fibreux obtenu comme plateforme pour incorporer d'autre(s) matériau(x), polymères ou nanoparticules, est également un aspect à étudier, d'un grand intérêt pour nous. Plus précisément, l'interaction entre les additifs nouvellement ajoutés et le PNIPAM, l'influence de ces additifs sur la structure fibreuse, et par la suite sur le comportement de réactivité à la température des hydrogels seront nos objectifs de recherche principaux. Afin d'avoir une compréhension globale des doubles composants (PNIPAM/additifs), des protocoles « avant électrofilage » et « après électrofilage » ont été utilisés pour intégrer respectivement la cellulose nanocristalline (CNC) et le polyaniline (PANI) dans l'hydrogel.

Dans ce travail, un agent de réticulation initié par UV a été développé et incorporé dans un copolymère à base de PNIPAM. Les hydrogels correspondants ont ensuite été fabriqués par électrofilage d'un copolymère à base de PNIPAM avant d'être réticulé par traitement UV. La morphologie de la structure fibreuse a ensuite été conservée après plusieurs cycles de gonflement et dégonflement induit par température. En changeant la température, il a été possible d'atteindre des rapports de degrés de gonflement et dégonflement importants, ainsi que d'excellentes vitesses de réaction. En termes de vitesse de réaction, les équilibres de gonflement et dégonflement ont été atteints en 10 min pour des échantillons de 0.7 mm d'épaisseur. Cependant, l'augmentation du rapport d'agent réticulant a montré un impact négatif important sur le rapport de gonflement et dégonflement (une diminution respective d'environ 700% et 15%). Un comportement viscoélastique, presque élastique a été observé pour les états d'équilibre de gonflement et dégonflement induit par cisaillement oscillatoire de faible amplitude.

Ensuite, le PANI a été introduit dans le domaine hydrogel via une polymérisation in-situ de l'aniline avec l'APS comme oxydant et l'acide phytique comme dopant en environnement aqueux. Plusieurs effets du PANI sur l'hydrogel sont investigués, notamment sur 1) la morphologie fibreuse dans les états gonflés et contractés, 2) la capacité de l'hydrogel à gonfler et se contracter et 3) la conductivité des hydrogels hybrides. Les hydrogels hybrides contenant plus de 1.4wt% de PANI se comportent différemment selon la baisse de résistance quand ils sont contractés à 40 °C. Cela peut être dû à leur structure hautement fibreuse. Par la suite, un système d'évaluation est établi dans le but de comprendre globalement et comparer les capacités de conduction et de réaction de ces hydrogels hybrides, afin de prévoir leurs potentielles applications.

Par ailleurs, la CNC a été incorporé avec cet hydrogel par la voie « avant électrofilage ». Une suspension de CNC stable a été préparé avec un mélange de DMF/formamide par ultrasonication. Cette suspension a été ensuite utilisé pour dissoudre le P(NIPAM-ABP) pour l'électrofilage. Il a été constaté que la CNC exerce une contrainte significative sur le gonflement des hydrogels quand sa concentration dépassait 5wt% alors que son effet sur la contraction est négligeable. La différence de comportement de réaction à la température entre les hydrogels avec des teneurs en CNC variables est utilisée pour fabriquer un hydrogel à deux couches. Nous avons démontré que ces hydrogels à deux couches sont capables de générer des géométries 3D dans l'eau. Plus précisément, ces hydrogels gonflent de manière anisotropique au premier contact avec l'eau et subissent des

changements dimensionnels réversibles suite au gonflement et à la contraction. De plus, il s'est avéré que ces géométries sont extrêmement ajustables en affinant le rapport d'épaisseur entre les deux couches.

ABSTRACT

Poly (N-isopropylacrylamide) (PNIPAM) is a well-known thermoresponsive polymer that undergoes reversible conformational transition at temperature of 32 °C, which is close to human body temperature. This appealing feature, along with its well-defined structure which could be tailored easily, makes it perfect candidate for delivering drugs. In addition, the corresponding hydrogel is therefore widely applied in cell culture and tissue engineering fields. To utilize its large swelling and contraction degree, some efforts have also been made to develop PNIPAM-based hydrogels for the application as sensors and actuators. However, the poor temperature response capacity and mechanical strength have hindered its further application in these fields. To improve these two drawbacks, technologies have been employed separately. Specifically, interpenetrating polymer network and crosslinking additives have been reported to strengthen the PNIPAM hydrogels; while large volume to surface ratio is the main principle to accelerate its temperature responsive rate. In most cases, a higher mechanical strength would result in a worse temperature responsive rate. Because either interpenetrating polymer network or crosslinking network would serve as a framework to limit the movement of PNIPAM chains with temperature change. Thus, a higher volume to surface ratio fabricated either by porous forming technology or by fibrous structure via electrospinning is of significance to offset the side effect resulting from higher mechanical strength. Considering the versatility, flexibility and ease of fiber production, electrospinning would be a perfect candidate to be employed to fabricate PNIPAM-based hydrogel with high surface to volume ratio.

On the other hand, the performance of obtained fibrous hydrogel as a platform to incorporate with other material(s), either polymers or nanoparticles, is also of our great interest to study. Specifically, the interaction between newly introduced additives and PNIPAM, the influence of these additives on fibrous structure and subsequently on hydrogel's temperature responsive behaviors would be our main research objectives. To have a comprehensive understanding on the dual components (PNIPAM/additives) systems, protocols of “before electrospinning” and “after electrospinning” were employed to introduce Cellulose nanocrystals (CNC) and polyaniline (PANI) into hydrogel respectively.

In this work, a UV-initiated crosslinking agent was developed and incorporated in a poly(*N*-isopropylacrylamide) (PNIPAM)-based copolymer. Corresponding hydrogels were then fabricated by the electrospinning of a PNIPAM-based copolymer and subsequently crosslinked under UV-treatment. The morphology of the fibrous structure was well maintained after many temperature-induced swelling and de-swelling cycles. Both considerable degree of swelling and de-swelling ratios, along with an excellent response rate, were achieved with temperature variation. In terms of response time, both swelling and de-swelling equilibrium were reached within 10 min for samples with 0.7 mm thickness. However, the increase of crosslinker ratio showed a significant negative impact on equilibrium swelling and de-swelling ratio (about 700% and 15% decrease respectively). A viscoelastic, but close to elastic, behavior in both swelling and de-swelling equilibrium states under small-amplitude oscillatory shear was observed.

Then PANI was introduced into hydrogel domain via in-situ polymerization of aniline with ammonium persulfate (APS) as oxidant and phytic acid as a dopant. The effect of PANI on hydrogel were investigated, including: 1) fiber morphology in both swollen and contracted states; 2) swelling/contraction capability of the hydrogels and 3) conductivity of the hybrid hydrogels. Hybrid hydrogels with >1.4 wt% PANI behaved distinctly in resistance alternation when hydrogel contracted at 40 °C, which could be due to their highly fibrous structure. Subsequently, an evaluation system, aiming at general understanding and comparison of both conductive and responsive capabilities for these hybrid hydrogels, was established to forecast their potential applications.

On the other hand, CNC was incorporated with this hydrogel via “before electrospinning” route. A stable CNC suspension was prepared in DMF/formamide mixture after ultrasonication treatment. This suspension was then employed to dissolve P(NIPAM-ABP) for electrospinning. CNCs were found to exert significant constraint effect on hydrogels swelling when it exceeded 5 wt% but negligible effect for contraction. The difference between hydrogels with various CNCs proportion regarding their temperature responsive behaviors is utilized to fabricate bilayer hydrogels. We demonstrated that these bilayer hydrogels were capable of generating 3D geometries in water. Specifically, these hydrogels swelled anisotropically at first time contacting water and underwent reversibly dimensional change in following swelling and contraction. In addition, these geometries were found to be highly tunable via finely tuned thickness ratio between two layers.

TABLE OF CONTENTS

DEDICATION	III
ACKNOWLEDGEMENTS	IV
RÉSUMÉ.....	V
ABSTRACT	VIII
TABLE OF CONTENTS	X
LIST OF TABLES	XIV
LIST OF FIGURES	XV
LIST OF SYMBOLS AND ABBREVIATIONS.....	XVIII
CHAPTER 1 INTRODUCTION.....	1
CHAPTER 2 LITERATURE REVIEW	4
2.1 Hydrogels	4
2.1.1 Smart hydrogels.....	5
2.2 PNIPAM.....	7
2.2.1 PNIPAM hydrogels	9
2.3 Electrospinning.....	18
2.4 Conductive hydrogels.....	21
2.4.1 Conductive hydrogels applications	25
2.5 Cellulose Nanocrystals	28
2.5.1 Low CNCs proportion.....	30
2.5.2 High CNCs proportion	34
2.6 Summary of literature review.....	37
CHAPTER 3 RESEARCH OBJECTIVES AND COHERENCE OF ARTICLES.....	40
3.1 Research objectives	40

3.1.1	Specific objectives of the research	40
3.1.2	Presentation of articles and coherence with research objectives.....	40
CHAPTER 4 ARTICLE 1: RESPONSE BEHAVIORS AND MECHANICAL STRENGTH OF THERMAL RESPONSIVE HYDROGELS FABRICATED BY ELECTROSPINNING.....		
4.1	Abstract	42
4.2	Introduction	43
4.3	Experimental	45
4.3.1	Materials.....	45
4.3.2	Preparation of polymerizable photo-crosslinker (ABP).....	45
4.3.3	Synthesis of p(NIPAM-ABP).....	46
4.3.4	Electrospinning.....	46
4.3.5	Characterization	46
4.3.6	Swelling behavior of hydrogels.....	47
4.3.7	Rheology	48
4.3.8	Compression tests.....	48
4.4	Results and discussion.....	49
4.4.1	Morphology of electrospun fibers	49
4.4.2	Effect of crosslinker	50
4.4.3	Response behaviors of P(NIPAM-ABP) hydrogels	51
4.4.4	Rheological characterization and compression tests	55
4.5	Conclusion.....	57
4.6	Acknowledgements	58
4.7	Support information	59

CHAPTER 5	ARTICLE 2: FAST THERMAL RESPONSIVE HYDROGELS CONSISTING WITH ELECTROSPUN FIBERS WITH HIGHLY TUNABLE CONDUCTIVITY	62
5.1	Abstract	62
5.2	Introduction	63
5.3	Results and discussions	65
5.3.1	Fibers morphology	65
5.3.2	Responsive behaviors	67
5.3.3	Conductive behaviours	69
5.4	Conclusions	72
5.5	Experimental	73
5.5.1	Materials	73
5.5.2	Electrospinning	73
5.5.3	Hybrid hydrogels preparation	74
5.5.4	Conductivity measurements	74
5.6	Supporting Information	75
5.7	Acknowledgements	75
CHAPTER 6	ARTICLE 3: TUNABLE TWO-STEP SHAPE AND DIMENSIONAL CHANGES WITH TEMPERATURE OF PNIPAM/CNCS HYDROGEL	78
6.1	Abstract	78
6.2	Introduction	79
6.3	Results and discussions	82
6.3.1	Fibers morphology	82
6.3.2	Hydrogel responsive behaviors	85

6.3.3	Deformation characterization.....	89
6.4	Conclusions	92
6.5	Experimental	93
6.5.1	Materials.....	93
6.5.2	Preparing PNIPAM/CNCs suspension.....	93
6.5.3	Electrospinning.....	94
6.5.4	Fibers morphology	94
6.5.5	Swelling/contraction equilibrium.....	95
6.5.6	Deformation characterization.....	95
6.6	Acknowledgements	95
CHAPTER 7	GENERAL DISCUSSION.....	99
7.1	Electrospinning of PNIPAM-based hydrogel	99
7.2	Multifunctional PNIPAM-based fibrous hydrogel.....	101
CHAPTER 8	CONCLUSION AND RECOMMENDATIONS.....	103
8.1	Conclusion.....	103
8.2	Recommendations	104
REFERENCES	106

LIST OF TABLES

Table 2.1 Different tensile strength values of PNIPAM hydrogels from various articles[11].	9
Table 2.2 Photo-initiators that are widely used in industry	14
Table 2.3 Preparation of Polyaniline hydrogels	24
Table 2.4 Techniques for incorporating CNCs into temperature and pH responsive hybrid systems.	30
Table 2.5 Summary on smart chiral nematic CNCs based materials	35
Table 6.1 Average fiber diameters for samples in as-spun, swollen and contracted states	82

LIST OF FIGURES

Figure 2.1 Schematic illustration of thermal response of PNIPAM polymers and mechanism of the change of polymer volume.[57]	8
Figure 2.2 SEM images of Poly (NIPAM-HMAAM) electrospun fibers before (a) and after (b) thermal crosslinking treatment. The fibers morphology after one cycle of temperature alternation(c) and hydrogel swelling ratio after cycles[87].	13
Figure 2.3 A scheme of the folding star-shaped polymer bilayer; folding of a four-arm microcapsules in high (a) and low temperature(b); six-arm microcapsules in high (c) and low temperature(d).[39]	17
Figure 2.4 self-regulated oscillating PNIPAM hydrogel system. (a, Cross-section schematic. (b, Three-dimensional schematic. (c, Top-view microscope images of upright and bent microfins corresponding to on (left) and off (right) reaction states.[99]	18
Figure 2.5 Applications of electrospun nanofibers in biological field. ^[102]	19
Figure 2.6 Typical electrospinning setup in laboratory.[100]	20
Figure 2.7 Structures of polyaniline (n represents reduced repeat units, m represents oxidized repeat units, $n+m = 1$).[119]	23
Figure 2.8 The trend of publications related to hydrogels, nanocomposite hydrogels, and nanocomposite smart hydrogels from 2003 to 2018.[171]	28
Figure 2.9 TEM images of dried dispersion of cellulose nanocrystals derived from different sources: (a) tunicate, (b)bacterial, (c)ramie, (d)sisal.[179]	29
Figure 2.10 (A)SEM images of shear-ordered CNCs films(a) and non-sheared CNCs films(b); (c)the color of shear CNCs films[214]. (B)Mechanism of chiral nematic structure unwinds to mechanical stress(a). CNCs-elastomer composite viewed with cross-polarizing lens(b)[216].	37
Figure 4.1 SEM images of (a) as-spun nanofibers, (b) nanofibers after UV-treatment, (c) crosslinked nanofibers after swelling at 20 °C and drying in vacuum, and (d) crosslinked nanofibers after swelling, de-swelling and then drying in vacuum (scale bar: 3 μ m).	50

- Figure 4.2 (a) The electrospun membranes obtained from p(NIPAM-ABP) and pure PNIPAM were immersed in water at 20 °C for given times. (b) Molecular weight of p(NIPAM-ABP) from different molar ratio between NIPAM and ABP.....51
- Figure 4.3 Thermal responsive behaviors of hydrogels with respect to dimensions. Length and width for sample as-spun (a), fully swollen (a') and fully shrunk (a''). Membrane thickness in as-spun (b), fully swollen (b') and fully shrunk (b'') states. The dimension change of hydrogels at temperatures of 20 °C (c) and 40 °C (c').53
- Figure 4.4 Thermal-responsive behaviors of P(NIPAM-ABP) hydrogels with respect to swelling and de-swelling ratios. The influence of original membrane thickness on the swelling (a) and de-swelling (b) ratios for hydrogels from copolymer with NIPAM: ABP=100:3. The effect of crosslinker ratios on swelling (c) and de-swelling (d) ratios for hydrogels with original membrane thickness of 0.5mm.....54
- Figure 4.5 Rheological characterization for hydrogels from copolymers with crosslinker ratios of 100:1, 100:3 and 100:5 in fully swollen (a) and shrunk (b) states.55
- Figure 4.6 Compression tests for hydrogels in fully swollen (a) and shrunk (b) states. Inset: detail showing strains between 0% and 30%. The elastic modulus for hydrogels in both swelling and de-swelling states by compression test (c). Volume phase transition temperature (VPTT) of hydrogels from P(NIPAM-ABP) with crosslinker ratio of 100:1, 100:3 and 100:5 (d).....57
- Figure 4.7 NMR results for 4-acryloylbenzophenone and 4-Hydroxybenzophenone59
- Figure 5.1 Schematics of the incorporation of PANI into PNIPAM fibrous hydrogels.64
- Figure 5.2 SEM images of electrospun fibers of neat PNIPAM in as-spun (a), swollen (b) and shrunk states (c); SEM images of hybrid hydrogels (with weight ratio: PNIPAM:PANI=100:1.44) before washing (d), after washing in swollen(e) and shrunk (f) states. The scale bar is 2 μm65
- Figure 5.3 Effect of PANI on hydrogels response behaviours. Weight percent of PANI incorporated in hybrid hydrogels for various aniline concentrations (a); swelling behaviours of hybrid

hydrogels (b); contraction behaviours of hybrid hydrogels (c); effect of PANI on hydrogels equilibrium swelling/contraction ratio (d).....67

Figure 5.4 The electric resistance of hydrogels in swelling and contraction. The electric resistance of dried samples with various amount of PANI (a); the resistance of hydrogels with PANI when swelling (b); the resistance of hydrogels with PANI when contracting (c); the correlation of hydrogels resistance with responsive properties when swelling and contracting(d).69

Figure 5.5 The resistance of hydrogels with all PANI weight percent when swelling.75

Figure 6.1 Schematics of building bilayer structured hydrogels using PNIPAM and CNC via electrospinning and UV-induced crosslinking. Specifically, A) the electrospinning of PNIPAM/CNC suspension, with insert illustrating PNIPAM and CNC molecules in single fiber; B) the obtained bilayer electrospun fibers mat were exposed under UV light for crosslinking, with insert showing that the crosslinking occurs between PNIPAM chains; c) cutting samples from fibers membrane (with length and width of 1 cm and 0.5 cm, respectively) and immersing in water to fabricate bilayer structured hydrogels.81

Figure 6.2 Electrospun fibers morphology in as-spun (A1~A5), swollen (S1-S5) and contracted (C1-C5) states with various CNC proportion (0%, 1.5%, 3%, 5% and 7.5%). Scale bars are 2 μm82

Figure 6.3 A) Schematic of ‘single layer’ hydrogels (with 1.5wt% CNCs) swelling and contraction; B) Conformational transition of PNIPAM in presence of CNCs and water molecules; C) Weights of hybrid hydrogels in swollen (blue bars) and contracted states (red bards).85

Figure 6.4 (A) geometry of bilayer hydrogels with thickness ratios in swollen and contracted states; weights comparison of swollen (B) and contraction (C) hydrogels among the bilayer hydrogels with thickness ratios and the sum of corresponding two separate layers.87

Figure 6.5 Curvatures of bilayer hydrogels in swollen (blue squares) and contracted (red circles) states with tunable thickness ratios. Inserts were pictures for corresponding hydrogels with scale bar of 1 mm.90

LIST OF SYMBOLS AND ABBREVIATIONS

PNIPAM	Poly(N-isopropylacrylamide)
NIPAM	N-isopropylacrylamide
DMF	N'-Dimethylformamide
LCST	Lower critical solution temperature
VPTT	Volume phase transition temperature
THF	Tetrahydrofuran
AIBN	Azobisisobutyronitrile
ABP	4-acryloylbenzophenone
UV	Ultraviolet
GPC	Gel permeation chromatography
NMR	Nuclear magnetic resonance
SR	Swelling ratio
DR	De-swelling ratio
CR	Contraction ratio
G'	Storage moduli
G''	Loss moduli
IPN	Interpenetrating polymer network
HCl	Hydrogen chloride
PANI	Polyaniline
APS	Ammonium persulfate
DI	Deionized water
CNC(s)	Cellulose nanocrystal(s)
3D	Three-dimensional

SEM	Scanning Electron Microscope
FTIR	Fourier-transform infrared spectroscopy
wt%	Weight percent

CHAPTER 1 INTRODUCTION

Background and problematic

With the emergence of nanoscience and nanotechnology, researchers started to realize the value of nanofibers and corresponding production technology^[1]. Nanofibers with large surface area to volume ratio, about a thousand time higher than that of a human hair, could significantly improve materials' properties as well as generating new feature(s) on current materials^[2]. As one of the best technologies to produce fibers in micro to nano scale, electrospinning possesses incomparable advantages to other methods, such as phase separation^[3] and template synthesis^[4], in terms of versatility, flexibility and ease of fiber production. Unlike conventional fiber spinning methods like dry-spinning and melt-spinning, electrospinning utilizes electrostatic forces to stretch the solution droplet. It has been reported to successfully produce nanofibers with polymers, composites, semiconductors and ceramics^[5-7]. Electrospun fibers have been reported to be employed as nanocatalysis, tissue scaffolds, protective clothing, filtration and in nano-electronics^[5, 8, 9]. Thus, electrospinning would be a feasible protocol to fabricate fibrous structured hydrogels to accelerate its mass exchange rate. However, many critical issues need to be addressed regarding fibers processing conditions of polymer solution and maintaining the fibers' morphology under the crosslinking environment.

Poly (N-isopropylacrylamide) (PNIPAM) is a thermoresponsive polymer with lower critical solution temperature(LCST) of 32°C^[10]. PNIPAM contains hydrophobic isopropyl groups (-CH(CH₃)₂-) as well as hydrophilic amide groups (-CONH-)^[11]. At temperatures below LCST, the polymeric chains are expanded with hydrophilic moiety exposing to water molecules; while above this temperature, these hydrophilic moieties are isolated by hydrophobic moiety and corresponding hydrogen bonds are disrupted^[12]. Resulting from the reversible formation and disruption of hydrogen bonds, PNIPAM illustrates reversible “soluble-insoluble” feature in water around LCST^[13]. The LCST of PNIPAM can be tailored by addition of salts, surfactants or copolymerization with various hydrophilic or hydrophobic comonomers^[14-16]. Specifically, hydrophobic monomers decrease the LCST while hydrophilic monomers result in elevating its LCST^[10].

PNIPAM undergoes a coil-to-globule conformational transition around this temperature which is

close to normal physiological body temperature^[17]. To utilize this feature, PNIPAM-based hydrogels have been applied in biological related fields, such as drug delivery, tissue engineering and cell culture^[18, 19]. On the other hand, its capability of swelling to high degree has also drawn a lot of attention and corresponding efforts have been made to apply them as soft robotics or actuators^[20, 21]. In these fields, both the fast response rate and relatively strong mechanical strength are required^[20, 21]. These two aspects are common weak points for most smart hydrogels and PNIPAM-based ones are not excluded. Although efforts have been made to improve either side, there are very few studies that have successfully improved both sides^[22]. Needless to mention the lack of comprehensive investigation on the relationship between capability of temperature response and mechanical strength of the improved PNIPAM-based hydrogel. In addition, how this hydrogel would perform when employed as a platform to incorporate with other polymers and nanoparticles remains unknown. Apart from the interaction between PNIPAM and new material(s), the impact of fibrous structure on temperature response capability and newly added feature(s) would be a complicated and systematic question, which worth being investigated further. All these aspects would be involved and investigated comprehensively in this thesis.

Organization of this thesis

This thesis is based on three articles submitted to scientific journals or already published, and consists of the following sections:

Chapter 2 provides a literature review on PNIPAM-based hydrogels, the unique feature of PNIPAM, the technologies developed to improve its weak mechanical strength and slow response rate and the properties and applications of two materials (PANI(polyaniline) and CNCs(cellulose nanocrystals)) which would be incorporated to the hydrogel matrix consisting of PNIPAM nanofibers. Chapter 3 states the research objectives and the coherence between the objectives and articles. The core results of this thesis, in the form of three peer reviewed scientific articles, are presented in the following three chapters. Chapter 4 includes the comprehensive study on fabrication of UV-crosslinkable PNIPAM via electrospinning. Its temperature responsive behaviors and mechanical strength were another core issue addressed in this chapter. Chapter 5 represents the

capability of this PNIPAM-based hydrogel to serve as a platform to be introduced conductive properties via in-situ polymerization of PANI. Chapter 6 focuses on the incorporation of CNCs into this hydrogel, the interaction between CNCs and PNIPAM and corresponding impact of reinforcement of obtained hydrogel which was illustrated in programming 3D geometries of bilayer hydrogels. In Chapter 7, a general discussion of the entire thesis is presented. Finally, Chapter 8 summarizes the conclusions and the recommendations for future work.

CHAPTER 2 LITERATURE REVIEW

2.1 Hydrogels

Over the past decades, many definitions have been made toward ‘hydrogels’ as increasing attention have been paid to their exceptional promise in wide range of applications.^[23, 24] The most common one is a crosslinked polymeric network, filled with water molecules, produced by the reaction of one or multiple monomers.^[25] Another definition is that they are polymeric materials with 3D network that can swell and retain a significant fraction of water within their structure.^[26] From both definitions, the key factor would be polymeric materials with durable network structure that can be filled with water molecules. Actually, a number of materials, both natural and synthetic, fit these definitions. However, natural hydrogels were gradually replaced by synthetic ones which are more durable and stronger in terms of gel strength. Apart from these, synthetic polymer structure can be well defined to yield tunable degradability and functionality.^[27]

In the scientific research field, hydrogel is a hydrophilic polymeric network illustrating elastic properties because of crosslinking. Based on the reversibility, it could be classified into either physical crosslinking or chemical crosslinking.^[28] Physical crosslinking includes entangled chains, hydrophobic interaction and crystallite formation. Hydrogels with physical crosslinking may not be permanent and could contain network defects due to free chain ends or chain loops.^[29] The more often seen hydrogels were developed via chemical crosslinking. For example, it could be synthesized via a number of organic chemistry protocols, including one-step procedures, such as simultaneously polymerization and crosslinking of multifunctional monomers, or reacting polymers with crosslinking agents; and multiple step procedure like synthesis of a polymer with reactive groups followed by crosslinking.^[27] The essential factors involved are monomers, crosslinker and initiator. The polymer networks could be precisely tuned under molecular scale to meet the requirements of specific properties, such as biocompatibility and biodegradation, mechanical strength, and responsive properties.^[30]

Since the first report of synthetic hydrogel by Wichterle and Lim in 1960^[31], this material immediately drew numerous attention and many efforts have been paid to extend its application fields by introducing new features and properties to both existing and newly synthesized hydrogel

materials. As of now, fields that hydrogels have been applied successfully include but are not limited to: hygienic products^[32], drug delivery^[33], food additives^[34], pharmaceuticals^[35], biomedical applications^[36], tissue engineering^[37], wound dressing^[38], separation of biomolecules or cells^[39], and sensors and actuators^[40, 41].

2.1.1 Smart hydrogels

Among all hydrogels, smart hydrogels that can respond to an external stimulation have grown tremendously in the last few decades.^[11] They originate from polymeric materials that possess phase transition and conformation change behaviors in response to stimuli, which are mainly controlled by hydrogen bonds between the corresponding materials and water molecules.^[19] Other factors involved are hydrophobic interactions, and van der Waals forces.^[42]

Many signals that exist in nature can act as stimuli for smart hydrogels, such as temperature, pH, humidity, light, specific molecules and solvent, electrical and magnetic fields, etc. Among them, temperature and pH responsive materials are the ones that are mostly studied because temperature and pH are easily controlled parameters and they have wide potential in applications such as drug delivery, tissue engineering, imaging, analytical separation and detection, antifouling coatings, flow control devices, soft robotics^[11] etc.

2.1.1.1 pH responsive hydrogels

pH responsive polymers are those with acidic or alkaline groups that are sensitive to external pH. These functional groups can be ionized (protonate or deprotonate) around the pKa in aqueous systems, which leads to a change of ion concentration in the hydrogel and results in a volume change to reach a new ion balance of the hydrogel.^[43]

The pKa of a polymer can be modified by incorporating hydrophilic and hydrophobic moieties, which changes the ion balance and then hydrogel volume. For example, by increasing the hydrophobicity of poly (acrylic acid) (PAA) hydrogel, the swelling-shrinking pKa is altered to alkaline pH.^[44] Using a similar method, pKa of the hydrogel formed by poly (2-ethylacrylic acid) (PEAA) can be designed and modified for specific applications.^[45] Many articles mentioned the modification of typical pH-responsive hydrogels including poly (acrylic acid) ^[46], poly(methacrylic

acid)^[47], poly(propylene imine)^[47] and chitosan^[48].

The changeable pKa of these hydrogels is widely utilized in some biomedical applications. For example, the pH of the stomach and intestine is 2 and 5.5 respectively, which can be used for the precise delivery of specific drugs.^[49] Also, the pH in the microenvironment around cancer cells is more acidic than in normal tissues, which can be targeted easily by specifically designed hydrogels to release drugs.^[50] In addition, other hydrogel behaviors were studied and reported. Nagasaki et al^[51] reported a silicone-based polysilamine gels with diamine and organosilyl functional groups, which interestingly hardened on swelling due to the molecular conformation transition. They also suggested the detailed mechanism of this change and applied this material for protein absorption.

2.1.1.2 Thermal responsive hydrogels

These polymers possess a critical solution behavior as a result of temperature dependent polymer-polymer and/or polymer-solvent interactions. At a specific temperature, the polymer undergoes phase separation associated with a volumetric change caused by the transition between polymer extended and contracted states.^[52] This temperature-dependent phenomenon is driven by the polymer-solvent interaction and corresponding conversion of free energy.^[53] Specifically, the molecular chains undergo coil-to-globule transition at a certain temperature, which determines the possibility of its hydrophilic moieties to be exposed to solvent molecules to form hydrogen bonding. With more hydrogen bonding formed, the material is more likely to be hydrophilic and vice versa. This coil-to-globule transition phenomenon has been observed on a nanometer scale using AFM (atomic force microscopy).^[54] Using confocal laser scanning microscopy (CLSM), the internal structures of polymers were shown to be composed of two continuous domains, one with dense and another one with sparse regions.^[55] Based on their behaviors, these kinds of polymers can be classified as ones with lower critical solution temperature (LCST) and upper critical solution temperature (UCST). The LCST polymers shrink when the temperature is above their critical temperature, while UCST polymers show similar behavior when the temperature is below their critical temperature.^[56]

This thermo-responsive behavior originates from the dynamic equilibrium between the hydrophobic and hydrophilic components in polymer molecules, which is altered by solution

temperature.^[52] Generally, the molecules of thermo-responsive polymers are hydrophilic and possess hydrophobic groups, such as methyl, ethyl and propyl groups. The most commonly used material is N-substituted poly(acrylamide), such as poly(N-isopropylacrylamide) (PNIPAM), poly(N,N-diethylacrylamide) (PDEAM), poly(N-ethylmethacrylamide) (PNEMAM), while others include poly(methylvinylether) (PMVE), poly(2-ethoxyethylvinylether) (PEOVE), poly(N-vinylisobutyramide)(PNVIBAM) and poly(N-vinylcaprolactam) (PNVCa).^[57] Some copolymers have been reported as thermo-responsive polymers, such as poly(ethylene oxide)-b-poly(propylene oxide)-b-poly(ethylene oxide) (PEO-b-PPO-b-PEO) and poly(ethylene oxide)-b-poly(D,L-lactic acid-co-glycolic acid)-b-poly(ethylene oxide) (PEO-b-PLGA-b-PEO), but there is not much study focusing on them due to difficulties in their preparation and relative high cost for large-scale production.^[58]

2.2 PNIPAM

Among all the temperature responsive polymers, PNIPAM is the most studied and promising material mainly because its LCST(32 °C) is close to that of the human body and can be modified precisely.^[11] The molecular structure of PNIPAM is well studied and characterized, and the swelling and shrinking behaviors are mainly controlled by two functional groups: amide (-CONH-) and propyl (-CH(CH₃)₂). Under aqueous environment, the amide groups in PNIPAM molecules form hydrogen bonds with water molecules, thus increase the solubility when temperature is low; while the hydrogen bonding is weakened and the hydrophobic propyl group is activated when temperature goes higher, which is observed as swelling and shrinking in macroscale, respectively (Figure 2.1).

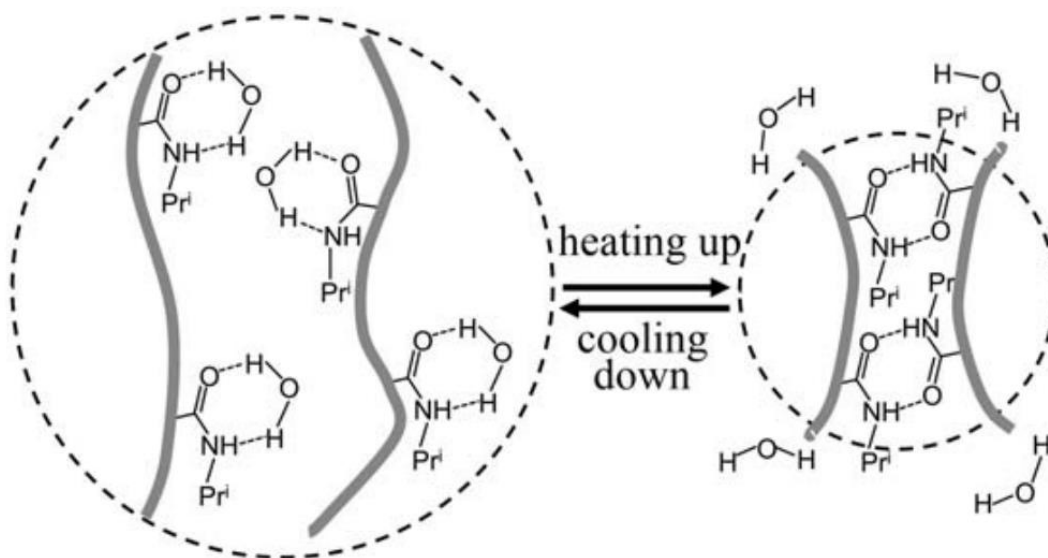


Figure 2.1 Schematic illustration of thermal response of PNIPAM polymers and mechanism of the change of polymer volume.[57]

The LCST of PNIPAM is reported to be independent on molecular weight.^[59] However, it can be tuned, according to specific applications, by incorporating hydrophilic or hydrophobic moieties in the polymer chain. When NIPAM is copolymerized with hydrophilic monomers (e.g. acrylamide or acrylic acid), its LCST increases.^[60] On the other hand, when copolymerized with hydrophobic monomers (e.g. N-tert-butyl acrylamide), the LCST decreases.^[61] For example, the LCST increased up to 45 °C, with 18% acrylamide incorporated, has been reported.^[62] In contrast, the LCST decreased to 10 °C with 40% of N-butyl acrylamide incorporated in the polymer.^[63]

We can easily find many other polymers that have similar responsive properties, such as poly(N,N-diethylacrylamide) (with LCST of 26–35°C), poly(N-1-hydroxymethyl) (with LCST of 30 °C) and poly(dimethylamino ethylmethacrylate) (with LCST of 50 °C).^[52] There are also some LCST polymers of interest today, for instance poly(N-vinylcaprolactam), poly(N-vinylcaprolactam) (LCST 25–35°C), poly[2-(dimethylamino)ethyl methacrylate] (LCST 50 °C) and poly(ethylene oxide) (PEO) (LCST 85 °C).^[64]

2.2.1 PNIPAM hydrogels

Basically, the PNIPAM hydrogels are prepared by copolymerization of NIPAM and other monomers, or by crosslinking of PNIPAM or the combination of both. Numbers of PNIPAM-based hydrogels have been reported and many researchers stepped further to introduce other functional groups or polymers at the stage of synthesis to extend its responsive triggers, for instance, pH. The most common functional groups added are acids/bases such as acrylic acid (AAc), methacrylic acid (MAc) and amine-containing N-(3-aminopropyl) methacrylamide hydro-chloride (APMAH). Furthermore, the functional groups can serve as reactive "handles" for further reactions with other functional molecules.

However, similar to other hydrogels, two drawbacks limit the applications of PNIPAM-based hydrogels: the slow response rate and the low mechanical strength. The mechanical strength of hydrogels formed by PNIPAM is not good due to their very high swelling degree which results in low density of polymer content in hydrogel. Another limitation is the poor response rate which results from the impenetrable surface that limits mass transfer of water molecules throughout the hydrogel.

The slow response rate can be increased by building a porous structure using pore forming additives, such as silica particles^[65] and poly(ethylene glycol) (PEG)^[66]. The porous structure enables a relative high diffusion of the solvent to the hydrogel, which can be used for building a hydrogel with fast response rate or increase the contact area of hydrogel and with solution.

Table 2.1 Different tensile strength values of PNIPAM hydrogels from various articles[11].

NIPAM concentration ¹	Crosslinker mole ratio	Measurement condition ²	Value (kPa)	REF
-------------------------------------	---------------------------	---------------------------------------	-------------	-----

¹ unit=mol/L

² room temperature

0.2	1.20E-02	SS ³	3.8	[67]
0.7	1.18E-02	SS	5.63	[68]
0.8	1.66E-02	CS ⁴	180	[69]
1.0	1.00E-02	SS	6.6	[70]

Many factors in polymerization process could affect the mechanical strength of the PNIPAM hydrogel, such as monomer concentration, crosslinker ratio, polymerization temperature and time. Besides, the state of the hydrogel during measurement also imposes influence to results significantly. Table 2.2 shows some articles involving the mechanical strength test result for PNIPAM in varying hydrogel states and measurement conditions.

The relatively low mechanical strength can be improved by building interpenetrating polymer network or crosslinking protocols. Incorporating other components physically or chemically can increase the mechanical strength by forming another network to ‘fix’ the PNIPAM linear molecular chain. Recent studies focus on ‘nanocomposite (NC) materials’ in which nanoparticles are added to the polymers to increase the surface reactivity or introduce new properties, such as the possibility to be functionalized or improvement on the compatibility. The use of nanoparticles (such as nanoclay) in a hydrogel was first reported in 2002 which extended the application on nanocomposites to hydrogel field.^[71] Many nanoparticles have been added to PNIPAM hydrogels such as graphene oxide^[72], laponite XLG^[73], tetramethoxysilane^[74], nano-starch^[75] and Fe₂O₃^[76]. These nanocomposite hydrogels show high tensile strength, specifically, the elongation at break can be up to 1000%. Particularly, the PNIPAM molecular chain can be adsorbed to the nano-clay by coordination and ionic interactions, thus forming a soft and flexible yet tough hydrogels.

³ SS= swollen state

⁴ CS=collapsed state

2.2.1.1 Interpenetrating polymer network

Interpenetrating polymer network (IPN) is normally defined as two polymer networks which are fully or partially interlaced on a molecular scale without covalent bonding to each other, while semi-IPN consists of one polymer with linear molecules and another crosslinked polymer which penetrate to each other physically.^[77] Many researchers reported the introduction of semi-IPN to PNIPAM hydrogels. For example, T. Kanai et al.^[78] introduced epoxy into PNIPAM hydrogels, S. Ekici et al.^[79] applied cellulose and PNIPAM building a semi-IPN hydrogel, C. Alvarez-Lorenzo et al.^[80] investigated the semi-IPN hydrogel by Chitosan and PNIPAM. Rathna et al.^[81] reported the semi-IPN hydrogel obtained from gelatin and PNIPAM, etc. Another interesting fact is that the response rate of these hydrogels was improved to some extent and was mainly due to the incorporation of the second polymer network, which resulted in a channel for water to get inside the hydrogel and thus shorten the contact time needed for response.^[11] Djonlagic et al.^[82] compared two semi-IPNs obtained from anionic and cationic poly(acrylamide) (PAAM) with PNIPAM, respectively. The mechanical strength of cationic PAAM containing hydrogels was twice that of pure PNIPAM gel, while the mechanical strength of hydrogel containing anionic PAAM was approximately one order of magnitude lower than that of the PNIPAM hydrogel. This result is due to the fact that the swelling ratio of anionic PAAM is higher than that of PNIPAM; while cationic PAAM is lower than that of PNIPAM. Thus, the density of polymer chains in hydrogel is different between the hydrogel with anionic and cationic PAAM.

2.2.1.2 Crosslinking agents

As mentioned above, the PNIPAM molecular chains are linear which cannot form a 3D network structure, thus a stable PNIPAM-based hydrogel can only be obtained by incorporation of physically or chemically crosslinkable moieties. The former means the additives can form a network themselves which builds a support structure for PNIPAM, while the latter means the crosslinkable moieties are covalently bonded to PNIPAM molecular chains. Among all the studies involving fabrication of PNIPAM hydrogels using the physical crosslinking, the best response rate (40s) was achieved by Gil et al.^[83] who used silk protein together with PNIPAM to build porous hydrogels. However, Jiang et al.^[84] reported a superfast PNIPAM based hydrogel that can respond to temperature within 1s via chemical crosslinking protocol. This huge gap in the response rate

may result from the fact that the network formed by physical crosslinking performs as a framework for PNIPAM linear molecules, which maintains the network and restricts the responsive capability. Whereas for the chemical crosslinking, the crosslinking points exist in molecular chain, which provides more space for PNIPAM's chains movement and illustrates a better response behavior.

There are a few crosslinking agents in polymer science field aiming to improve or modify the properties of various materials, such as organic polymers (like polyethylene^[85]), natural product (like starch^[86]), biomacromolecule (like RNA^[87]), etc. These crosslinking agents are applied depending on the properties of target materials and solvents as well as the specific requirement for reaction conditions, such as temperature, pH and light.

Among all the classic crosslinking agents, some were reported successfully applied to PNIPAM electrospun nano-fibers to conduct crosslinking under non-aqueous condition.^[88, 89] For example, Kim et. al. introduced N-hydroxy methyl acrylamide (HMAAm) to NIPAM as thermally-crosslinkable monomers and the copolymer was electrospun into nanofibers mats which were then crosslinked under 110 °C. The resulting PNIPAM-based hydrogels showed rapid and reversible volume changes in response to the water temperature alternation. They also reported that the fibrous structure was maintained after several volume change cycles (Figure 2.2).

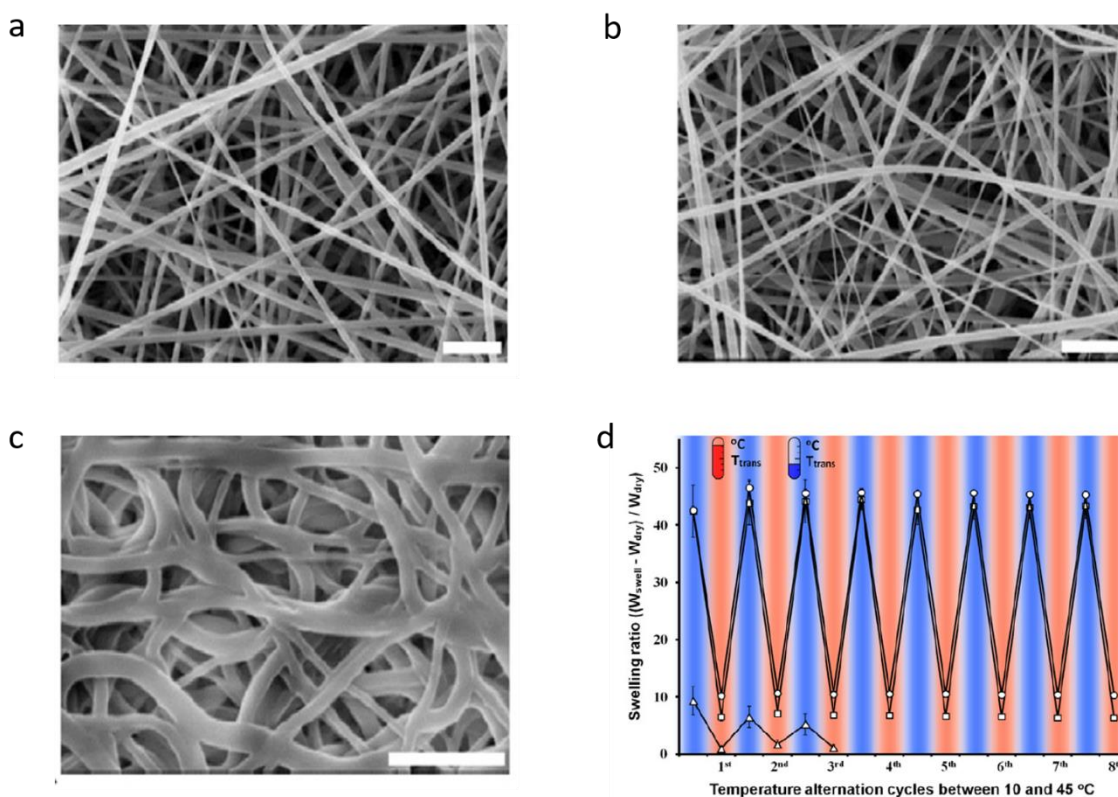


Figure 2.2 SEM images of Poly (NIPAM-HMAAM) electrospun fibers before (a) and after (b) thermal crosslinking treatment. The fibers morphology after one cycle of temperature alternation(c) and hydrogel swelling ratio after cycles[87].

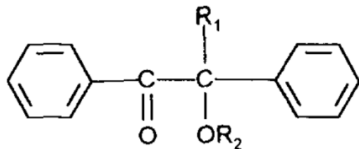
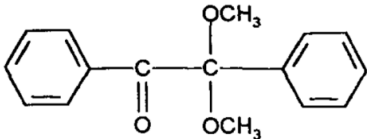
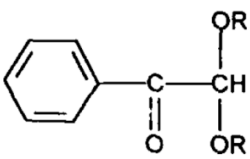
Similarly, Wang et. al^[89] introduced polyhedral oligomeric silsesquioxane (POSS) as thermal-crosslinking agent and 2-ethyl-4-methylimidazole (EMI) as a catalyst to PNIPAM solution. After electrospinning, the as-spun fibers mat was transferred to vacuum oven at 160 °C for 4 hours for crosslinking. Also, they had investigated the morphology of nanofibers followed by a comprehensive study on the volume change of the hydrogel toward the temperature alternation in water. They also introduced laser scanning confocal microscope (CLSM) to observe the swelling/de-swelling of electrospun fibers.

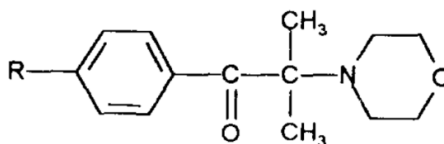
Although these two articles claimed a successful fabrication of PNIPAM-based hydrogels from electrospun fibers, it is still questionable to expose the PNIPAM electrospun fibers at temperature above 100 °C for crosslinking. Fibers morphology would be significant impacted, considering the glass transition temperature (T_g) of PNIPAM is approximately 100 °C -120 °C.^[90] However, the

influence of crosslinking temperature on both PNIPAM and the morphology of nanofibers were not mentioned. The absence of these key results would discourage further steps to build hydrogels through this protocol. Alternatively, photocuring has drawn a lot of attention as a replacement of thermal curing, as it is a more energy-saving and controllable choice for polymer crosslinking.^[91] Numbers of chemicals and functional groups were reported to be photo-cured with rapid reaction rates, energy efficiency and excellent temporal and spatial control.^[92]

Upon light absorption, the covalent bond in a photo-initiator is dissociated and generates energy, which will promote it into an excited state and yield new chemical initiation species by subsequent reactions. Most photo initiators involved are aromatic carbonyl compounds. Depending on the location of the group in molecules, the dissociation reaction mostly occurs at carbon-carbon bond between the carbonyl group and the alkyl residue in alkyl aryl ketones. Other bonds, such as C-S, O-O or N-O bonds (Table 2.3) can be cleaved, but they are relative low efficiency and cannot be stored for a long time, due to the possibility of thermal activation at low temperature.

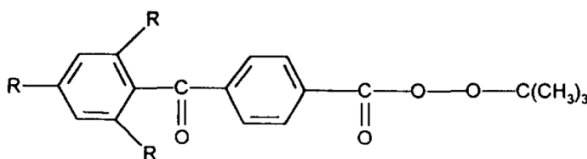
Table 2.2 Photo-initiators that are widely used in industry

Name	Chemical formula	Bonds
Benzoin derivatives		C-C
Benzil derivatives		C-C
Dialkoxy acetophenones		C-C

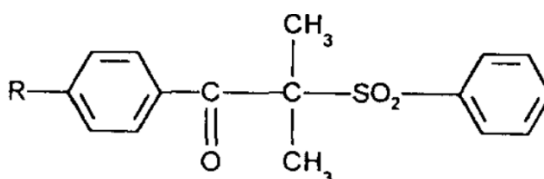
Amino alkylphenones


C-C

Organic peroxides



O-O

Organic
compounds sulfur

C-S

Some photo-initiation reactions are more complex reaction system because it can only work together with other compounds that can provide or receive an electron or proton, then the molecules undergo a series of recombination and form new chemical species, such as aromatic ketone/co-initiator systems, thioxanthone/amines system, miscellaneous ketone-amine systems, etc. The light absorption efficiency is mainly controlled by the concentration of the photo-initiator under the assumption that the material is transparent and there are no additives or pigments that can absorb light within a specific range ($\lambda > 300$ nm). Commonly, a higher proportion of light is absorbed in the upper layers and less is available for lower layers of a film. Therefore, an optimum concentration of photo-initiator could be obtained for a given layer thickness, below which the highest rate of initiation cannot be achieved and above which the overall rate of initiation will decrease. Most of light initiation reactions are carried out in air where oxygen can scavenge the free radicals generated by the photo-initiator. This problem can be solved by conducting the reaction in a vacuum or in nitrogen atmosphere, however, considering the relative high cost, most of the photo chemistry reactions are carried in air when feasible.

Many studies have been performed on the copolymerization of the photo-initiators and other monomers to produce light-sensitive materials.^[93-96] The efficiency of the photo-initiation is largely dependent on the molecular weight of the polymer, the molecular interactions between the photo-

initiator and monomers and other factors. Although the incorporation of photo-initiator to other monomers will decrease the initiation efficiency, the covalent bond between photo-initiator and monomer will extend the application of the photo-initiator in different solvent systems as well as the compatibility with various polymer materials.^[93]

Recently, Lonov's group^[41] has reported a UV-sensitive benzophenone derivative(ABP) and introduced it to NIPAM. Under UV irradiation, ABP was initiated and crosslinked to other ABP from the molecular chains nearby.^[97] By copolymerization of NIPAM and ABP, the poly(NIPAM-ABP) is thermal-responsive and UV-crosslinkable, which are from NIPAM and ABP, respectively. The crosslinked poly(NIPAM-ABP) served as the active layer for a bilayer structured microcapsules with PCL as the passive layer. Since the PCL layer was premixed with ABP, these bilayers were able to be patterned by UV irradiation. The covalent bonds formed between the two layers were to avoid the delamination when a large-scale deformation occurred (Figure 2.3). As an example for potential application, the author proposed a starlike microcapsule and showed its capability to capture and release yeast cells.

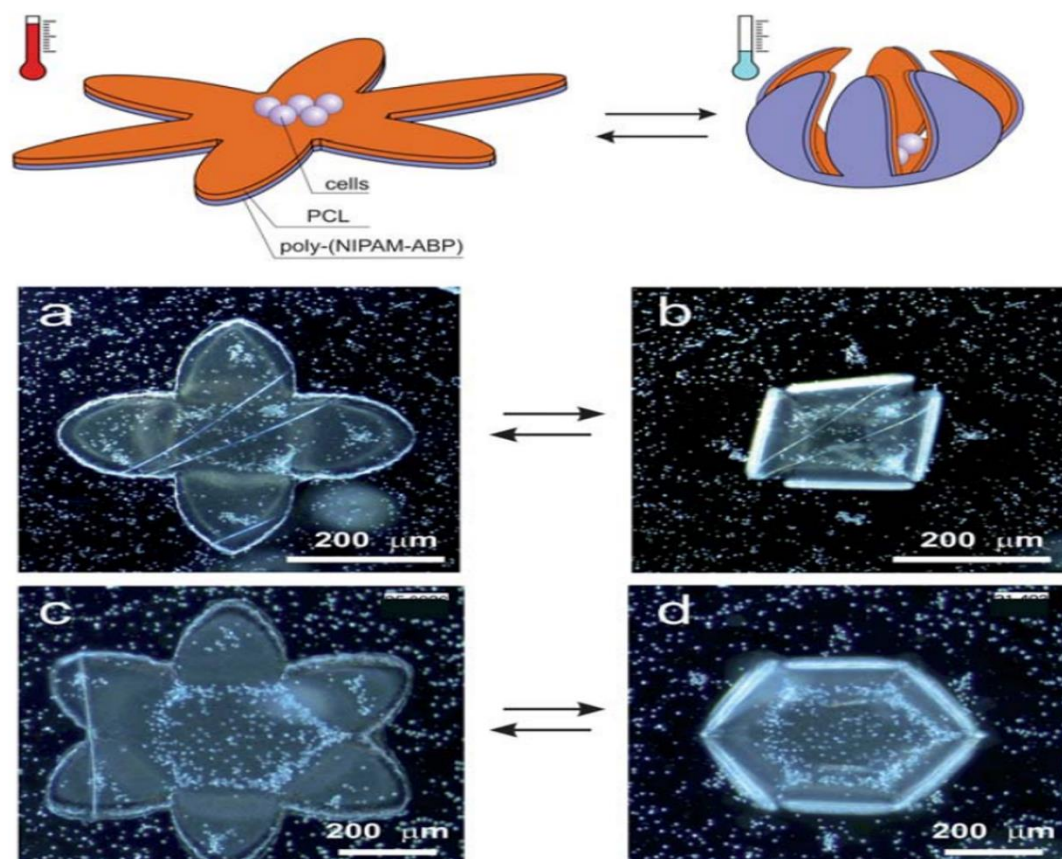


Figure 2.3 A scheme of the folding star-shaped polymer bilayer; folding of a four-arm microcapsules in high (a) and low temperature(b); six-arm microcapsules in high (c) and low temperature(d).[39]

This research provided a valuable protocol to prepare the poly(NIPAM-ABP) that is UV-crosslinkable, it should be well suited to fabricate the hydrogels from electrospun nano-fibers mats. The PNIPAM-based hydrogels prepared with this method could perform well regarding the temperature responsiveness because of the fibrous structure.

Apart from the traditional hydrogel application fields mentioned above, the PNIPAM hydrogel can be employed in the actuator field due to its high degree of deformation, such as soft robotic, shape memory and injectable hydrogel. Many studies reported the application of PNIPAM hydrogels as actuators^[98]. In 2012, He et al.^[99] reported a self-regulated oscillating system using PNIPAM hydrogel (Fig. 2.4). In this system, the PNIPAM was partly embedded into flexible microfins which

were incorporated with a catalyst in the top. The microfins and hydrogels were then placed into a biphasic system that can conduct a bilayer stable laminar flow: upper layer flow with reagents that can be catalyzed by the components fixed on the top of microfins to generate heat, the bottom layer was just water. At the beginning, the hydrogel was swelling at room temperature and the microfins were straight, so the chemical reaction was catalyzed and generated heat rapidly. Then, as temperature increased and reached above the LCST of PNIPAM, the hydrogel contracted and the flexible microfins bent down, which terminated the heat generation. When the system cooled down, the hydrogel swelled again and the microfins ‘stood up’ to generate heat. Thus, forming a self-powered and self-regulated loop.

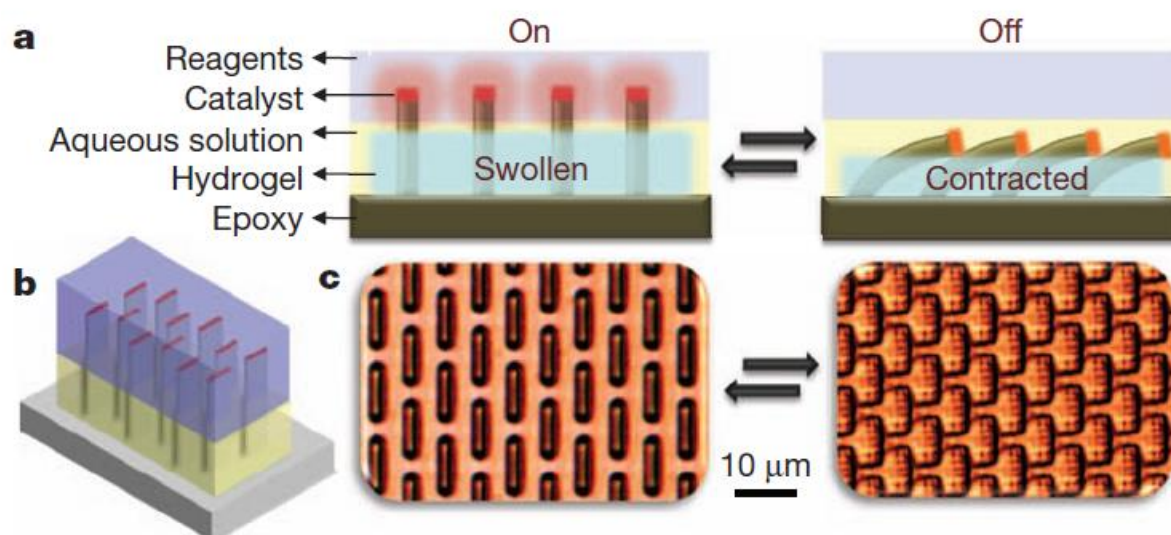


Figure 2.4 self-regulated oscillating PNIPAM hydrogel system. (a, Cross-section schematic. (b, Three-dimensional schematic. (c, Top-view microscope images of upright and bent microfins corresponding to on (left) and off (right) reaction states.[99]

2.3 Electrospinning

Electrospinning, as a simple and highly versatile technique to fabricate nano-scale fibers from a variety of materials, did not draw too much attention until the late 1990's when nanotechnology was emerging.^[100] Apart from the easy to conduct and high surface-to-volume ratio feature, many other advantages, such as the possibility to produce fiber alignment with the potential to be

functionalized^[101], are fully utilized in biological fields (Figure 2.5).

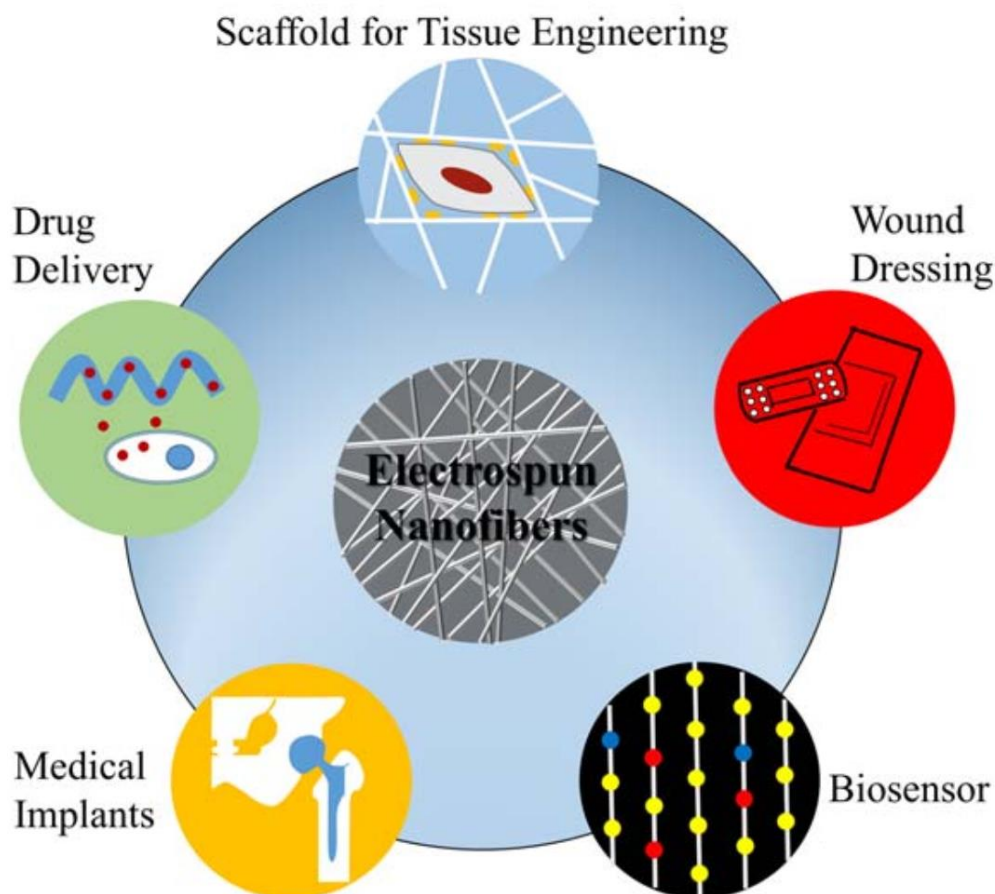


Figure 2.5 Applications of electrospun nanofibers in biological field.^[102]

Normally, four components are necessary for an electrospinning setup (Figure 2.6): a high voltage power supply, a feeding system, a spinneret, and a grounded collector.^[102] A rotating drum collector or coaxial spinneret may be needed for more advanced applications, such as aligned fiber and core-shell fibers.

The positive electrode of high voltage power connects to the spinneret and the collector (usually a piece of aluminum foil) connects to the ground. Between them, a strong electric field is applied. The solution droplet could carry a certain amount of charges under the electric field, which tends to move under the electrical force. Once the force overcomes the surface tension of the material solution, it brings the charged droplet to the collector. A so-called Taylor Cone is generated from the droplet as a balance between the stretching force and the surface tension of the solution.

Besides, almost all the solvent evaporates in air during their flight to the collector.^[101]

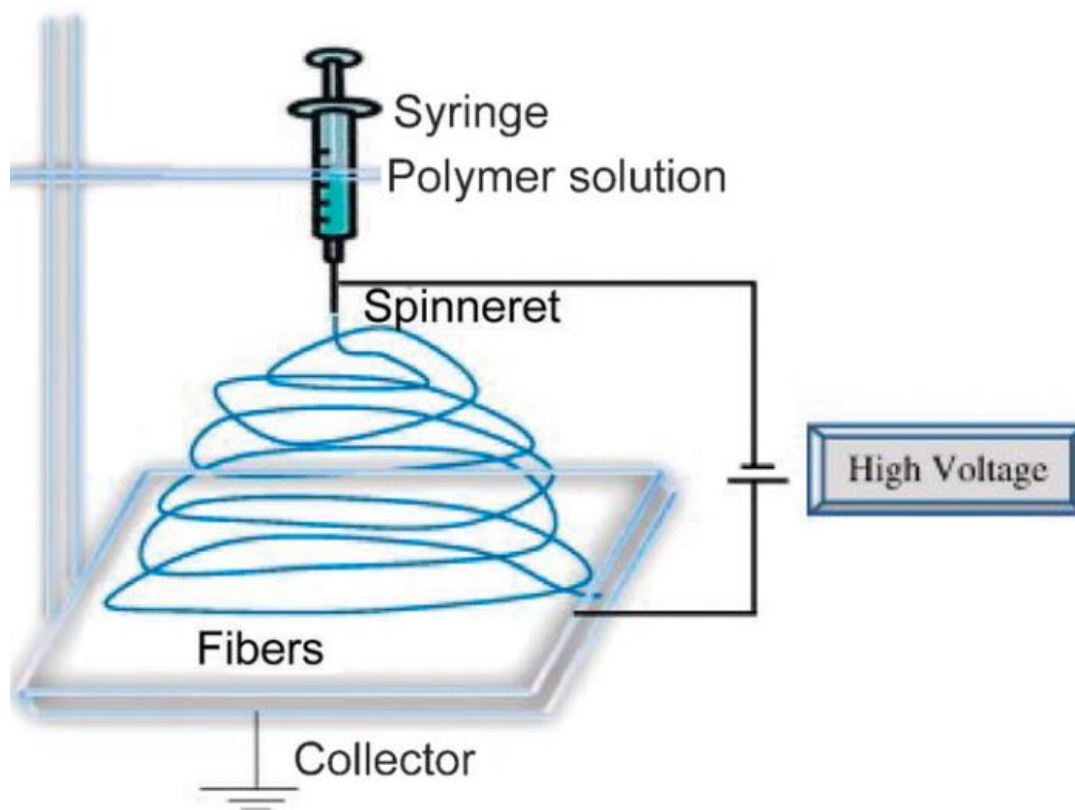


Figure 2.6 Typical electrospinning setup in laboratory.[100]

Many process parameters (such as the flow rate, voltage applied, spinneret size, distance between the spinneret and collector and rotation speed of the collector), environmental parameters (such as relative humidity and air temperature), and material parameters (such as solvent properties, polymer molecular weight, solution viscosity and volatility, the conductivity of the solution), can affect the fibers diameters, morphology, structure, secondary structure and alignment.^[101]

The response rate of a material upon stimulus is mainly controlled by the diffusion rate of the stimulus into the material. The application of normal stimuli responsive materials is limited due to the rather low response rate which can be improved by the electrospun nanofibers because of their high-surface-to-volume ratio. For example, a hydrogel obtained from electrospun nanofibers is reported to have 10 times faster response rate than the corresponding hydrogel films.^[103] Besides, the mass transfer can be improved further with the high porosity in electrospun fibers obtained by

adding pore generating components.^[104] Many stimuli-responsive materials have been reported to be prepared using the electrospinning technique.

For pH responsive electrospun fibers, Qi et al.^[105] reported a pH-sensitive electrospun fibers which were stable at pH 7.4, but degrade at lower pH to enhance the release efficiency. Kuo et al.^[106] designed a pH sensitive sensor to monitor culture environment using electrospun fibers fabricated with a copolymer solution. These fibers exhibited a dramatic shifting of the emission maximum in response to environmental pH.

For electrospun temperature responsive fibers, Rockwood et al.^[107] reported the fabrication of electrospun poly(NIPAM) fibrous mats and investigated the influence of the electrospinning process on molecular structure. Fu et al.^[108] reported another method to fabricate a thermally responsive fiber mats. They coated the PNIPAM into electrospun fiber mat obtained from block copolymers of 4-vinylbenzyl chloride (VBC) and glycidyl methacrylate (GMA) (PVBC-b-PGMA) through chemical reaction.

Many other stimuli responsive electrospun fibers were also studied. For example, magnetic targeting of drugs encapsulated in magnetic responsive nano-fibers^[109]; some photo responsive electrospun fibers obtained from fluorescent polymers can be used for light detecting sensors^[110]; fibers that can respond to chemicals, including protein^[111], gas^[112], ethanol^[113] and glucose^[114], were also reported in literature.

For potential applications of these PNIPAM-based hydrogels, multifunctional hydrogels are among the hottest research fields in past decades^[115], and numerous studies have been focused on introducing interesting features, such as conductivity^[116], permeability^[117] and optical properties^[118] to PNIPAM-based hydrogels. Among all these features, conductivity is one of the most promising features when added to volume change of the hydrogels.^[119]

2.4 Conductive hydrogels

Normally, conductivity could be introduced into PNIPAM-based hydrogels either by coating and/or blending with metallic or conductive polymeric particles.^[119] Considering the polymer compatibility and the processing difficulties, the conductive polymeric particles would be our

priority. There is a class of polymers, known as ‘synthetic metals’, that possess similar electrical, electronic, magnetic, and optical properties to metallic material while retaining the mechanical properties, material compatibility and processability of polymers. Conducting polymers are extensively conjugated molecules with alternating single and double bonds. These π -conjugated electrons spreading along the backbone of the polymer and their movement generate electrical conductivity. They completely differ from conventional “conducting polymer materials” that are usually a physical mixture of a nonconductive polymer with a conducting material, such as a metallic particles or carbon nano tubes, distributed throughout the material.^[119]

The conductivity of these polymers could be increased by several orders of magnitude by ‘doping’. Dopant, usually in small amounts with respect to polymers, could lead to dramatic changes in the electronic, electrical, optical, magnetic and structural properties of the polymer.^[119] The significant improvement towards conductivity of polymer via ‘doping’ was first discovered in 1977.^[120] And the following research has grown in a rapid rate and continued to accelerate until now.^[121] Professor Alan MacDiarmid, along with Japanese chemist Hideki Shirakawa and the American physicist Alan Heeger, were awarded the Nobel prize in 2000 to honor their contribution on the historic discovery of metallic conductivity in an organic polymer.^[119]

Among all the polymers that were discovered with metal-like conductivity in ‘doping’ state, Polyaniline (PANI) always holds a special position because it could be doped by protonic acid, which is an excited step from conventional redox doping. The protonic acid doping does not alter the number of electrons associated with the polymer backbone, instead, it rearranges the energy level along the back bone of the polymer chain^[122]. Actually, PANI could represent a class of polymers, which consist of alternating reduced and oxidized repeat units^[123], as is shown in figure 2.7. Based on the ratio between oxidized and reduced unites existing in PANI chain, the polymer is defined as ‘leucoemeraldine’, ‘emeraldine’, and ‘pernigraniline’ which represents the polymer in completely reduced, half-reduced and fully oxidized states. By introducing protonic acid, all these 3 polymer states could be protonated to corresponding salts form, for example, emeraldine salt. The imine nitrogen atoms on PANI molecules could be protonated based on the oxidation state and on the pH of the aqueous acid. Although the fully protonated emeraldine salt form of PANI possesses much higher conductivity, partly protonated emeraldine hydrochloride salt of PANI was

mostly investigated and mentioned in past research due to its properties, such as ease of synthesis, and unique protonic doping process^[124, 125]. However, two limitations on its processability need to be improved before further applications, which are thermal degradation and compatibility issues between doped and undoped form^[126]. However, hydrogels may help by providing a matrix with stability in aqueous environment and some interesting features from the matrix, like biocompatibility and volume change^[127]. This would extend the application of conductive polymers into biosciences, such as the stimulation or monitoring of cardiac^[128-130] or neural^[131, 132] cells and tissues. Recent research trends suggest applications in energy conversion and storage^[133, 134] which may be equally promising.

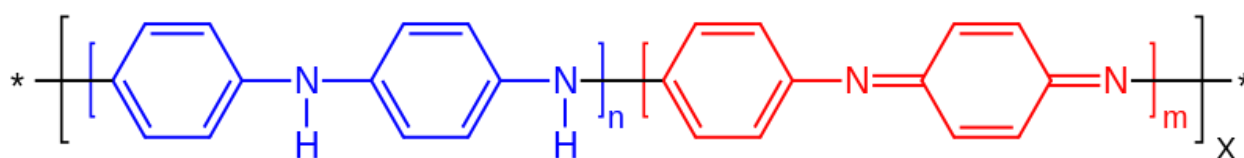


Figure 2.7 Structures of polyaniline (n represents reduced repeat units, m represents oxidized repeat units, $n+m = 1$).^[119]

Regarding the preparation of hydrogels with incorporation of conducting polymers, the most reported approach was the preparation of hydrogels from polymers, which was subsequently used as a matrix for the preparation of conducting polymers (Table 2.4). Specifically, the preparation is started by hydrogels produced by cross-linked water-soluble polymers, followed by diffusion of the solution of conductive monomer, such as aniline, into a hydrogel matrix. The last step would be the contact of monomer-containing hydrogel with the solution of oxidants.^[127] The ideal expectation in this scenario is that the oxidant could diffuse into hydrogel matrix loaded with conductive monomers and the conductive polymer will be formed once the oxidant meets the monomer. However, things run different in real world where the diffusion of monomer and oxidant occurs simultaneously and in opposite direction. The monomer tends to escape out of the hydrogel matrix while the oxidant diffuses into the matrix, all driven by the concentration difference.^[135] As a result, the polymer could form at the surface of the hydrogel where the oxidant and the monomer first meet. In addition, the monomer outside the hydrogel and the oxidant inside the hydrogel, as the result of diffusion, would also produce a concentration gradient. This would lead to the diversity of the polymer molecular weight and/or various degrees of protonation and oxidation.^[127] All these

would finally produce a hydrogel matrix with inhomogeneous conductivity. However, the formation of PANI at the surface of the hydrogels does not prevent the further polymerization inside the hydrogels. When formed at the surface of the hydrogel, polyaniline acts as the separation layer, and the polymerization could continue on one side where the monomer is dominant but not on the other side where oxidant plays the lead role.^[136] The oxidant and aniline molecules need not physically to meet to maintain the reaction because the electrons removed from aniline, during the polymerization, are transferred to the oxidant through the conducting polyaniline layer formed before.^[127] It was reported that the interface in contact with the aniline and oxidant is going to be coated with a thin polyaniline film after successful polymerization.^[137] This phenomenon has been utilized to coat the surface of poly(vinyl alcohol) hydrogel by the immersion of the hydrogel in the reaction mixture for polymerization of polyaniline.^[138] Many studies have been done introducing PANI into hydrogels, the table below is a summary of current works that have been reported.

Table 2.3 Preparation of Polyaniline hydrogels

Hydrogel matrix	Oxidant	Additive	Authors
Alginate, sodium salt	APS ⁵	Calcium ions	Srinivasan et al. ^[139]
		Sn nanoparticles	Zheng et al. ^[140]
Cellulose	Silver nitrate	silver	Wan and Li ^[141]
Chitosan	X ⁶	(Blending)	Kim et al. ^[142]

⁵ Ammonium peroxydisulfate

⁶ None

Gelatin	APS	X	Blinova et al. ^[136] ; Wu et al. ^[143]
	APS	NiO	Zhang et al. ^[144]
Polyacrylamide	APS	MWCNT ⁷	Chen et al. ^[145]
	KPS ⁸	SWCNT ⁹	Zhang et al. ^[144]
		X	Tang et al. ^[146]
Poly(acrylic acid)	APS	Graphene	Moussa et al. ^[147]
Poly(N-isopropylacrylamide)	APS	X	Rivero et al. ^[148]
	APS	Phytic acid	Shi et al. ^[149]
Poly(vinyl alcohol)	APS	X	Adhikari and Banerji ^[150]
No organic matrix	APS	Graphene, MnO ₂	Jayakumar ^[151]

2.4.1 Conductive hydrogels applications

Conductive hydrogels represent a series of materials with promising application potential. These

⁷ Multi-wall carbon nanotube

⁸ Potassium peroxydisulfate

⁹ Single-wall carbon nanotube

applications of conducting hydrogels are mainly focused on biosciences and energy conversion/storage fields.^[127] Specifically, conductive hydrogels mainly serve as biomedicine involved biosensors, electro-stimulated drug-release devices, and neural prostheses.^[152-154] These include the stimulation of tissues or cell growth, monitoring of vital functions, or the design of artificial muscles. As most of these conductive materials are environmentally stable, their biodegradability could be improved by the combination with other biodegradable polymers, such as pectin^[155].

Various energy-conversion and energy-storage devices utilize the electrical capability of these conductive materials^[133, 134, 156]. For example, batteries convert the chemical energy into electric one, while capacitors store electric energy by exploiting physical principles, such as the formation of electrostatic double layer. Widely diverse applications of conducting polymer hydrogels have been reported in literature.

2.4.1.1 Actuators

Actuators' principle is based on the mechanical strain resulting from volume change or electrical stimuli. For example, it was illustrated on polyaniline hydrogel's movement as a result of applied voltage.^[157] Another interesting example was the propulsion of hydrogel on water surface by asymmetric release of ethanol from polyaniline/alginate hydrogel matrix.^[139] Similar study showed polyaniline hydrogel crawled under the electric field towards with a maximum 15.1 mm s^{-1} speed. The oscillatory bending of polyaniline/chitosan hydrogels was observed with applied DC voltage and was applied as fishlike swimming robots or simple pump shave.^[158]

2.4.1.2 Biomedicine

As was mentioned above, the biocompatibility of polyaniline was improved by incorporation of other biocompatible materials for purpose of biological applications. For example, polyaniline hydrogel based on bacterial cellulose was found to be cytotoxic-free to the growth of human skin fibroblasts.^[159] Cytotoxicity and cell proliferation of polyaniline-containing injectable hydrogel were found to satisfy conditions for biomedical applications.^[160] Polyaniline/gelatin hydrogel was reported to be suitable for the growth of mesenchymal stem cells and myoblast cells.^[160] The cells

growth was illustrated to be sensitive to polyaniline particles with applying electric potential.^[161] Polyaniline based hydrogels were also applied to control drug release. For instance, the release of amoxicillin trihydrate, was controlled on polyaniline-based hydrogels by tailoring pH.^[135]

2.4.1.3 Electrodes and electrolytes

The electrical property of polyaniline hydrogels were exploited to serve as electrodes in supercapacitors^[162] and especially in flexible types^[147]. Their practical applications including lithium ion battery electrodes designed with polyaniline hydrogels with phytic acid^[163], tin^[140] or silicon nanoparticles^[164]. The polyaniline gel electrolytes also have been used for dye-sensitized solar cells.^[165]

2.4.1.4 Smart materials

Thermoresponsive materials undergo significant volume change with temperature change. Polyaniline hydrogel incorporated into such materials was applied as a heating element when certain current could generate Joule heat^[166] or as absorbent of microwave^[148] or near-infrared laser irradiation^[167]. The thermoresponsive conductive hydrogels have also been applied as a pressure sensor, electrical switch, or drug-delivery device driven by microwaves^[148]. Similar studies were reported regarding pH responsiveness for polyaniline/polyacrylate^[146] or polyaniline/poly (acrylamide-co-sodium methacrylate) hydrogels.^[168]

2.5 Cellulose Nanocrystals

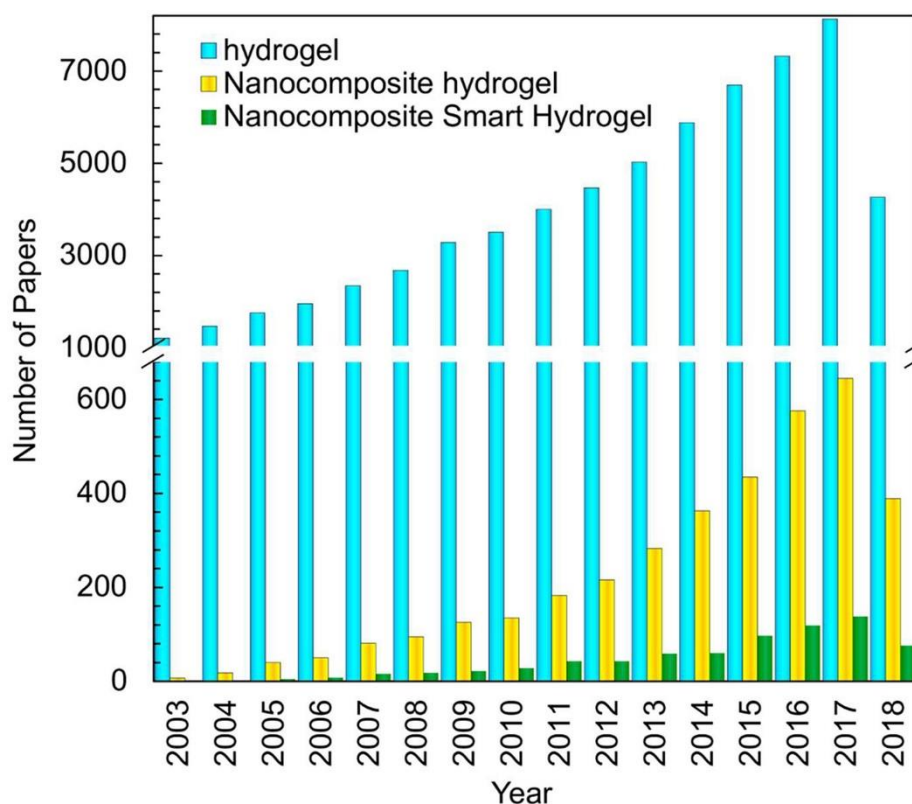


Figure 2.8 The trend of publications related to hydrogels, nanocomposite hydrogels, and nanocomposite smart hydrogels from 2003 to 2018.[171]

In addition to smart polymers, smart hybrid systems allow for better functionality to be achieved. These smart materials combine a stimuli-responsive component with at least another component(s) that alters the responsive behavior or introduces additional desired properties.^[169] For example, smart systems with targeted bioactivity have been achieved by conjugating smart polymers to biomacromolecules.^[170] Alternatively, inorganic components can be incorporated into smart polymer/hydrogels to materials with tunable optical properties.^[171] In recent years, more and more attention has been drawn to nanocomposite smart hydrogels (figure 2.8). In particular, a number of works have been reported with smart hybrid systems containing cellulose nanocrystals (CNCs).^[169]

CNCs are rod-like nanoparticles extracted from nature products, like plants and agricultural biomass.^[172] Apart from their excellent sustainable and biodegradable properties, they can also be

surface modified with specific functionality.^[173] There are many sources of cellulose, such as wood fibers, tunicates, and some bacteria.^[174] The nanocrystals can be obtained from precursors via acid hydrolysis, sonochemical fragmentation, microbial or enzymatic digestion, etc.^[175] Interestingly, the morphology of the CNCs produced largely depend on both the source(Figure 2.9) and extraction method used, and they generally possess lateral and length dimensions of 3~5 nm and 100~300 nm, respectively.^[176] Another attractive feature is their desirable physical characteristics, such as a high surface area ($\sim 250 \text{ m}^2/\text{g}$), high tensile strength (7500 MPa), and high stiffness (Young's modulus up to 140 GPa).^[177] Additionally, the abundance of reactive hydroxyl groups on their molecules provide an excellent platform for further chemical modifications that can be integrated into smart hybrid systems.^[178]

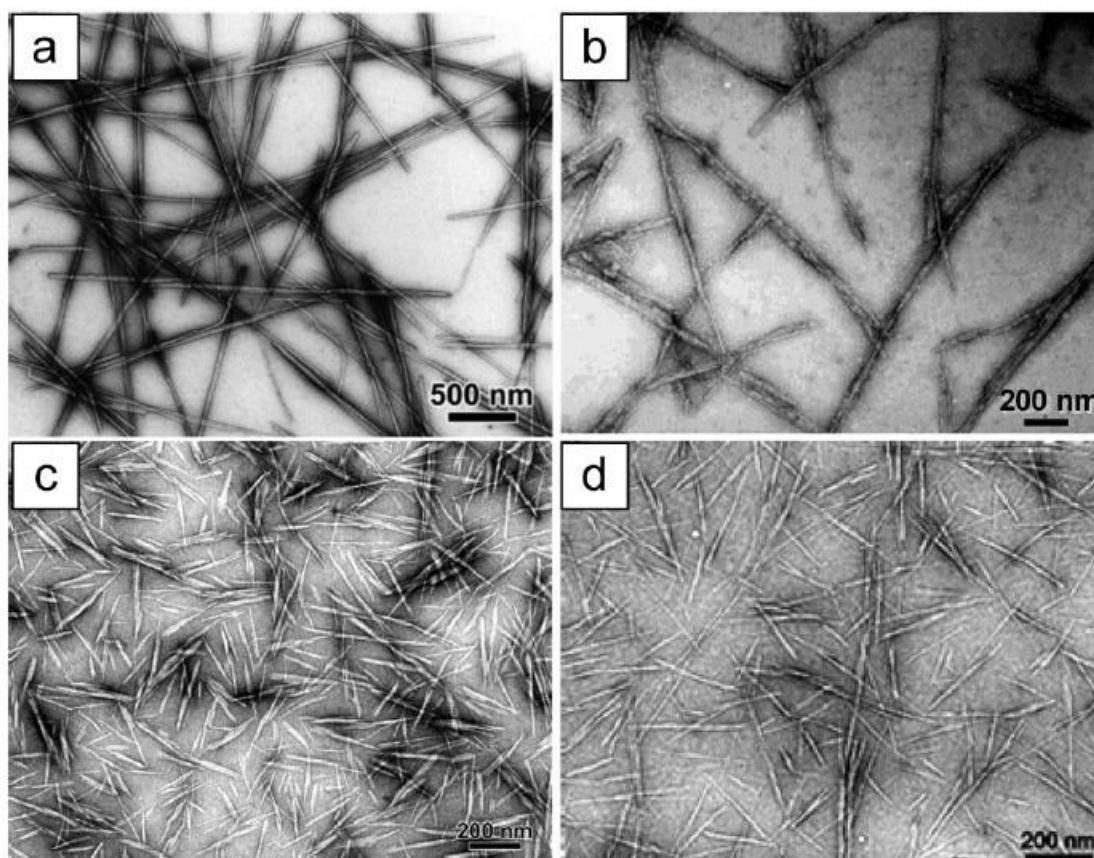


Figure 2.9 TEM images of dried dispersion of cellulose nanocrystals derived from different sources: (a) tunicate, (b) bacterial, (c) ramie, (d) sisal.[179]

Based on the objectives of specific research, CNCs proportions in hybrid system could be higher than 90% or lower than 10%. In most hybrid systems with low CNCs incorporated, CNCs normally provide a platform to either introduce new functionality or improve mechanical properties. For example, a number of efforts have been made to incorporate CNCs into temperature or pH responsive systems. Whereas for systems with high CNCs amount, optical properties or self-healing capability resulting from CNCs self-assembly feature were mainly utilized.

2.5.1 Low CNCs proportion

The most well-studied stimuli used to control smart polymeric systems is heat and pH. Three strategies have been employed to introduce CNCs into these hybrid systems, “grafting to”, “grafting from”, and physical mixing.^[169] Related works are summarized in Table 2.5. The “grafting to” and “grafting from” methods were employed in polymerization where the polymer brushes are to be covalently bonded to the CNCs. Specifically, well-defined polymer brushes can be synthesized with the “grafting to” technique. This method provides more flexibility in the synthesis of polymers and allows large-scale production. However, steric hindrance limits the grafting density, as the reactive sites would be blocked by already grafted brushes to continue the reaction^[179]. To improve this, the “grafting from” method was utilized, where the initiator molecules are first attached to the surface of CNCs, and then monomers are polymerized directly from the initiator sites^[180].

Table 2.4 Techniques for incorporating CNCs into temperature and pH responsive hybrid systems.

Fabrication protocols	Polymers	References
Grafting From CNCs		
ATRP	Poly(oligo(ethylene glycol)) methacrylate	[181]
ATRP	Poly[2-(2-(2-methoxyethoxy)ethoxy) ethyl acrylate]	[182]

FRP	Poly(N-isopropylacrylamide)	[183]
SI-ATRP	Poly(poly(ethylene glycol) methyl acrylate)	[184]
LRP	Poly(N-isopropylacrylamide-co-stearyl methacrylate)	[185]
Grafting To CNCs		
Peptide Coupling	Jeffamine polyetheramines M2005 and T5000	[186]
Peptide Coupling	Jeffamine polyetheramine M2005	[187]
Covalent Bonding	poly(4-vinylpyridine)	[188]
Covalent Bonding	poly[2-(dimethylamino)ethyl methacrylate]	[189]
Covalent Bonding	poly(4-vinylpyridine)	
Physical Mixing		
H-Bonding	Pluronic 407	[190]
Hydrophobic Bonding	Hydroxypropyl methylcellulose	[191]
Electrostatic Attraction	Poly(2-(dimethylamino)ethyl methacrylate)	[192]

Cudjoe et al. prepared a nanocomposite consisting of CNCs, grafted with a temperature responsive polymer, called amine-end-capped poly[2-(2-(2-methoxyethoxy)ethoxy)ethyl acrylate] (POEG3A)^[182]. Below the LCST, the grafted polymer chains hindered the structure forming among cellulose nanoparticles, limiting their reinforcing effect. Once exposed to water above the LCST, the grafted chains undergo a coil-to-globule transition, reducing the inter-particle separation of

CNCs that stiffen the nanocomposite.

Zubik et al. fabricated a CNC-g-PNIPAM thermo-responsive hydrogel and proposed a potential application in wound dressing.^[183] Increasing the CNC in the hybrid system led to an improvement in the mechanical stability, while clear thermo-responsive behavior was preserved. Antibiotic and antiprotozoal compounds were loaded into and released from the hydrogel to evaluate the potential application for wound dressing. This hybrid system produced rapid and sustained release, which is aimed for wound treatment.

Lee et al. grafted poly(N-isopropylacrylamide-co-stearyl methacrylate) (poly(NIPAM-co-SMA)) brushes onto the CNC employed via living radical polymerization to fabricate a thermo-responsive rheology modifier.^[185] The strength of the hydrophobic interactions could be manipulated with altering CNCs ratios. Above the LCST of PNIPAM, the enhanced hydrophobic interactions resulted in the increase of viscosity, storage, and loss modulus of the solution.

Pickering emulsions are one of the most important applications of CNCs-based pH-responsive systems. Pickering emulsifiers with pH-responsive CNCs can cause alternate stabilization and destabilization of emulsions in response to variations in pH. Additionally, these hybrid systems are recoverable and reusable because the CNC-based emulsifiers can desorb selectively from the emulsion interface. For example, Tang et al. reported a Pickering emulsion stabilized by poly[2-(dimethylamino)ethyl methacrylate] (PDMAEMA) grafted CNCs. The hydrophobicity of the synthesized polymer brushes was altered in different pH due to the protonation and deprotonation of PDMAEMA chains, which led to the emulsification and demulsification of oil droplets.^[189] Zhou et al. prepared a CNC/fluorinated polyarylated soap-free emulsion. The surface functionalized CNCs were grafted to two polymers: poly(2-(dimethylamino) ethyl methacrylate) (PDMAEMA) and poly(2,2,3,4,4,4-hexafluorobutyl acrylate) (PHFBA), which are hydrophilic and hydrophobic respectively. At low pH, the protonated PDMAEMA resulted in the coalescence of the oil droplets. With increasing pH, the size of oil droplets decreased significantly because of the increased hydrophobicity.^[193]

Apart from the application in Pickering emulsions, tailoring the surface charge and hydrophobicity of functionalized CNCs could also impact the dispersity, like flocculation in industrial processes.

Kan et al. fabricated poly(4-vinylpyridine)-grafted CNCs via surface-initiated polymerization with ceric(IV) ammonium nitrate. Its flocculation and sedimentation was controlled by pH and the hydrophilic components of the CNCs. At low pH, it exhibited excellent stability in water. At pH > 5, the pyridyl groups on the polymer chains were deprotonated and this material became hydrophobic and precipitated in aqueous solution.^[194] Zhang et al. applied this poly(4-vinylpyridine)-grafted CNCs to stabilize gold nanoparticle (Au NPs) nanocatalysts. At pH lower than 5, these particles acted as an efficient nanocatalyst, while at pH greater than 5, this nanocatalyst could be recovered via flocculation.^[188]

Some pH-responsive CNCs have also been applied to biomedicine fields, such as drug release and drug delivery. For example, Rahimi et al. functionalized CNCs with tris(2-aminoethyl)amine for the delivery of methotrexate (MTX). This drug was loaded via the electrostatic attraction between amino groups on the CNCs and carboxylate group on the MTX at pH of 7.4. The drug release was controlled by the protonation of carboxylate groups on MTX which was pH-responsive. They proposed the potential application in targeted drug delivery field.^[195]

Although temperature and pH responsive material systems are most of the recent research that contributed to smart CNCs-based hybrid systems, a few efforts have also been devoted to the systems that respond to other stimuli, including water, magnetic fields, strain, and combinations of stimuli like temperature and pH have been developed. For example, Low et al. developed a drug delivery system based on CNCs decorated Fe₃O₄ with magnetic responsive capacity. A colon cancer drug, curcumin, was loaded into a Pickering emulsion stabilized with these CNCs. About 53% drug was released from the system under a magnetic field over a 4-day period.^[196] Similarly, Nylepö et al. also prepared a CNCs-based system with magnetic responsiveness via surface modification on cellulose with magnetic nickel/cobalt particles.^[197]

CNCs were introduced into electroactive polymers to generate movement in the presence of an applied electric field. Kim et al. designed an electro-responsive actuator using poly(vinylidene fluoride)/CNCs electrospun membranes and found that increasing the CNCs concentration benefit its properties as an actuator in both actuator's displacement and the response lag time. The actuator's electrolyte holding capacity was significantly increased because of CNCs incorporation.^[198]

In addition to single-stimulus responsive systems, multi-responsive CNCs-based systems have also drawn attention in recent years. Haqani et al. [79] grafted CNCs to a copolymer that can respond to pH and temperatures and propose this material for drug delivery applications. CNCs were first surface modified with crosslinked poly(2-hydroxyethylmethacrylate) (PHEMA) to increase the content of hydroxyl groups. NIPAM and acrylic acid (AA) were then polymerized from the surface of CNC-PHEMA with different sequences. The LCST of obtained material was shifted to near-body temperature and pH-sensitivity were observed at pH values of 7.0-10.0.^[199] Similarly, Malho et al. reported a temperature and pH-responsive system with surface-functionalized CNCs. Thermal-responsive polypeptides and pH-sensitive PAA were grafted onto CNCs via the surface initiated atom transfer radical polymerization (SI-ATRP). The colloidal stability was controlled by the temperature and pH of the CNCs dispersion, which was proposed for various biological applications.^[200]

2.5.2 High CNCs proportion

For all research that CNCs are at dominant proportions, their objectives are mainly about the utilization of CNCs' chiral nematic structure and corresponding optical properties. When CNCs' concentration is above 70 wt% in dispersion or solution, they form chiral nematic films via self-assembly during solvent evaporation.^[201] This chiral nematic structure is always lefthanded, allowing them to reflect lefthanded polarized light with a specific wavelength which equals the total distance it takes for the chiral structure to make a full turn.^[202] This distance can be tailored through the infiltration of small molecules, solvents, and polymeric materials into the gaps between each chiral layer.^[203] Thus, the maximum reflected wavelength and the corresponding color illustrated, can be easily controlled.

Numbers of research have been done regarding optically changeable CNCs based films, with proposed applications such as security and anticounterfeiting to sensors.^[204, 205] An overview of the most recent research related is summarized in Table 2.6. A vast majority of this recent work has been focused on CNC films that change color in response to applied mechanical stress and relative humidity.

Table 2.5 Summary on smart chiral nematic CNCs based materials

Stimuli	Film composition	Ref
Chemoresponsive		
Humidity	3.8% glycerol/96.2% CNCs (w/w)	[206]
Humidity	20% polyethylene glycol/80% CNCs (w/w)	[207]
Water	54.5% polyethylene glycol diacrylate/45.5% CNCs (w/w)	[205]
Ethanol	30% waterborne polyurethane/70% CNCs (w/w)	[208]
Mechanoresponsive		
Compression	100% desulphated CNCs	[209]
Uniaxial Strain	Glucose/ethyl acrylate/2-hydroxyethyl acrylate/CNCs	[210]
Multiresponsive		
Uniaxial Strain+ Humidity	30-50% glucose/50-70% CNCs (w/w)	[203]
Compression+ Ionic Strength	30% acrylamide/70% CNCs (w/w)	[211]
Heat+ Humidity	Poly(N-isopropylacrylamide)/glutaraldehyde/CNCs	[212]

As was mentioned above, many CNCs-based materials could change color resulting from the change of chiral pitch because of the infiltrating water molecules into each nematic layer with high

humidity. However, the rigidity of CNCs-based materials would be a problem in fabricating these humidity responsive systems because of the difficulty in processing. Thus, small hygroscopic molecule that can also act as a plasticizer would be an ideal selection. Some research was conducted via this protocol. For example, He et al. incorporated varying amounts of glycerol into CNCs chiral nematic structure and the self-assembly of CNCs by evaporation was observed. The pitch increased proportionally to the increasing glycerol content, thus red-shifting the maximum reflected wavelength from under 400 nm to almost 650 nm. Regarding the improvement on mechanical strength, the maximum elongation at break was 4% more than those without glycerol. The color of the glycerol/CNC composite film changed from its native green at 16% RH to orange at 98% RH^[206](Fig. 2.10C). Yao et al. have mixed PEG with CNCs and then casted the solution, CNCs/PEG composites were formed with weight ratios of 100/0 to 60/40. Similarly, the incorporated polymer generated a progressive red shift, while the color of this hybrid system changed from green to colorless reversibly with the humidity it was exposed to. The maximum elongation at break was improved about 2.5% with increasing PEG content^[207](Fig. 2.10D).

A wide range of mechano-induced photonic CNCs materials have been developed currently, including aerogels, hydrogels, and composite films. For example, Hiratani et al. fabricated a pressure-responsive hydrogel from the composite with CNCs and polymerized acrylamide. Before polymerization, the hydrogel was subjected to alternating shear along structural anisotropic films as shown in Fig. 2.10A(a). An anisotropic order was clearly observed in the sheared sample but not in the untreated sample. The sheared sample also showed drastically color change at pressures from 1.4 kPa. The color illustrated a blue shift as the pressure increased as shown in Fig. 2.10A(c). This developed CNCs-polyacrylamide hydrogel represented a remarkable and reversible color change with pressure and could be applied as an optical pressure sensor.^[211] Kose et al. prepared a CNCs composite with elastomer that can also responds to strain(Fig. 2.10B). Interestingly, its responsive behavior rely on the changes of nematic structure instead of the pitch. CNCs and glucose units were mixed and dried to form chiral nematic structures which allows the penetration of ethyl acrylate and 2-hydroxyethyl acrylate monomers in DMSO solution.^[213]

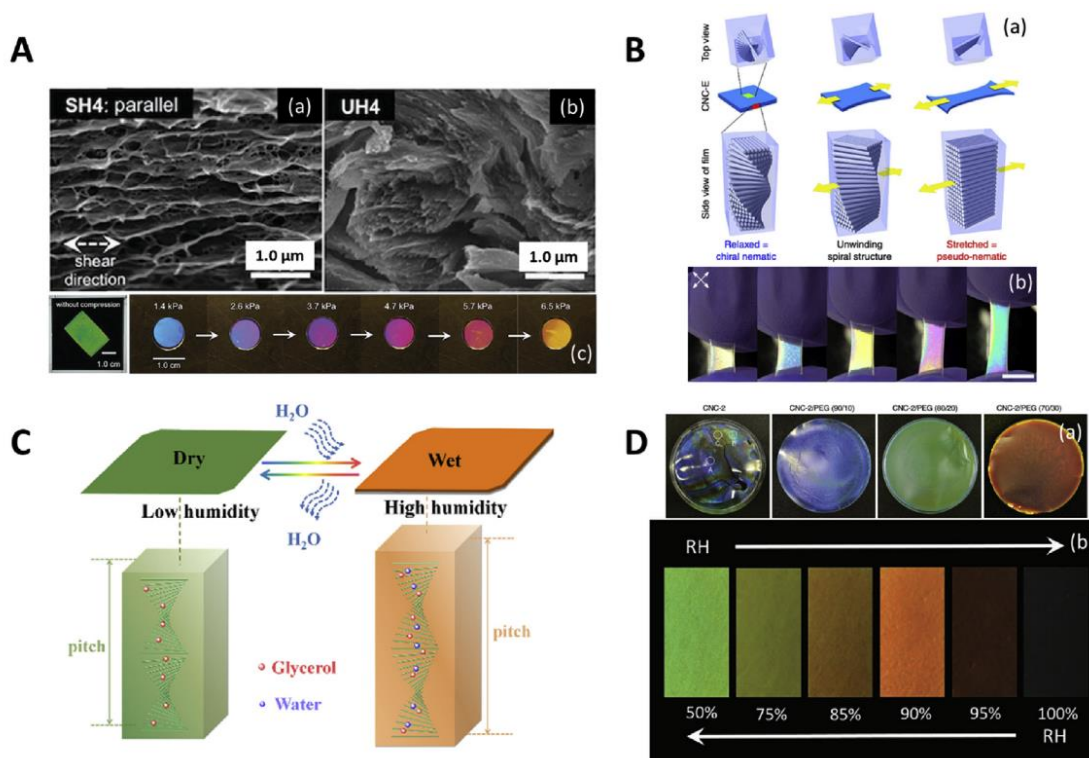


Figure 2.10 (A) SEM images of shear-ordered CNCs films(a) and non-sheared CNCs films(b); (c) the color of shear CNCs films[214]. (B) Mechanism of chiral nematic structure unwinds to mechanical stress(a). CNCs-elastomer composite viewed with cross-polarizing lens(b)[216].

2.6 Summary of literature review

PNIPAM is a well-studied and promising smart material mainly because its LCST is close to temperature of the human body and the capability of being finely modified molecularly. This wonderful feature is thus also present in PNIPAM-based hydrogels which represents a particularly important category of temperature responsive hydrogels in biological fields, for applications such as drug delivery and tissue engineering, and actuation/sensing fields, which utilize its large-scale volume change toward temperature alternation.

However, two main limitations hinder further application of these hydrogels. They are poor mechanical strength and slow response rates. In fact, the mechanical stability of neat PNIPAM is good but poor for corresponding hydrogels which is caused by its very high degree of swelling. On the other hand, the relatively slow response rate normally results from the impenetrable surface

that limits the mass transfer of water molecules throughout the hydrogel.

To accelerate the temperature responsive rate, the objective would be preventing the formation of impenetrable surface structurally. This is achieved by building pores structure on PNIPAM-based hydrogels, which results in multi-paths for water molecules to pass. This could be achieved either by porous-forming protocol where some additives generate pores under certain conditions; or by electrospinning technology where the material was electrospun under electrical field into fibers with very high surface-to-volume-ratio to facilitate faster mass exchange rate. The electrospinning is a widely used technology to fabricate smart material to accelerate their response rate.

The poor mechanical strength is being improved continuously via two main technologies: interpenetrating polymer network or crosslinking. Actually, the principle of both technologies is to limit the PNIPAM chain movement when swelling. Specifically, interpenetrating polymer network serves as a framework for linear PNIPAM chains; while crosslinking protocols build the 3D network among PNIPAM chains, either physically or chemically depending on the feature of crosslinking agents. Particularly, some crosslinking agents that can be introduced into PNIPAM chains via covalent bonds and work under non-solvent environment are extremely important for electrospun fibers. Because the fibrous and porous structure would be impaired in some solvent environment which is necessary for some crosslinking reactions.

Multifunctional hydrogels that can respond to more than one stimuli is a promising direction for potential applications of PNIPAM-based hydrogels. This could be fulfilled via either introducing functional groups into PNIPAM chains or incorporate other smart materials. Conductive polymers, such as PANI, is an ideal polymer to be introduced into PNIPAM-based hydrogels. The combination of PANI and PNIPAM-based hydrogel could maximize advantages from both sides: 1) conductive polymer could provide the electronic conductivity and redox activity; 2) the supporting polymer networks endow the hydrogels with integrity, elasticity and mechanical properties. It has been reported on successful incorporation of PANI along with dopants within the fibrous hydrogel matrix and potential applications as actuators, biomedicine or electrodes and electrolytes, etc.

With the aim of improving the mechanical properties and functionality of the PNIPAM-based hydrogel but without reducing its biocompatibility. CNCs, as one of the newest nanofiller in recent research field of nanocomposite, would be an ideal material to be introduced to the PNIPAM-based hydrogel to meet the requirements mentioned above. There are a number of research focused on the combination of CNCs with smart materials. In some systems that CNCs content remain low, it serves as: 1) a platform to introduce other functional group(s); 2) a reinforcement additive to improve the mechanical stability of the target system. While in some systems that CNCs are in dominant level (>70 wt%), its chiral nematic structure formed via self-assembly and corresponding optical properties are the focus to be investigated.

Few efforts have been devoted to fabricating UV-crosslinkable PNIPAM electrospun fibers membrane and investigating the response behaviors of corresponding hydrogels. Although PNIPAM is a well-studied material and widely applied in drug delivery field, it would be of our great interest to have a comprehensive study on this system. In addition, what role of nanofibers would play in the hydrogel system when it is incorporated with the conductive polymer (PANI) and nanofiller with unique structure(CNCs) remains unknown until now. Not to mention the interactions between two materials at molecular scale, nanofiber scale and hydrogel matrix scale, which would be a complicated and systematic questions to be explored.

This thesis aims at addressing issues mentioned above and the general and specific objectives are presented in next chapter.

CHAPTER 3 RESEARCH OBJECTIVES AND COHERENCE OF ARTICLES

3.1 Research objectives

The main objective of this research is to develop PNIPAM-based hydrogels with fibrous structure and apply them as a platform to introduce new polymer and nanoparticles.

3.1.1 Specific objectives of the research

- 1) Develop UV-crosslinkable PNIPAM for electrospinning and investigate its temperature response behaviors and mechanical strength comprehensively.
- 2) Introduce PANI into PNIPAM-based hydrogel matrix via *in-situ* polymerization and study the relationship between the temperature responsiveness and conductive behaviors of this hybrid hydrogel.
- 3) Develop PNIPAM/CNCs stable suspension for electrospinning, investigate the interaction between CNCs and PNIPAM and apply this interaction in designing bi-layer structure hydrogels for tunable deformation.

3.1.2 Presentation of articles and coherence with research objectives

Chapter 4, 5 and 6 present the core results of this thesis with three articles in the form of published (Chapter 4) or, submitted (Chapters 5 and 6) states. These articles cover the three specific research objectives and are described in the following section:

Chapter 4 presents the first article “*Response behaviors and mechanical strength of thermal responsive hydrogels fabricated by electrospinning*”, published in Polymer (DOI: 10.1016/j.polymer.2019.121880). This journal was chosen because of its great reputation in the polymer synthesis and processing field. This paper was submitted on June 20, 2019 and accepted on Oct 3rd, 2019. In this work, a UV-initiated crosslinking agent was incorporated in a poly(N-isopropylacrylamide) (PNIPAM)-based copolymer. Thermally responsive hydrogels were then fabricated by the electrospinning of a PNIPAM-based copolymer and subsequently crosslinked under UV treatment. The fibers morphology and hydrogel’s temperature responsive behaviors were

investigated as a function of crosslinker ratio. In addition, hydrogel's mechanical strength was measured via compression and rheology testing. Specific objective 1 is covered in article 1.

Chapter 5 shows the content of the second article, “*Fast thermal responsive hydrogels consisting with electrospun fibers with highly tunable conductivity*”, submitted in Sep. 3rd 2020 to Macromolecular Rapid Communications (manuscript number marc.202000518). This journal was chosen because it focuses on polymer science, ranging from chemistry and physics of polymers to polymers in materials science and life sciences. In this paper, poly(N-isopropylacrylamide) based hydrogels consisting of electrospun nanofibers are fabricated and applied as hydrogel matrices to introduce doped poly(aniline) (PANI) via in-situ polymerization (specific objective 2). The electric conductive properties of this hybrid hydrogel were found to be consistent with its swelling degree in response to temperature alternation. Subsequently, an evaluation system, aiming at general understanding and comparison of both conductive and responsive capabilities for these hybrid hydrogels, was established.

Chapter 6 shows the third article “*Tunable two-step shape and dimensional changes with temperature of PNIPAM/CNCs hydrogel*”, submitted to Small (submission number: smll.202006140). In this work, stable well dispersed PNIPAM/CNCs suspensions (with various CNCs proportion) were prepared and electrospun into nanofiber membranes (specific objective 3). The difference between hydrogels with various CNCs proportion regarding their temperature responsive behaviors was utilized to fabricate bilayer hydrogels. These bilayer hydrogels were capable of generating 3D geometries which were found to be tunable via finely tuned thickness ratio between two layers.

CHAPTER 4 ARTICLE 1: RESPONSE BEHAVIORS AND MECHANICAL STRENGTH OF THERMAL RESPONSIVE HYDROGELS FABRICATED BY ELECTROSPINNING

Yinghao Xu, Abdellah Ajji[†] and Marie-Claude Heuzey[†]

Published: Polymer, 2019, 183: 121880

[†]Department of Chemical Engineering, Research Center for High Performance Polymer and Composite Systems (CREPEC), Polytechnique de Montréal, 2900 Boulevard Edouard-Montpetit, Montréal, Quebec, Canada

Corresponding Author E-mail: Abdellah.ajji@polymtl.ca and marie-claude.heuzey@polymtl.ca

KEYWORDS: PNIPAM, HYDROGEL, ELECTROSPINNING

4.1 Abstract

A UV-initiated crosslinking agent was incorporated in a poly(N-isopropylacrylamide) (PNIPAM)-based copolymer. Thermally responsive hydrogels were then fabricated by the electrospinning of a PNIPAM-based copolymer and subsequently crosslinked under UV-treatment. The morphology of the fibrous structure was well maintained after many temperature induced swelling and de-swelling cycles. Both considerable degree of swelling and de-swelling ratios, along with an excellent response rate, were achieved with temperature variation. The influence of the crosslinker incorporated in the copolymer was investigated in terms of swelling/de-swelling ratios and rate, as well as the compressive strength and viscoelasticity of the hydrogels. Incorporation of crosslinker led to a 15% increase in copolymer molecular weight and 2 ° C decrease of the volume phase transition temperature (VPTT). The diameters of fully swollen and shrunk electrospun fibers were around 10 times and 3 times those of as-spun fibers, respectively. Also, compared to as-spun fiber membrane, 4 times swelling in thickness and an unusual 0.6 time shrinking in the length and width are reported and explained for the first time. In terms of response time, both swelling and de-swelling equilibrium were reached within 10 min for samples with 0.7 mm thickness; negligible impact on the response rate was observed when the crosslinker to monomer ratio increased from 100:1 to 100:5. However, the increase of crosslinker ratio showed significant negative impact on equilibrium swelling and de-swelling ratio (about 700% and 15% decrease respectively). A

viscoelastic, but close to elastic, behavior in both swelling and de-swelling equilibrium states under small-amplitude oscillatory shear was observed. The results of this work are expected to accelerate research in applications such as actuators and soft robotics.

4.2 Introduction

Stimuli-responsive materials, also called ‘smart materials’, have received considerable attention in both scientific and industrial communities. This is mainly due to their phase transition properties in response to stimuli such as temperature, pH, humidity, ionic strength, electric or magnetic fields, light, etc.^[97] The majority of these smart materials are polymers because their moieties can respond to different stimuli from the environment.^[19] As one of the most important applications, smart hydrogels built from crosslinked smart polymers can be applied for biomedical purposes e.g. drug delivery and tissue engineering.^[18]

Among the well-known stimulus-responsive polymers, PNIPAM (Poly(N-isopropyl acrylamide)) undergoes a hydrophilic (swollen in aqueous media) to hydrophobic (contraction) transition at a temperature of lower critical solution temperature (LCST, $\approx 32\text{ }^{\circ}\text{C}$) which is close to the human body temperature. Further, new properties could be obtained by incorporation of other materials either by co-polymerization, blending or layering to make it double or triple sensitive materials.^[17]

However, one of the most significant challenges for PNIPAM-based hydrogels, like most other hydrogels, is their extremely low mechanical properties. This is due to the quite low density of polymer in hydrogels when they swell to very high degrees in aqueous medium.^[11] This has been a great hurdle in many applications. For instance, in some specific molecules filtration and water purification fields, the thermo-responsive coating or membrane must be capable of withstanding high pressure and shear force.^[20, 21] Many efforts have been made to overcome the low polymer density and improve the mechanical strength of PNIPAM hydrogels. For example, interpenetrating polymer networks (including semi-IPN or full IPN)^[82, 214], modification on molecular chain^[215] and the addition of various nanoparticles^[216] have been performed on PNIPAM hydrogels and great enhancements have been reached in comparison with pure PNIPAM hydrogel. Nonetheless what should be realized is that several parameters impact the mechanical properties. For instance, variables such as the ratio between monomer and crosslinker, polymerization method and applied temperature, show a great influence on the results. Other experimental factors, like swelling degree

of the sample, technique and condition of measurement and even the pre-treatment of the sample, also have a considerable impact on its mechanical strength.^[11] Thus it is very difficult to compare among all the results reported. Besides, when it comes to enhancing mechanical strength, the response rate is always neglected and vice versa.

Another problem is the relative slow response rate following environmental temperature change. However, it has been proven by Zhang et al.^[214] that PNIPAM chains are capable of fast response. This issue is mainly caused by the impenetrable surface that is formed when the hydrogels contact water, which slows down the inward flow of water to access the hydrogels. To this end, nano-structures are considered as an ideal solution. Electrospinning is regarded as a robust technique to fabricate nanofiber nonwoven membranes with the feature of large surface to volume ratio and high porosity. Both can accelerate the stimulus and mass transportation in comparison to the corresponding bulk films. Electrospinning has been utilized in a few investigations to produce PNIPAM or its copolymer materials applied in drug delivery and cell culture fields.^[217-219]

PNIPAM-based hydrogels are normally prepared by two methods: direct co-polymerization of N-isopropylacrylamide (NIPAM) with other components; or by crosslinking of copolymers consisting of NIPAM and other moieties capable of crosslinking.^[89] The former one is not suitable for electrospinning because of the corresponding highly viscous polymer solution. The extremely high molecular weight of the copolymer makes it difficult to be dissolved by solvents and electrospun. The ideal strategy could be electrospinning of a linear high molecular weight PNIPAM followed by chemical crosslinking. However, very few studies have applied electrospinning to the fabrication of smart hydrogels. Wang et al.^[89] prepared a PNIPAM-based hydrogel by electrospinning of PNIPAM with polyhedral oligomeric silsesquioxane (POSS) and an organic-based catalyst. They investigated the influence of the catalyst on the morphology of fibers and found that the fibrous structure of hydrogels was maintained very well after catalyzed heat-treatment.

Currently, Jiang et. al. reported the fabrication of actuators with bi-layer structure of PNIPAM and TPU by electrospinning.^[84] They studied the capability of fast folded-unfolded response with temperature change and the correlated the bending curvature and the Young's modulus and thickness. Whereas, the fundamental investigation on PANIPAM-based hydrogels fabricated by electrospinning remain unclear. Specifically, the investigation of both mechanical strength and

response behaviors of PNIPAM hydrogels prepared by electrospinning has not yet been reported in recent scientific literature. These fundamental researches are necessary and helpful for these material's further applications either in actuators with double/multi-layer structure or self-controlled scaffolds for tissue engineering.

In this work, we study, for the first time, the response behaviors (including response rate and maximum swelling/de-swelling equilibrium ratio) and mechanical properties of PNIPAM hydrogels obtained from electrospun fibrous membranes. The response rate (which means how fast can the hydrogels reach equilibrium) and maximum equilibrium ratio (which represents how much water can the hydrogels uptake) in both swelling and de-swelling process are investigated. We also proposed the influence of nanofibers morphology and fibers mats interspace on the anisotropy deformation behaviors. In addition, the mechanical properties are also studied through compression and small-amplitude oscillatory shear tests. Besides, the influence of crosslinker is investigated through both response rate and mechanical properties comparison. Considering the difficulty on comparing the results of response behaviors and mechanical strength among many hydrogel research articles, these contributions would be significantly meaningful to accelerate the research progress in responsive hydrogels field.

4.3 Experimental

4.3.1 Materials

The following materials were used as received from Sigma Aldrich (Canada): 4-hydroxybenzophenone, benzophenone, N, N'-dimethylformamide (DMF) (99.8%), Tetrahydrofuran (THF) (99.9%), N, N'-diisopropylethylamine and acryloyl chloride. Azobisisobutyronitrile (AIBN) (Aldrich) was recrystallized from ethanol and N-isopropylacrylamide (NIPAM) (Aldrich) was recrystallized from n-hexane before use, respectively.

4.3.2 Preparation of polymerizable photo-crosslinker (ABP)

The photo-crosslinker 4-acryloylbenzophenone (ABP) was synthesized based on G. Stoychev's method ^[41] with slight modification. Solution A: 4-Hydroxybenzophenone (20 g, 0.1009 mol) was

dissolved into a mixture of N, N-diisopropylethylamine (19 ml) and methylene chloride (100 ml). Solution B: 9 ml of acryloyl chloride were mixed with 20 ml of methylene chloride. Solution A was added to a 200 ml round-bottom flask kept in ice bath and using magnetic stirring. Then solution B was added dropwise into the flask by a syringe. The methylene chloride was removed by rotary evaporation. The residue was washed with 20% HCl and neutralized with saturated solution of sodium hydrocarbonate and dried by rotary evaporation. The product was purified with the mixture solution of methional and deionized water with volume ratio of 1:1 and 2:3 respectively. The purity of ABP was verified by ^1H NMR(in support information).

4.3.3 Synthesis of p(NIPAM-ABP)

p(NIPAM-ABP) and PNIPAM were synthesized by free radical polymerization in a 1,4-dioxane solution with AIBN as initiator. AIBN (with molar ratio of 0.75:100 to NIPAM) and ABP (with molar ratio of NIPAM to ABP as 100:1, 100:3 and 100:5) were dissolved into an oxygen-free NIPAM solution (20 wt%). After 20 h polymerization at 70 °C, the solution was cooled down to room temperature and precipitated with n-hexane 3 times to remove the monomers. Pure PNIPAM was also synthesized with the same conditions but without ABP addition. All the molar ratio (100:1 100:3 and 100:5) mentioned in this article means the ratio of NIPAM: ABP in p(NIPAM-ABP).

4.3.4 Electrospinning

To produce nanofibers, p(NIPAM-ABP) and pure PNIPAM were prepared in DMF at a concentration of 45 %wt. The applied voltage on the needle (outer diameter: 0.6 mm) was 21 kV; the flow rate was fixed to 0.5 mL/h and the distance between the needle and collector was 20 cm. All fibers were collected on a grounded metal plate. The obtained fibers mats were dried under vacuum overnight to remove any residual solvent. Then the dried fibers mats were placed under a home-made UV-treatment device for 2 h to achieve crosslinking. By spinning different amount of solutions, electrospun membranes with selected thicknesses were obtained.

4.3.5 Characterization

The molecular weights of pure PNIPAM and p(NIPAM-ABP) were obtained before crosslinking by gel permeation chromatography (GPC) with THF as the eluent. All electrospun samples

investigated were taken from as-spun electrospun fibers mats with varying thicknesses (0.1, 0.3, 0.5 and 0.7 mm). Fibers morphology was observed under a scanning electron microscope (HITACHI TM3030Plus) following by vacuum evaporation at 20°C and 40°C for swollen and contracted samples respectively. The thickness of the samples in both as-spun and hydrogel states were sandwiched with two metallic plate and measured under optical microscopy (BX-61, Olympus). The optical images were analyzed by Image J software.

4.3.6 Swelling behavior of hydrogels

The gravimetric method was utilized to study the swelling and de-swelling behavior of PNIPAM-based hydrogels^[220]. The weights of swollen hydrogels were obtained at given time intervals in water with the temperature above/below the LCST of PNIPAM. To eliminate the potential change of LCST by the incorporation of crosslinker, the temperature for swelling and de-swelling of the hydrogels was fixed to 20 °C and 40 °C, which was confirmed to have no impact on the swelling and de-swelling kinetics from our preliminary experiments (data not shown). The excess water on the surfaces was removed with filter paper. The average value of three measurements was taken for each sample.

For swelling kinetics

The samples were immersed in water at 20 °C to reach equilibrium state, then dried under vacuum. The weight of the as-spun fiber mat was defined as W_o ; W_t represents the weight of the swollen hydrogels. The swelling ratio (SR) at time t was obtained as follows^[220]:

$$SR = \frac{W_t - W_o}{W_o}$$

For de-swelling kinetics

The weight of a fully swollen hydrogel was determined as W_d ; the sample was placed under water at 40 °C and the weight of sample at given time intervals was measured as W_T ; the definition of W_o is the same as that in the swelling part. The de-swelling ratio (DR) at time t was calculated as follows^[221]

$$DR = \frac{W_T - W_o}{W_d - W_o}$$

4.3.7 Rheology

An Anton Paar rheometer MCR 501 (PhysicaTM, Graz, Austria) equipped with CTD200 temperature control unit and parallel plate flow geometry was used to investigate the viscoelasticity of the hydrogels. A piece of double-sided tape was applied to fix sandpaper on the bottom plate to prevent the hydrogel from slipping during the measurements. Small-amplitude oscillatory shear tests were carried out with frequency sweep in the range of 0.1–50 rad/s and keeping the strain at 1%. This strain was confirmed to be in the linear viscoelastic range by strain amplitude sweep experiments (with frequency of 1, 10 and 50 rad/s) that showed non-linear effects starting from strain of 2%. The hydrogel samples were characterized by examining the storage (G') and loss moduli (G'') in both fully swollen and contracted states. The reproducibility of the measurements was carefully verified with an accuracy of up to 5%.

4.3.8 Compression tests

The same rheometer was used to investigate the compressive strength of the hydrogels in water at 20 °C and 40°C. The gels were compressed with a 12 mm diameter cylinder probe. A normal stress-strain curve was obtained at a crosshead speed of 0.5 mm s⁻¹.^[222] To protect the instrument, the software was set to terminate the test when the normal force reached 50 N, or the gap was less than 0.5 mm. Hydrogels obtained from electrospinning of copolymer with varying NIPAM and ABP ratio were compressed in both fully swollen and shrunk states. Considering the significantly rapid changes of the water-absorption capacity of PNIPAM hydrogels during heating/cooling processes, each sample was kept in a water bath at the selected temperature both before and during the measurement process.

In addition, the effect of ABP on the VPTT (volume phase transition temperature) of the hydrogels was investigated. A cylindrical probe was kept compressing the fully swollen hydrogels with 50% strain to make sure it was in contact with the hydrogel. Temperature was increased at a rate of 0.2 °C min⁻¹ to transfer heat homogeneously along the thickness direction. With the temperature increase, the forces generated and the corresponding temperature from hydrogel contraction, which due to the volume phase transition, were recorded.

4.4 Results and discussion

4.4.1 Morphology of electrospun fibers

All the samples were fully dried under vacuum to constant weight for SEM observation. Figure 1 shows SEM images of nanofibers after various treatments. Both as-spun fibers (Fig. 4.1a) and fibers after UV treatment (Fig. 4.1b) showed smooth surfaces and no preferential alignment. The diameters of as-spun fibers and fibers after UV-treatment were in the range of 150-250 nm. The fibers after 20 swelling/de-swelling cycles were examined by SEM again and no significant difference was observed. Then 20 nanofibers mats were selected for following tests. All the samples were immersed in water at 20 °C until full swelling. Then 10 swollen samples were dried under vacuum at 20 °C for the following SEM observations. As shown in Fig. 4.1c, significant swelling and bending/twisting was observed. The corresponding fibers diameters were in range of 1.2-1.5 μm . Another 10 fully swollen hydrogel samples were transferred to water at 40 °C to shrink. After drying under vacuum at 40 °C, these samples were observed also under SEM. As is shown in Fig. 4.1d, the contraction of fibers can be clearly seen and the fibers diameters were in range of 450-600 nm.

Two interesting things were noticed: 1) the fibers were bending and twisting instead of stretching to straight in the swollen state. Due to hydration, polymer chains relax and move to a more entropically favourable conformation which is random coils.^[84] This leads to morphological changes of the fibers as a result of polymer chain movement within the fibers; 2) the fibers could not go back to the original size after full contraction at 40 °C, in contrast the weight of the sample went back to the same value as in the original as-spun state. This phenomenon is hardly seen to be reported and no literature related was found to discuss it. To explain this, the following hypotheses were stated: the fibers cannot keep shrinking with more and more water expelled from polymer chain during the dehydration process. Specifically, the water molecules cannot be expelled completely during the dehydration balance at high temperature. After transferring to vacuum at 40 °C, the water molecules were volatilized quickly and completely from both inside and outside of the nanofibers. The weight of samples went back to that of corresponding as-spun state. On the other hand, during the rapid volatilization, the fiber cannot contract as much as under aqueous

conditions. Since with less and less water left, there is no more space for fibers to ‘move’, in other words, the fibers are ‘fixed’ and cannot shrink to original size.

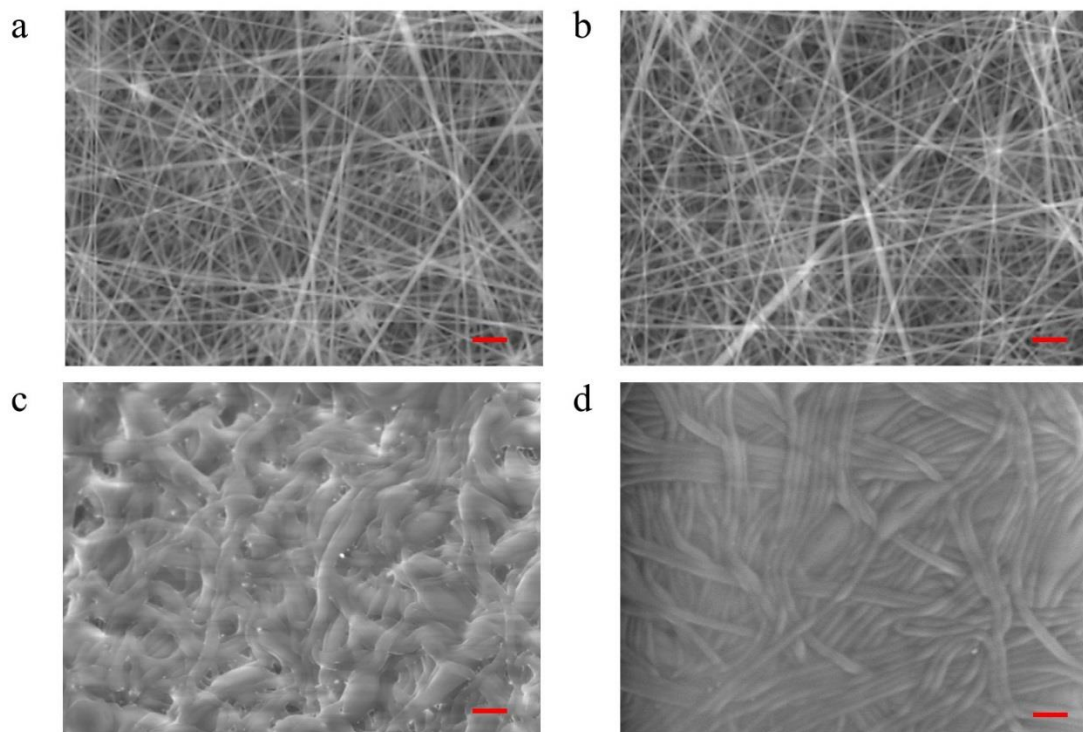


Figure 4.1 SEM images of (a) as-spun nanofibers, (b) nanofibers after UV-treatment, (c) crosslinked nanofibers after swelling at 20 °C and drying in vacuum, and (d) crosslinked nanofibers after swelling, de-swelling and then drying in vacuum (scale bar: 3 μ m).

4.4.2 Effect of crosslinker

The effect of crosslinker is shown in Fig. 4.2. For visual clarity, 1 wt% of Rhodamine B was added to the polymer solution before electrospinning. As can be easily observed, after electrospinning and UV-treatment, the electrospun membrane from pure PNIPAM dissolved rapidly in water at 20 °C. In contrast, membrane from P(NIPAM-ABP) was able to maintain its fibrous structure (Fig. 4.2a). The amount of crosslinker also affects the molecular weight of P(NIPAM-ABP). Normally, higher molecular weight results in highly viscous solutions and higher mechanical strength.^[11] About 15% increase in both number-average (M_n) and weight-average (M_w) molecular weights was observed when the crosslinker (ABP) increased from 0% (pure PNIPAM) to 1%, 3% and 5%,

respectively (Fig. 4.2b). The polydispersity index (M_w/M_n) was maintained well around 4.5, which is reasonable for free-radical polymerization.

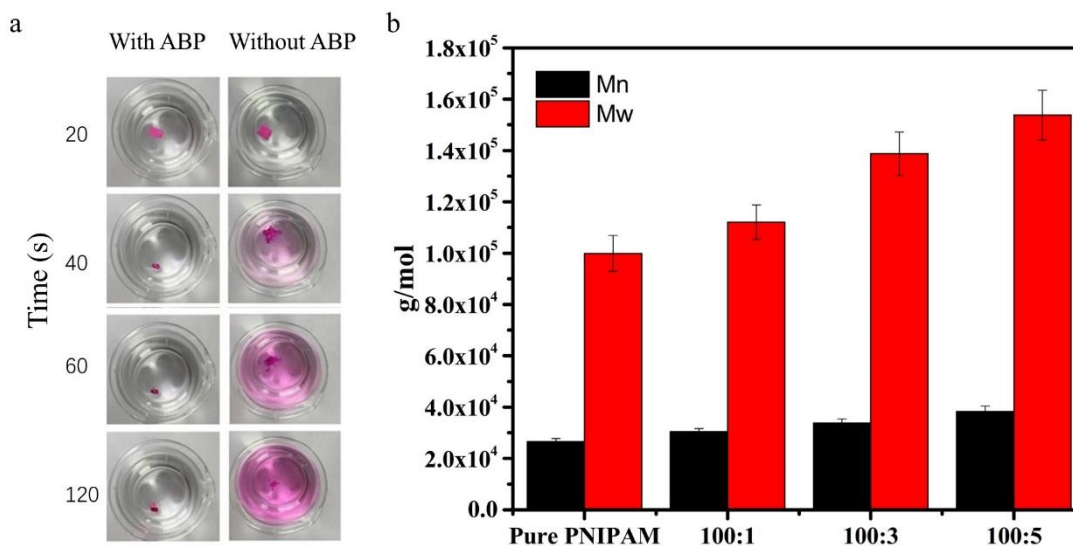


Figure 4.2 (a) The electrospun membranes obtained from p(NIPAM-ABP) and pure PNIPAM were immersed in water at 20 °C for given times. (b) Molecular weight of p(NIPAM-ABP) from different molar ratio between NIPAM and ABP.

4.4.3 Response behaviors of P(NIPAM-ABP) hydrogels

The hydrogels from copolymer with a monomer and ABP ratio of 100:3 was used for the investigation of volume change in response to temperature. The same trends were also observed for hydrogels from the copolymer with a monomer and ABP ratio of 100:1 and 100:5 (results not shown). By measuring the dimension changes of one sample at time intervals of 2 min., the thermal-responsive behaviors of hydrogels were studied. The as-spun samples were dipped in water at 20 °C for 5 min, a contraction in both length and width could be observed clearly. After transferring the samples to 40 °C water, both the length and width were observed to shrink further (Fig. 4.3a-3a"). However, the thickness of hydrogels in swollen state was observed to be much higher in comparison with as-spun membrane (4 times). Even for the shrunk state, it was observed to be still thicker than the original membrane (2 times) (Fig. 4.3b-b"). More details are provided in Fig. 4.3c-3c'. The swelling ratios were normalized with the original size of samples (as-spun nanofibers mats), while the de-swelling ratios were normalized with the size of fully swollen

samples to show the contraction capability of the hydrogels. Fig. 3c shows the dimension change for hydrogels in water at a temperature of 20 °C. Both length and width decreased rapidly in the beginning, slowed down after 2 min and reached an equilibrium after 5 min; while the increase in thickness happened simultaneously. The exposure of fully swollen hydrogels to water at a temperature of 40 °C induced a slight decrease in thickness and a higher degree of contraction was found in planar direction (Fig. 4.3c').

In fact, the swelling and de-swelling in both planar and thickness directions is a balance between the movement or relaxation of stretched fibers and the swelling of the polymer chains.^[223] The former leads to contraction in planar direction and the latter results in the expansion in thickness. Due to the specific layer-by-layer micro-structure of randomly oriented electrospun fibers, the contact points existing along the thickness direction are much more than those along the planar direction^[224]. This means the space between fibers is larger along planar direction in comparison with that along the thickness direction. When swelling, the fibers ‘prefer’ to swell homogeneously in both planar and thickness directions. However, the voluminous inter-fiber space reduces the overall expansion along the planar direction. Correspondingly, when the temperature goes above LCST, the dehydration of the polymer makes the hydrogels shrink more in the planar direction.^[225]

Interestingly, it was reported by Wang et al. that in comparison with original size, the length and width of their electrospun PNIPAM fibers mats increased in water at 20 °C.^[89] The increase in thickness direction is consistent with our results; while the increase in planar direction is opposite to ours. This could result from the balance between the fibers swelling and the inter-fibers space. Specifically, the swelling of fibers always tends to fill the inter-fibers space first. Thus, depending on the balance of the swelling degree (which is dictated by the properties of the copolymer) and the inner space of the hydrogels (which is determined by the density of the electrospun membrane), the swelling could be increased or decreased along the planar direction.

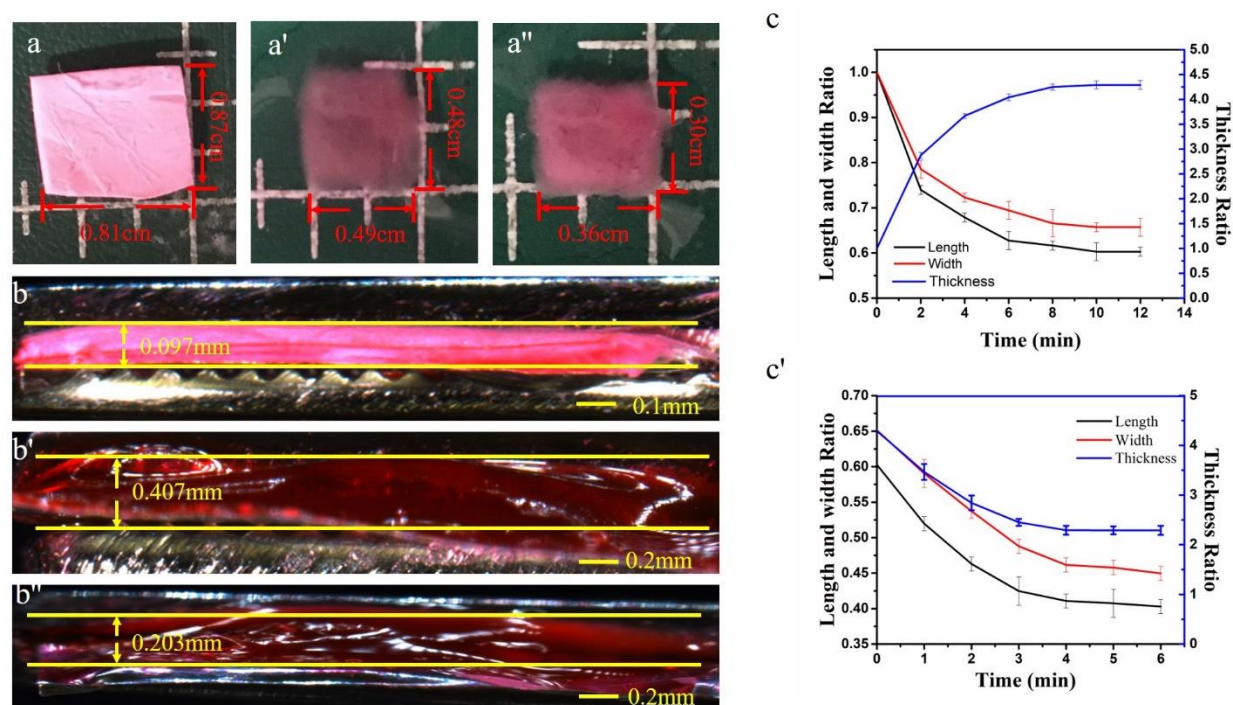


Figure 4.3 Thermal responsive behaviors of hydrogels with respect to dimensions. Length and width for sample as-spun (a), fully swollen (a') and fully shrunk (a''). Membrane thickness in as-spun (b), fully swollen (b') and fully shrunk (b'') states. The dimension change of hydrogels at temperatures of 20 °C (c) and 40 °C (c').

The swelling and de-swelling ratios and rates of P(NIPAM-ABP) hydrogels in terms of hydrogels weight are illustrated in Fig. 4.4. In addition, the effect of sample thickness and the ratio between NIPAM and ABP for the copolymer are also shown. The swelling ratios reflect the weight of the swollen hydrogel water uptake at a given time vs. the weight of the as-spun membrane. Whereas, the de-swelling ratio means the weight of water remaining in the contracted hydrogel at a given time vs. the weight of water in the fully swollen hydrogel. The swelling and de-swelling ratios at equilibrium, along with the response rate, are regarded as the most important properties of hydrogels and widely studied for various responsive hydrogels.^[226]

The effect of membrane thickness on response rate was investigated using electrospun membranes with thickness of 0.1, 0.3, 0.5 and 0.7 mm, for both swelling and de-swelling, respectively (Fig. 4.4 a, b). In both processes, the thickness showed negligible impact on the swelling and de-swelling ratio at equilibrium. The membrane with higher thickness always response slower than that with

smaller thickness. But the difference is not significant in comparison with PNIPAM based hydrogel films, which normally respond at least 10 times slower for thicker samples.^[227]

The influence of crosslinker ratios were studied with hydrogels in both swelling and de-swelling tests (Fig. 4.4 c, d). For hydrogels with higher ABP ratio, they responded more slowly in both swelling and de-swelling processes. Lower swelling and de-swelling ratios at equilibrium states were also found. These results are consistent with those of Yao et al.^[226] who used nanoclay (Laponite XLG) together with photoinitiator (1-hydroxy-cyclohexylphenylketone, Irg. 184) to polymerize NIPAM monomer under UV in an iced water bath. In addition, the de-swelling ratio here represents the relative value by weight of water kept in contracted hydrogels vs. that of hydrogels in swollen state.

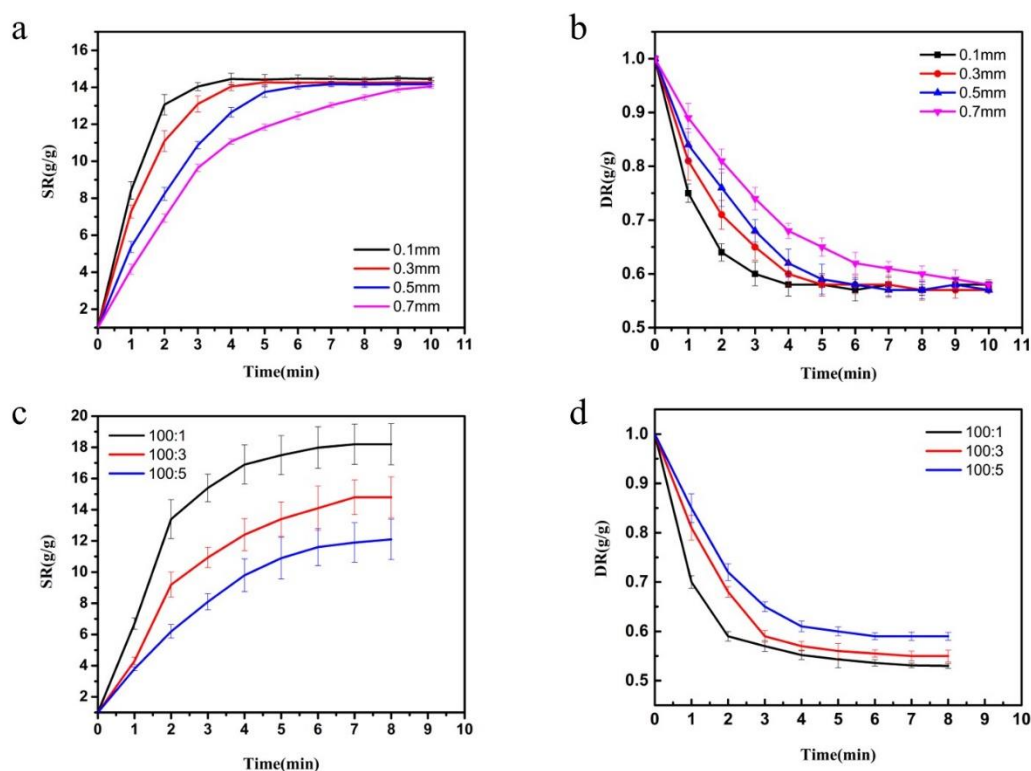


Figure 4.4 Thermal-responsive behaviors of P(NIPAM-ABP) hydrogels with respect to swelling and de-swelling ratios. The influence of original membrane thickness on the swelling (a) and de-swelling (b) ratios for hydrogels from copolymer with NIPAM: ABP=100:3. The effect of

crosslinker ratios on swelling (c) and de-swelling (d) ratios for hydrogels with original membrane thickness of 0.5mm.

4.4.4 Rheological characterization and compression tests

The viscoelasticity of hydrogels with different crosslinker ratios was also investigated through small-amplitude oscillatory shear (Fig. 4.5 a, b) in both shrunk and swollen states. For hydrogels at all crosslinker ratios, 8 times or higher increase in both storage and loss moduli were noticed in the shrunk state (Fig. 4.5b) compared with the swollen state (Fig. 4.5a). The storage modulus (G') was always much higher than loss modulus (G''), indicating a solid-like character. In addition, the influence of crosslinker was more significant on the storage modulus (G') of hydrogels in shrunk states (Fig. 5b) in comparison to that in swollen states (Fig. 4.5a). Specifically, at 0.1 rad/s, the storage modulus (G') for hydrogels in shrunk states was 54 Pa with the highest crosslinker ratio (100:5) and 30.9 Pa with the lowest crosslinker ratio (100:1). In contrast, the corresponding values in swollen states were 17.2 Pa and 8.4 Pa respectively. These results show that the crosslinker ratio has more effect on the strength of hydrogels in shrunk states, which is consistent with our results from the upcoming compression tests.

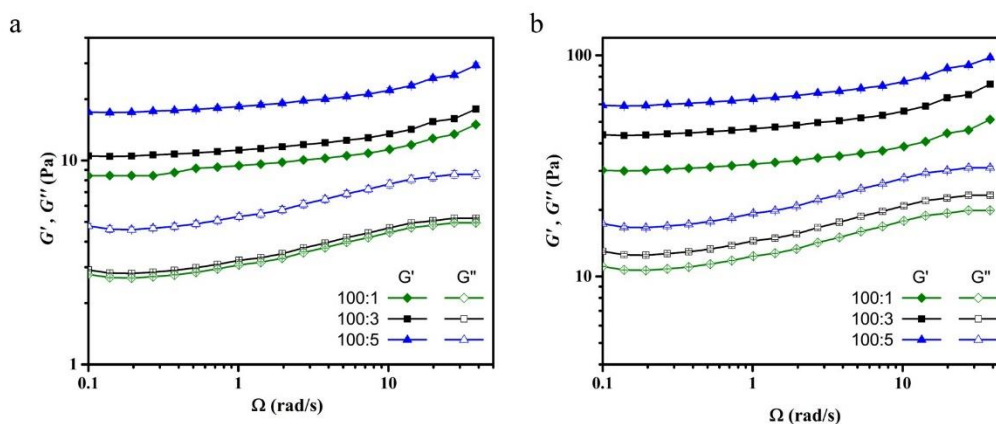


Figure 4.5 Rheological characterization for hydrogels from copolymers with crosslinker ratios of 100:1, 100:3 and 100:5 in fully swollen (a) and shrunk (b) states.

The hydrogel samples from copolymer with NIPAM:ABP ratio of 100:1, 100:3 and 100:5 was also characterized in compression using a rheometer in both fully swollen and shrunk states.

The hydrogel from copolymer with crosslinker ratio of 100:3 was first characterized in the compression test. The stress-strain curve was similar to a previous work done by Puleo et al.^[67] They synthesized the PNIPAM hydrogels with 1.2 mol% N,N-methylenebis(acrylamide) MBAAM as crosslinker and compressed their hydrogels. They reported an elastic response behavior for strains within 30% deformation under a crosshead speed of 1 mm/min. In our case, the compression elastic modulus E_c was calculated for up to 30% deformation in both fully swollen (Fig. 4.6a) and shrunk states (Fig. 4.6b). The values obtained were 2.9 kPa and 6.1 kPa respectively. The same tests were performed on hydrogels from P(NIPAM-ABP) with crosslinker ratios of 100:1 and 100:5 (Fig. 4.6c). It was found that the compression elastic modulus of the hydrogels in fully shrunk state were always higher than those in fully swollen state, which is within expectation. Besides, the difference was more significant for shrunk hydrogels when the ratio of ABP increased. This is in accordance with the results of equilibrium swelling and de-swelling ratios discussed earlier (Fig. 4.4 c, d). For the hydrogels with all three crosslinker ratios, their capability of swelling more than 10 times (Fig. 4.4c) leads to a similar elastic modulus in fully swollen state. On the other hand, crosslinking was the main factor in compression test when most water was expelled from hydrogels in the shrunk state.

In addition, the VPTT of the hydrogels was determined using the compression tests (Fig. 4.6d). It was found that the VPTT decreased from 28.2°C to 25.2 °C when increasing the ratio of ABP from 100:1 to 100:5. Since the hydrophilicity of ABP is lower than for NIPAM, the incorporation of ABP to NIPAM led to a higher content of hydrophobic moieties than in pure PNIPAM. Thus, the volume phase transition temperature VPTT, which results from the balance between hydrophilic and hydrophobic moieties^[97], occurred earlier than in pure PNIPAM.

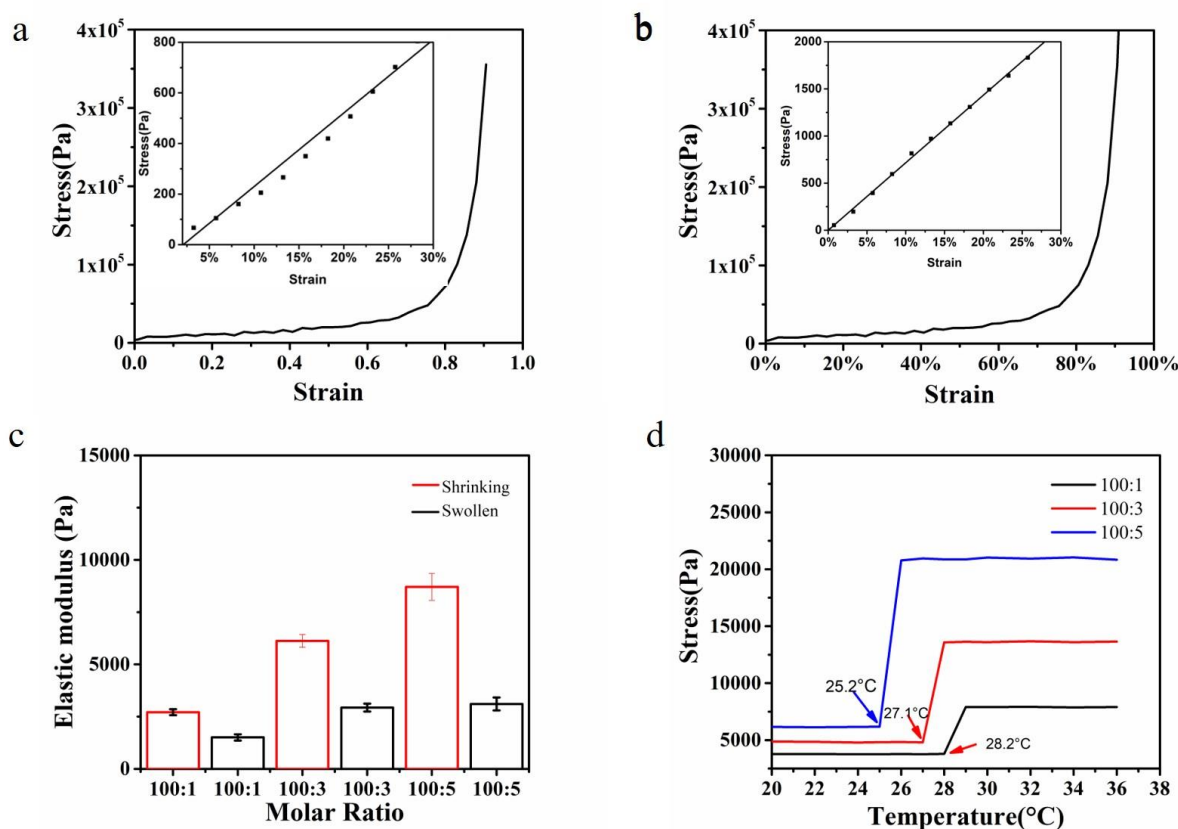


Figure 4.6 Compression tests for hydrogels in fully swollen (a) and shrunk (b) states. Inset: detail showing strains between 0% and 30%. The elastic modulus for hydrogels in both swelling and de-swelling states by compression test (c). Volume phase transition temperature (VPTT) of hydrogels from P(NIPAM-ABP) with crosslinker ratio of 100:1, 100:3 and 100:5 (d).

4.5 Conclusion

In summary, electrospinning was utilized to prepare P(NIAPM-ABP)-based hydrogels successfully with an excellent response rate/ratio and high mechanical strength. Specifically, in comparison with as-spun state samples, over 10 times swelling ratios were reached. Both swelling and de-swelling equilibrium were reached within a very short time. A higher ratio of crosslinker had a negligible impact on the response rate but significant influence on maximum swelling and de-swelling equilibrium ratios. Besides, the fibrous structure and fiber morphology were maintained very well after swelling/de-swelling for 20 cycles.

In terms of mechanical strength, results from both compression tests and rheological characterization showed that a higher ratio of crosslinker lead to higher strength for hydrogels in shrunk state but had less impact on the hydrogels in swollen state, which is due to their quite high swelling degree. A solid-like behavior was observed in both swelling and de-swelling equilibrium states under small amplitude (1%) and low angular frequencies (0.1-50 rad/s).

This approach not only improves the response rate and deformation degree for PNIPAM-based smart hydrogels prepared by electrospinning, but also provides criteria for the strength characterization of soft hydrogels. The influence of crosslinker on both responsive and mechanical properties was demonstrated. The methods developed in this work can be applied to build other stimuli-responsive hydrogels and perform corresponding characterization. These results are expected to accelerate related studies on highly promising applications for actuators, robotics, microsystems and architecture, among many others.

4.6 Acknowledgements

The authors acknowledge financial support from Natural Sciences and Engineering Research Council of Canada (NSERC) and the Canada Foundation for Innovation (CFI). We also thank Farhad Farnia, Chemistry Department, Sherbrooke University, Canada, for the help with synthesis of the crosslinker and Richard Silverwood, chemical engineering Department, Polytechnique, Canada, for the suggestions on paper writing. A scholarship is provided by the China Scholarship Council (CSC) to Y.H. Xu.

4.7 Support information

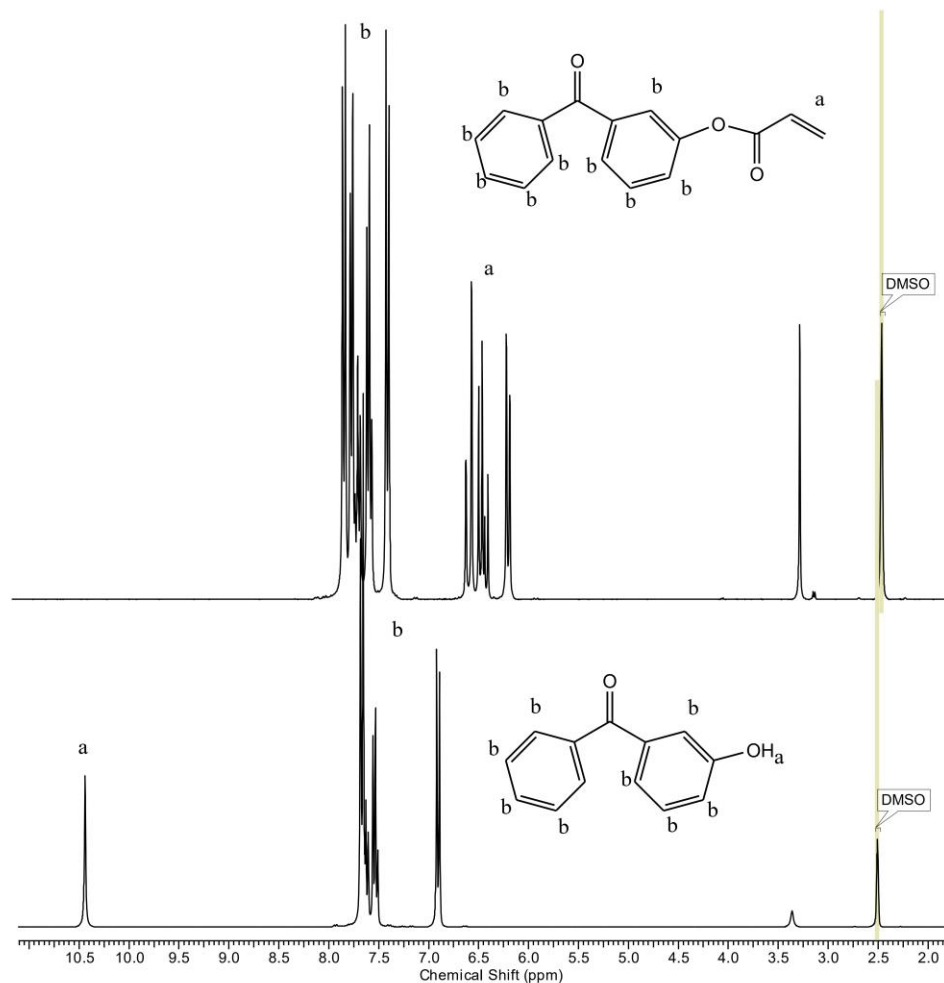


Figure 4.7 NMR results for 4-acryloylbenzophenone and 4-Hydroxybenzophenone

References

- [1] F. Natalia, G. Stoychev, N. Puretskiy, I. Leonid, V. Dmitry, *European Polymer Journal* **2015**, 68, 650.
- [2] E. A. Di Marzio, *Progress in polymer science* **1999**, 24, 329.
- [3] A. Alexander, J. Khan, S. Saraf, S. Saraf, *European Journal of Pharmaceutics and Biopharmaceutics* **2014**, 88, 575.
- [4] C. Yoon, R. Xiao, J. Park, J. Cha, T. D. Nguyen, D. H. Gracias, *Smart Materials and Structures*

2014, 23, 094008.

- [5] M. A. Haq, Y. Su, D. Wang, *Mater Sci Eng C Mater Biol Appl* **2017**, 70, 842.
- [6] B. P. Tripathi, N. C. Dubey, F. Simon, M. Stamm, *RSC Advances* **2014**, 4, 34073.
- [7] J. Höpfner, C. Klein, M. Wilhelm, *Macromolecular rapid communications* **2010**, 31, 1337.
- [8] X. Z. Zhang, C. C. Chu, *Journal of applied polymer science* **2003**, 89, 1935.
- [9] J. Djonlagić, Z. S. Petrović, *Journal of Polymer Science Part B: Polymer Physics* **2004**, 42, 3987.
- [10] K. Ito, *Polymer journal* **2007**, 39, 489.
- [11] P. Schexnailder, G. Schmidt, *Colloid and Polymer Science* **2009**, 287, 1.
- [12] F. Song, X.-L. Wang, Y.-Z. Wang, *Colloids and Surfaces B: Biointerfaces* **2011**, 88, 749.
- [13] D. N. Rockwood, D. B. Chase, R. E. Akins Jr, J. F. Rabolt, *Polymer* **2008**, 49, 4025.
- [14] Y. J. Kim, M. Ebara, T. Aoyagi, *Advanced Functional Materials* **2013**, 23, 5753.
- [15] J. Wang, A. Sutti, X. Wang, T. Lin, *Soft Matter* **2011**, 7, 4364.
- [16] S. Jiang, F. Liu, A. Lerch, L. Ionov, S. Agarwal, *Advanced materials* **2015**, 27, 4865.
- [17] G. Stoychev, N. Puretskiy, L. Ionov, *Soft Matter* **2011**, 7, 3277.
- [18] M. Liu, H. Su, T. Tan, *Carbohydrate Polymers* **2012**, 87, 2425.
- [19] R. Fei, J. T. George, J. Park, A. K. Means, M. A. Grunlan, *Soft Matter* **2013**, 9, 2912.
- [20] C. S. Wang, N. Virgilio, P. M. Wood-Adams, M. C. Heuzey, *Macromolecular Chemistry and Physics* **2018**.
- [21] S. Jiang, F. Liu, A. Lerch, L. Ionov, S. Agarwal, *Advanced Materials* **2015**, 27, 4865.
- [22] L. Li, Y. L. Hsieh, *Nanotechnology* **2005**, 16, 2852.
- [23] X. Jin, Y.-L. Hsieh, *Polymer* **2005**, 46, 5149.
- [24] C. Yao, Z. Liu, C. Yang, W. Wang, X.-J. Ju, R. Xie, L.-Y. Chu, *Advanced Functional Materials* **2015**, 25, 2980.
- [25] M. Liu, H. Su, T. Tan, *Carbohydrate polymers* **2012**, 87, 2425.
- [26] G. L. Puleo, F. Zulli, M. Piovaneli, M. Giordano, B. Mazzolai, L. Beccai, L. Andreozzi,

Reactive & Functional Polymers **2013**, 73, 1306.

CHAPTER 5 ARTICLE 2: FAST THERMAL RESPONSIVE HYDROGELS CONSISTING WITH ELECTROSPUN FIBERS WITH HIGHLY TUNABLE CONDUCTIVITY

Yinghao Xu, Abdellah Ajji[†] and Marie-Claude Heuzey[†]

Submitted: Polymer, 2020

[†]Department of Chemical Engineering, Research Center for High Performance Polymer and Composite Systems (CREPEC), Polytechnique de Montréal, 2900 Boulevard Edouard-Montpetit, Montréal, Quebec, Canada

Corresponding Author E-mail: Abdellah.ajji@polymtl.ca and marie-claude.heuzey@polymtl.ca

KEYWORDS: PNIPAM, hydrogel, electrospinning, conductivity

5.1 Abstract

In this paper, poly(N-isopropylacrylamide) based hydrogels consisting of electrospun nanofibers are fabricated and applied as hydrogel matrices to introduce doped poly(aniline) (PANI) via in-situ polymerization. Regardless of the PANI introduced, the fast thermal-responsive feature brought by the fibrous structure is maintained successfully. The continuous channel for electron transfer is provided by PANI located at fiber surfaces and inside fibers. The effect of PANI incorporated in hydrogel matrices on: 1) fiber morphology in both swollen and contracted states; 2) swelling/contraction capability of the hydrogels and 3) conductivity of the hybrid hydrogels are investigated. The electric conductive properties of this hybrid hydrogel vary consistently with its swelling degree in response to temperature alternation. Specifically, hybrid hydrogels with contents higher than 1.4 wt% PANI behave distinctly regarding resistance drop when contracted at 40 °C, in comparison with those with lower PANI proportion, which could be due to their highly fibrous structure. Subsequently, an evaluation system, aiming at general understanding and comparison of both conductive and responsive capabilities for these hybrid hydrogels, is established. This evaluation system is applied to forecast their potential applications based on corresponding thermal-responsive and conductive properties. Finally, a fibrous-structured hydrogel with excellent temperature responsive capability featuring tunable conductive properties is fabricated.

5.2 Introduction

Smart hydrogels, with stimulus-responsive and biocompatible characteristics, have received increasing attentions in recent years.^[1] Among them, poly(N-isopropylacrylamide) (PNIPAM) based temperature responsive hydrogels were investigated especially in drug-delivery field. This is mostly because it undergoes a reversible hydrophilic to hydrophobic transition at a temperature (32 °C) close to physiological human body temperature. The drawbacks of these kind of hydrogels are mainly related to their poor mechanical strength^[2] and slow response rate towards temperature changes.^[3] The first weakness is due to the large degree of swelling, thus few polymer chains but high water content in hydrogel domain.^[4] On the other hand, its slow response towards temperature change generally results from the poor mass transportation between the hydrogel matrix and the solvent, hence these hydrogels are reported to reach their swelling equilibrium after a few hours or days, depending on the size of the hydrogels.^[5] To improve their mechanical strength, interpenetrating polymer networks, multi-block polymer chains and addition of various nanoparticles were considered.^[6-8] Whereas, electrospinning and pores-forming protocol were applied to accelerate the response rate by increasing contact surface of hydrogels and solvent.^[9, 10]

However, most of the PNIPAM-based hydrogels are non-conductive, which limit their applications as electrochemical sensors, nerve electrodes, solar cells and electronic skins.^[11-14] Many efforts have been devoted to impart conductive properties to smart hydrogels by adding conductive particles, such as carbon nanotubes, metal particles, and graphite materials or by introducing conductive polymers, including polyaniline (PANI), polypyrrole, and polythiophene.^[15, 16] But a few problems remain unsolved, for example, the randomly distributed particles and poor interfacial compatibility between the various materials, which leads to unsatisfactory conductive properties and weaker mechanical strength of the hybrid hydrogels.^[15, 17]

In recent years, Shi et al. introduced PANI into PNIPAM-based hydrogels by in-situ reaction.^[17] A mesh-like structure was formed due to the presence of a dopant (phytic acid) to increase the conductivity of the hybrid hydrogels. In addition, they also reported that the mechanical strength of the hybrid hydrogels was improved by the PANI network. However, the PNIPAM-based hydrogels that served as the substrate were not optimally designed. They were neither fibrous nor

porous structured, which led to a slow response rate of the hybrid hydrogels. Alternatively, electrospinning is a robust technique to fabricate materials with fibrous and porous structures. Hydrogels consisting of electrospun fibers would possess excellent responsive properties, whereas PANI would presumably not affect both fibrous structure and response behaviours, although this hybrid system has never been investigated. Most importantly, how these fibrous structured hybrid hydrogels would perform regarding their resistance when they are swollen and de-swollen is of great interest.

Based on our previous work, we incorporated PANI into PNIPAM hydrogels consisting of electrospun fibers for the first time and developed a hybrid hydrogel with fast temperature responsive properties and reversible conductivity during swelling/contraction cycles.^[18] By controlling the concentration of the aniline (monomer of PANI), the proportions of PANI introduced into the hydrogels were tailored and the corresponding effect on hydrogel response behaviours was investigated (figure 5.1). Furthermore, the kinetics of hydrogels swelling and contraction were correlated to the resistance of the hydrogel's matrix. An evaluation system established in this study may be of great importance to forecast the potential applications of these fibrous-structured hydrogels based on their temperature responsive and conductive features, such as flexible electronics and smart switchers.^[19, 20]

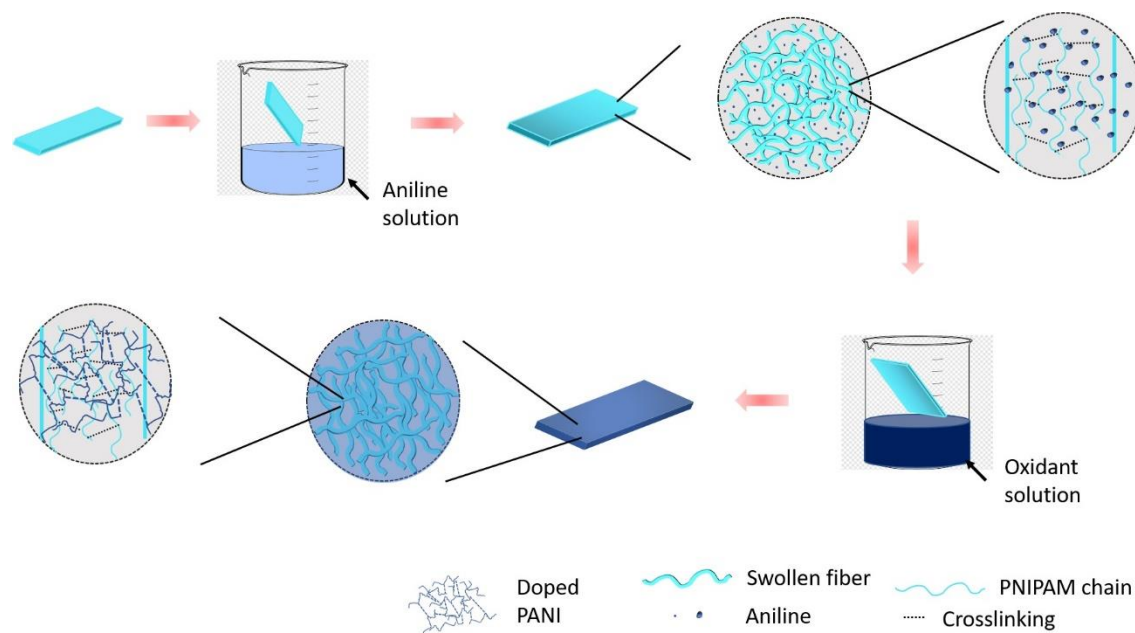


Figure 5.1 Schematics of the incorporation of PANI into PNIPAM fibrous hydrogels.

5.3 Results and discussions

5.3.1 Fibers morphology

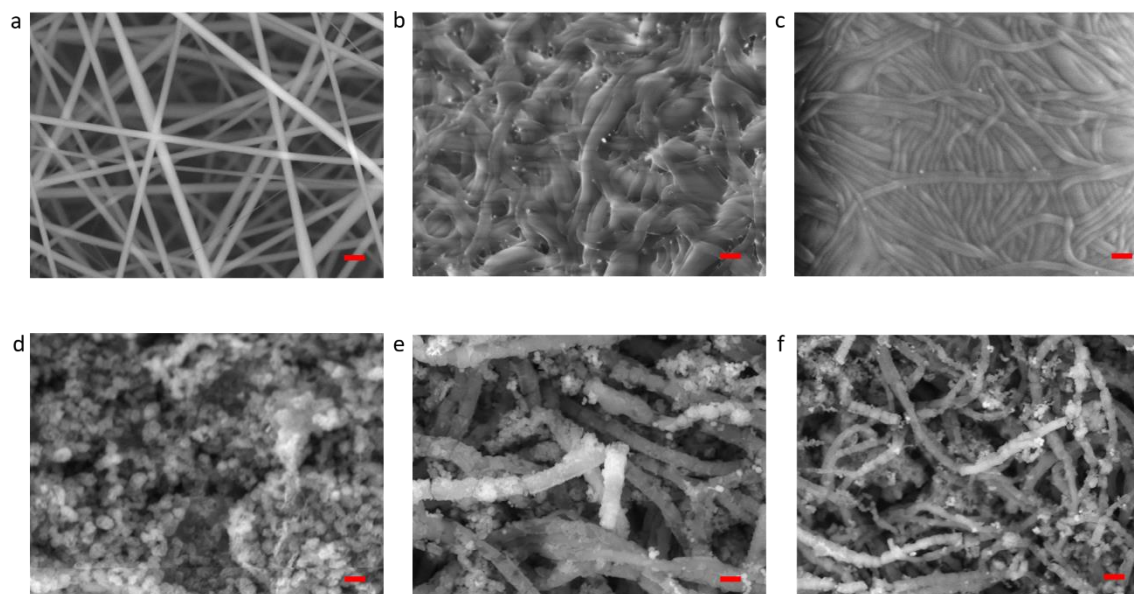


Figure 5.2 SEM images of electrospun fibers of neat PNIPAM in as-spun (a), swollen (b) and shrunken states (c); SEM images of hybrid hydrogels (with weight ratio: PNIPAM:PANI=100:1.44) before washing (d), after washing in swollen(e) and shrunken (f) states. The scale bar is 2 μm .

Figure 5.2 (a, b and c) show the morphology of electrospun fibers of neat PNIPAM in the as-spun, swollen and contracted states, respectively. The average fiber diameter increased from 0.37 μm to 1.84 μm after full swelling at 20 $^{\circ}\text{C}$ and all fibers were clearly seen twisted and banded. This significant change of fiber morphology was caused by the hydration of the fibers, which means simultaneously swelling and movement of fibers when in contact with water. The material, that was stretched to straight nanofibers during electrospinning, relaxed irreversibly when contacting water. After transfer to water at 40 $^{\circ}\text{C}$, almost all water absorbed was expelled out and a sharp drop (about 70%) in fibers average diameter was observed consequently.

Interestingly, the variation of fibers morphology can be more clearly observed after incorporation of PANI. After in-situ polymerization of PANI, the hybrid hydrogels were

covered by continuous PANI particles aggregates and/or agglomerates (Figure 5.2d). This morphological change makes sense considering the way PANI was introduced into the PNIPAM hydrogels. In the beginning, aniline and dopant (phytic acid) were introduced into PNIPAM hydrogels domains by swelling of the dried PNIPAM electrospun mats in solution of aniline and phytic acid. At this stage, aniline and phytic acid were present both inside the swollen nanofibers and in the space between them because they were introduced along with the solvent. In a second step, the fully swollen hydrogel was transferred to the solution of oxidant (APS) at 20 °C. Although the hydrogels could not swell further, the ongoing mass exchange between the hydrogel and APS solution continued due to the concentration gradient. In the hydrogel domain, the concentration of aniline and phytic acid is higher than that in APS solution and vice versa. As a result, a part of aniline and phytic acid transferred from hydrogels matrix to APS solution and some APS molecules diffused from solution to hydrogel matrix, simultaneously and in opposite directions.^[21] Once they are in contact with each other, the in-situ polymerization of PANI occurs, mostly at the surface of hydrogels where the oxidant and the monomer first meet.^[22] It was reported that the interface in contact with the aniline and oxidant is going to be coated with a thin polyaniline film after successful polymerization.^[23] In ideal conditions where sufficient mass exchange has taken place before the reaction is finished, a good polymerization level of PANI throughout the hydrogel domains could be expected.^[24] The PANI present in the space between fibers in the hydrogel matrix was successfully removed after 5 times washing, with each time a swelling/contraction cycle, thus the fibrous structure was recovered (Figure 5.2e). Obviously, the presence of PANI exerted significant influence on the smoothness of the nanofibers. However, it was difficult to have an accurate conclusion on PANI's effect on the average fibers diameter because the interface of each fiber was not clear anymore, especially in the swollen state (Figure 5.2e). Whereas for shrunken hybrid hydrogels, the fibers contracted showed an average diameter of 0.62 μm (Figure 5.2f), slightly higher than the fibers without PANI (0.41 μm in Figure 1c). This could result from the presence of PANI which is a non-thermally responsive material. When temperature increased, PANI hydrogels could not de-swell as much as PNIPAM, thus limiting the contraction of each fiber at 40 °C. However, the fibers did not

completely lose their thermal response capability, which suggests that PANI presence on the surface did not ‘fully cover’ the fibers. Water could still be absorbed and desorbed into fibers when they swell and de-swell, respectively.

5.3.2 Responsive behaviors

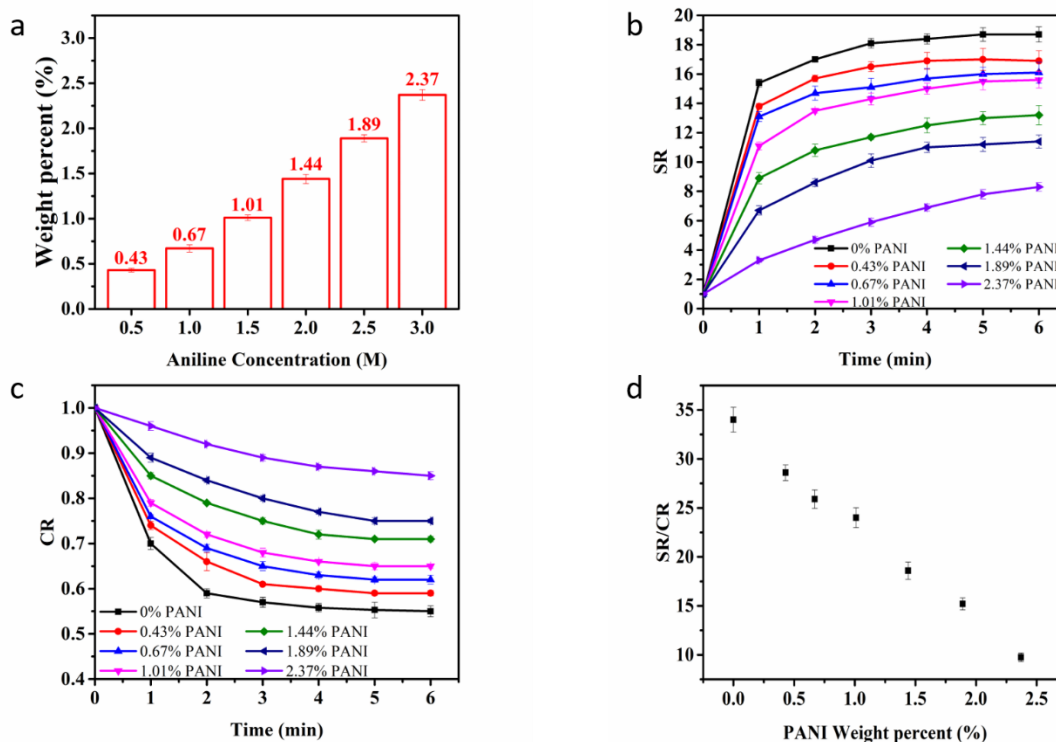


Figure 5.3 Effect of PANI on hydrogels response behaviours. Weight percent of PANI incorporated in hybrid hydrogels for various aniline concentrations (a); swelling behaviours of hybrid hydrogels (b); contraction behaviours of hybrid hydrogels (c); effect of PANI on hydrogels equilibrium swelling/contraction ratio (d).

The effect of PANI incorporated in hybrid hydrogels on its thermal responsive capability was investigated. Before washing, the hybrid hydrogels were solid-like without temperature responsive swelling/contraction right after the reaction. Since the PANI filled up the space between fibers in hydrogel domain, there is no room for fibers to swell when being in contact with water at 20 °C.^[17] However, the temperature responsive capability of this

hybrid hydrogel was successfully recovered after removing most of PANI present in hydrogel domain after 5 times swelling/contraction washing.

As is shown in Figure 5.3a, the weight percent of PANI incorporated was calculated by measuring the weight of dried samples before and after incorporation of PANI. The results confirmed that most of the PANI was preserved in the hydrogel domain and the loss of PANI was not significant with increasing aniline concentration. This suggests an excellent mass exchange inside and outside each fiber during PANI polymerization. A poor mass exchange could lead to a shell-like structure that could prevent further reaction in fibres.^[23] In that scenario, the unreacted aniline could re-dissolve afterwards and the amount of PANI incorporated in hydrogels would reach a plateau with increasing aniline concentration. In our case, the highest and lowest percent of PANI incorporated were around 2.4% and 0.5% respectively.

Then all the after-washing hybrid hydrogels with various PANI proportion were investigated in terms of temperature responsive behaviors. The swelling and contraction kinetics are shown in Figure 3b and 3c. When swelling (Figure 5.3b), the hybrid hydrogels with less than 1% PANI swelled as fast as the one without PANI. Whereas the only difference lies in the swelling equilibrium, they swelled slightly less compared with pure PNIPAM hydrogels. This is because the swelling of PANI is lower than PNIPAM, which means the higher amount of PANI in hydrogels, the lower the maximum swelling ratio the hybrid hydrogel can reach. For the hydrogels with 1%~2% PANI, they appeared to swell slower and reaching equilibrium 1 minute later in comparison with hydrogels with less than 1% PANI. The most significant effect was observed for the hydrogels with 2.37% PANI, not only in response rate but also in the much lower equilibrium swelling ratio. Other than all other samples, the one with most PANI content swelled slowly until equilibrium, at constant rate. As for the maximum swelling ratio, it was halved with 2.37% PANI compared with hydrogels without PANI. Considering the weight percent of PANI in hybrid hydrogels was only 2.37%, this significant drop indicated the presence of PANI constrained the swelling of PNIPAM fibers. Similar results were observed for hydrogels contraction in Figure 5.3c: the incorporation of PANI decreased the equilibrium contraction ratio and from

proportion of 1.44%, PANI would start to exert negative impact on hydrogels contraction rate.

The influence of PANI on hydrogels responsive capability was evaluated (Figure 5.3d). The hydrogels responsive capability was interpreted as the maximum swelling ratio divided by maximum contraction ratio. A higher value represents better responsive ability, which means this hydrogel could swell to higher degree in water at 20 °C and de-swell to a lower degree in water at 40 °C. As shown in Figure 2d, the higher PANI weight percent, the lower the responsive capability. For example, the hydrogels with 2.37% PANI swelled the least and most of the water remained when de-swelling, thus leading to the lowest value.

5.3.3 Conductive behaviours

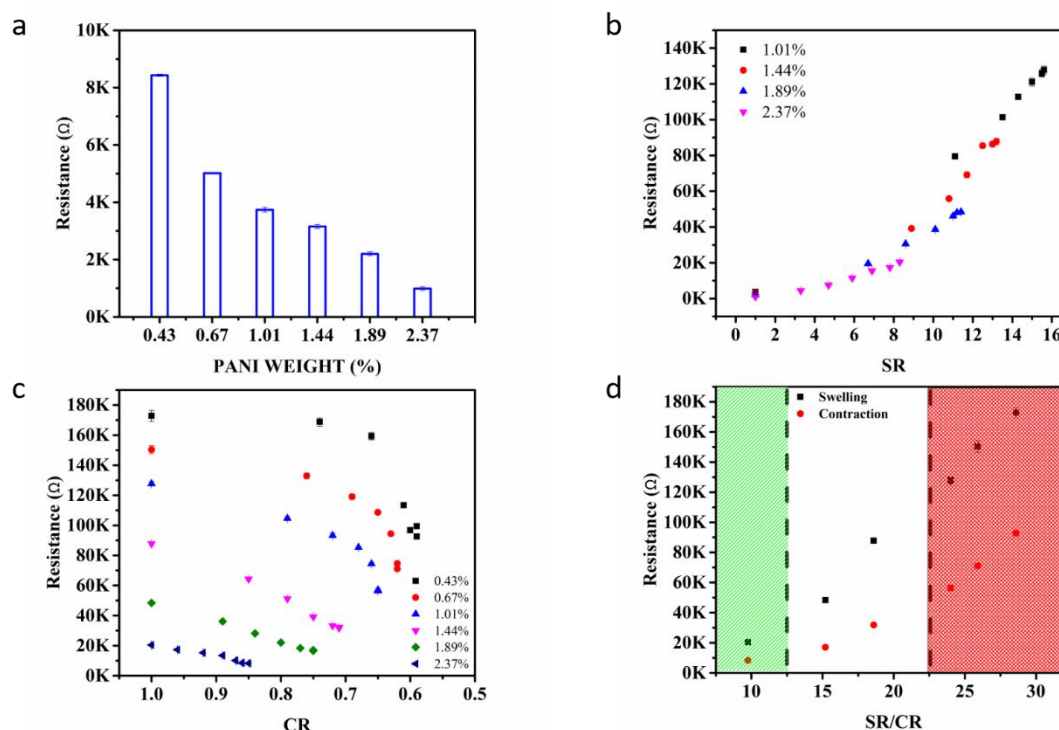


Figure 5.4 The electric resistance of hydrogels in swelling and contraction. The electric resistance of dried samples with various amount of PANI (a); the resistance of hydrogels with PANI when swelling (b); the resistance of hydrogels with PANI when contracting (c); the correlation of hydrogels resistance with responsive properties when swelling and contracting(d).

The resistance of the hybrid hydrogels was then investigated in dried, swollen and contracted states. In all our conductivity tests, resistance instead of conductivity was measured because the dimensions of hydrogels varied with time during swelling and contraction. It is thus difficult to correlate real-time resistance with the corresponding hydrogels dimensions to have accurate results of conductivity.

The washed hybrid hydrogels were dried at room temperature under vacuum until constant weight. Then the resistance of each sample was measured by electrometer with two flat pliers connected to the edges of samples at a fixed distance. The electrical resistance results of these dried samples are shown in Figure 5.4a. As the PANI was introduced and polymerized in PNIPAM hydrogels in fully swollen state, PANI was distributed all over the fully extended hydrogels matrix. When dried, the space left by evaporated water was narrowed and the PANI that was separated before had more chances to get closer to each other, thus, building more channels for electrons to pass through to achieve higher conductivity (lower resistance). Apart from the sample with 0.43 wt% PANI, all dried samples showed good conductive properties (resistance below 5 k Ω). Whereas the samples with the highest PANI content presented an excellent conductivity, with resistance below 1 k Ω .

We studied the correlation between resistance and the swelling ratio of the hybrid hydrogels. As the hydrogels with less than 1 wt% PANI swelled too fast to obtain more data within 1~10 times swelling due to manipulations difficulty, Figure 5.4b shows only the results for samples with higher content than 1 wt% PANI (full results are provided in support information S1). The resistance for each hydrogel was recorded at corresponding swelling ratio. It is significant that all samples showed strong positive correlation between resistance and swelling ratio, which suggests that electrons paths were reduced smoothly with the expansion of the hydrogels. Another interesting phenomenon was that the resistances of the samples increased at different rates along with increasing swelling ratio. Specifically, the resistance for hydrogels with more PANI rose slower with hydrogel swelling, which suggests the structure for electrons transfer was preserved better. However, the hybrid hydrogels with higher swelling degree (>12 times) illustrated that PNIPAM was able to break up the constraint of PANI structure and swelled further. Thus, the slopes for resistance

increased as the structure for electrons transfer was collapsed more quickly with further swelling.

However, the conductive properties of these hydrogels performed distinctly when contracting hybrid hydrogels with high and low PANI content (Figure 5.4c). For the hydrogels containing 0.43 wt%, 0.67 wt% and 1.01 wt% PANI, there were significant drops in terms of resistance when they contracted below 0.7, in contrast, their resistance remained stable in the beginning of contraction (1.0~0.8 times). This suggests that a critical point in de-swelling ratio may exist and for which electron transfer channels cannot be built rapidly and effectively when above it; whereas the resistance drops significantly once the hydrogel de-swells further below this critical point. But for hydrogels with higher content (>1%) of PANI, this critical point was not reached as their resistance kept decreasing continuously with contraction of hydrogels. Even for the slopes of resistance curves for hydrogels with 1.44 wt %, 1.89 wt% and 2.37 wt% PANI, there were no obvious difference observed.

It is an interesting phenomenon that the same hybrid hydrogels with different PANI proportions behaved distinctly when contracting regarding their conductive property. To understand the mechanism behind, we propose the de-swelling ratio of 0.7 as a critical point for the hydrogels containing 0.43 wt%, 0.67 wt% and 1.01 wt% PANI. These hydrogels were able to swell to relative high degree, so more PANI on fibers was detached from each other and more space left between fibers at that high swelling ratio. Therefore, we see no obvious resistance drop as very few electron transfer paths were recovered at the beginning of contraction. Whereas hydrogels with higher content of PANI (1.44 wt%, 1.89 wt% and 2.37 wt%) would swell less, under which condition more PANI was able to remain in contact. Therefore, their resistance kept dropping constantly because the electron transfer paths increased constantly when the hydrogel de-swelled to reduce the intra-space of the hydrogel domain. From the above speculations, the proportion of PANI on fibers that remained continuous would determine the way their conductivity changes when the hybrid hydrogels are contracted.

Based on the results above, we have built an evaluation system for these hybrid hydrogels regarding their conductive capabilities with consideration of their temperature responsive properties, as shown in Figure 5.4d. For hydrogels with all PANI proportions, those in

contraction states always showed better conductivity than corresponding swollen states. The higher the responsive ability (SR/CR value), the higher the resistance in both swollen and contraction states, which means their conductivity decreased. Another interesting and significant point was that the resistance difference gaps between each sample in the swollen and contraction states were wider with increasing hydrogel responsive capabilities (SR/CR value). This illustrates that they are capable to show significant differences in terms of resistance just by swelling/contraction depending on temperature.

Taking all discussions above into considerations, we propose a criteria to predict the potential applications for these fibrous structured hydrogels with thermal-responsive and conductive properties as follows: 1) for hybrid hydrogels with SR/CR less than 15 (green zone of figure 5.4d), they show excellent conductive properties in both swollen and contraction states with very close resistance. These materials are ideal alternatives for applications in flexible electrodes and soft electronics fields.^[25] 2) For fibrous hydrogels with excellent responsive properties (SR/CR>20, red zone of figure 5.4d), they are capable of both swelling and contracting to very high degree and demonstrate significant differentiation in these states in terms of the resistance. These materials could be applied for applications in sensor and smart switchers fields.^[26, 27] 3) Between these two zones, which could be called ‘blank zone’, which means both the conductive property and responsive capability of these hydrogels could be finely tuned for specific requirements. Although all these conclusions are drawn only from the results of PNIPAM/PANI fibrous hydrogels system, this evaluation system that combine the thermal-responsive capability and conductive properties is not limited to this model.

5.4 Conclusions

In summary, fibrous structured PANI-PNIPAM hydrogels with phytic acid as dopant obtained via in-situ polymerization have been successfully fabricated. The fibrous structure of the hybrid hydrogels was well maintained in both swollen and contraction states. The tunable conductive properties have been introduced by PANI addition to this material without sacrificing its temperature-responsive capability. The resistance of hybrid hydrogels varied highly consistently with their corresponding swelling and contraction

degree. Especially for contraction, the resistances of hydrogels with high and low PANI proportions were found to drop in different ways due to the fibrous structure. The correlation between the conductive and thermal-responsive properties was further investigated to propose an evaluation system for this type of hydrogels. The potential applications for these hybrid hydrogels with various PANI proportions are proposed based on these evaluation results. In addition, the possibility of introducing other conductive materials, either polymer and/or nanocomposite to this fibrous structured PNIPAM hydrogels may be considered.

5.5 Experimental

5.5.1 Materials

The following materials were used as received from Sigma Aldrich (Canada): N, N'-dimethylformamide (DMF) (99.8%), ammonium persulfate (APS) and phytic acid. Azobisisobutyronitrile (AIBN) (Aldrich) was recrystallized from ethanol and N-isopropylacrylamide (NIPAM) (Aldrich) was recrystallized from n-hexane before use, respectively. The preparation of crosslinker ABP(4-acryloylbenzo-phenone) and photo-crosslinkable P(NIPAM-ABP) (NIPAM:ABP = 98:2 molar ratio) was the same as in our previous report.¹⁸ The deionized water (DI) used for the conductivity tests was obtained from Barnstead Easypure II Purification System.

5.5.2 Electrospinning

To produce nanofibers, P(NIPAM-ABP) was dissolved in DMF at a concentration of 40 %wt. The applied voltage on the needle (outer diameter: 0.6 mm) was 24 kV; the flow rate was fixed to 0.3 mL/h and the distance between the needle and collector was 20 cm. All fibers were collected on a grounded metal plate. The obtained fibers mats were dried under vacuum overnight to remove any residual solvent. By controlling the volume of solutions, electrospun membranes with original thicknesses of 0.2 mm were obtained.

5.5.3 Hybrid hydrogels preparation

The electrospun mats were placed under a home-made UV-treatment device for 2 h to conduct crosslinking. A small piece of electrospun mats was cut (2 cm x 1 cm) and immersed into deionized water (DI) at room temperature for swelling. Then the fully swollen hydrogel was transferred to DI at 40 °C to obtain a hydrogel in the shrunken state. Subsequently, the shrunken hydrogel was moved to a pre-cooled (4 °C) solution containing phytic acid (50%, w/w in water), aniline and DI to re-swell again. At the final step, the swollen hydrogel loaded with phytic acid and aniline was moved into a pre-cooled (4 °C) APS solution and the container was kept at 4 °C using an ice bath for 10 min until the solution turned from light brown to dark green. The hybrid hydrogels were washed by DI 5 times to remove excess phytic acid and unattached PANI that remained in the space between fibers in the hydrogel domain.

5.5.4 Conductivity measurements

The resistance of the hybrid hydrogel samples was measured by a Keithley 6517A electrometer connected to a Keithley 8009 test fixture (Keithley Instruments, USA) under a voltage of 5 V. The electric resistance of the hydrogels was measured by applying two flat pliers, which were connected to the electrometer, on two sides of the hydrogel matrix. As swelling and contraction are highly reversible, all the resistance results presented here were repeated 5 times. Although the measurements were performed with a 2-point technique instead of 4-point, we believe these results are reliable and can support our conclusions.

5.6 Supporting Information

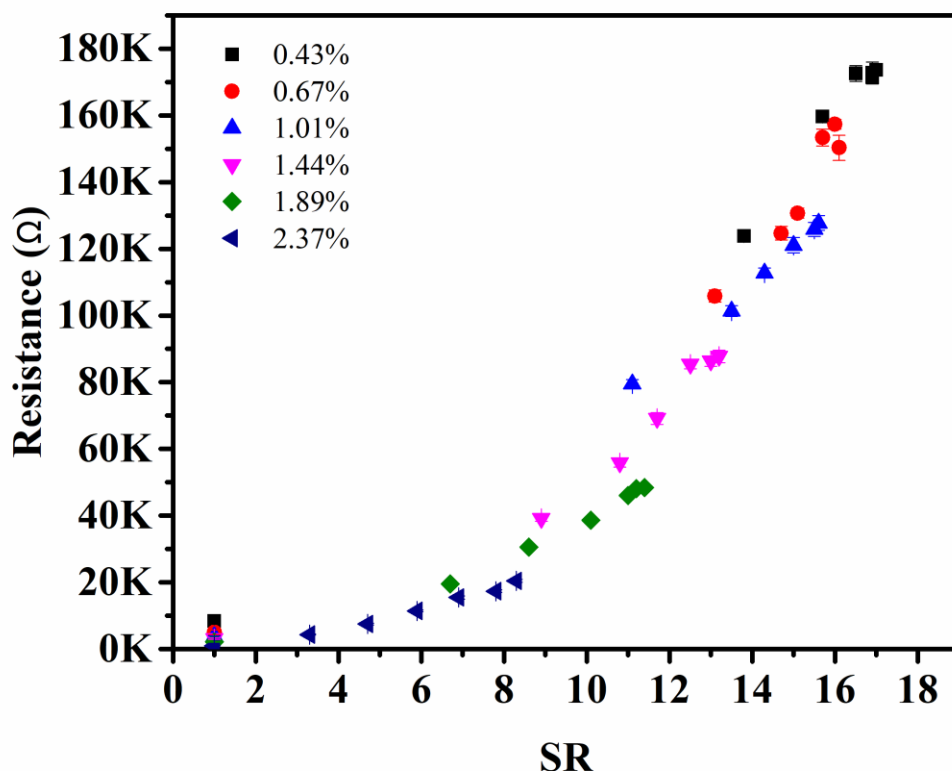


Figure 5.5 The resistance of hydrogels with all PANI weight percent when swelling.

5.7 Acknowledgements

The authors acknowledge financial support from Postgraduate Scholarship Program of China Scholarship Council Natural Sciences and Engineering Research Council of Canada (NSERC) and the Canada Foundation for Innovation (CFI). We also thank Hanan Abdali, Chemical Engineering Department, Polytechnique Montreal, Canada, for the suggestions on PANI polymerization.

References

- [1] P. Chakraborty, P. Baire, B. Roy, A. K. Nandi, ACS applied materials & interfaces 2014, 6, 3615.
- [2] M. A. Haq, Y. Su, D. Wang, Mater Sci Eng C Mater Biol Appl 2017, 70, 842.
- [3] X. Z. Zhang, C. C. Chu, Journal of applied polymer science 2003, 89, 1935.

- [4] S. Jiang, F. Liu, A. Lerch, L. Ionov, S. Agarwal, *Advanced materials* 2015, 27, 4865.
- [5] L. Liu, A. Ghaemi, S. Gekle, S. Agarwal, *Advanced Materials* 2016, 28, 9792.
- [6] G. Puleo, F. Zulli, M. Piovaneli, M. Giordano, B. Mazzolai, L. Beccai, L. Andreozzi, *Reactive and Functional Polymers* 2013, 73, 1306.
- [7] F. Alsubaie, A. Anastasaki, P. Wilson, D. M. Haddleton, *Polymer Chemistry* 2014, 6, 406.
- [8] N. Singh, L. A. Lyon, *Chemistry of Materials* 2007, 19, 719.
- [9] H. Okuzaki, K. Kobayashi, H. Yan, *Synthetic metals* 2009, 159, 2273.
- [10] K. Depa, A. Strachota, M. Šlouf, J. Hromádková, *European Polymer Journal* 2012, 48, 1997.
- [11] L. Li, Y. Shi, L. Pan, Y. Shi, G. Yu, *Journal of Materials Chemistry B* 2015, 3, 2920.
- [12] D. N. Heo, S.-J. Song, H.-J. Kim, Y. J. Lee, W.-K. Ko, S. J. Lee, D. Lee, S. J. Park, L. G. Zhang, J. Y. Kang, *Acta biomaterialia* 2016, 39, 25.
- [13] Q. Li, Q. Tang, L. Lin, X. Chen, H. Chen, L. Chu, H. Xu, M. Li, Y. Qin, B. He, *Journal of Power Sources* 2014, 245, 468.
- [14] N. N. Jason, M. D. Ho, W. Cheng, *Journal of Materials Chemistry C* 2017, 5, 5845.
- [15] L. Liu, S. Luo, Y. Qing, N. Yan, Y. Wu, X. Xie, F. Hu, *Macromolecular rapid communications* 2018, 39, 1700836.
- [16] J. Wu, Q. e. Zhang, A. a. Zhou, Z. Huang, H. Bai, L. Li, *Advanced Materials* 2016, 28, 10211.
- [17] Y. Shi, C. Ma, L. Peng, G. Yu, *Advanced Functional Materials* 2015, 25, 1219.
- [18] Y. Xu, A. Ajji, M.-C. Heuzey, *Polymer* 2019, 183, 121880.
- [19] M. Tahhan, V.-T. Truong, G. M. Spinks, G. G. Wallace, *Smart materials and structures* 2003, 12, 626.
- [20] B. Mutharani, P. Ranganathan, S.-M. Chen, *Sensors and Actuators B: Chemical* 2020, 304, 127232.
- [21] K. Sharma, V. Kumar, B. Chaudhary, B. Kaith, S. Kalia, H. Swart, *Polymer Degradation and Stability* 2016, 124, 101.
- [22] J. Stejskal, *Chemical Papers* 2017, 71, 269.
- [23] S. Fedorova, J. Stejskal, *Langmuir* 2002, 18, 5630.
- [24] N. V. Blinova, M. Trchová, J. Stejskal, *European polymer journal* 2009, 45, 668.

- [25] D.-W. Wang, F. Li, J. Zhao, W. Ren, Z.-G. Chen, J. Tan, Z.-S. Wu, I. Gentle, G. Q. Lu, H.-M. Cheng, ACS nano 2009, 3, 1745.
- [26] N. V. Lavrik, M. J. Sepaniak, P. G. Datskos, Review of scientific instruments 2004, 75, 2229.
- [27] J. Liu, J. Liu, F. Ma, J. Liu, ACS Applied Polymer Materials 2019, 1, 152.

CHAPTER 6 ARTICLE 3: TUNABLE TWO-STEP SHAPE AND DIMENSIONAL CHANGES WITH TEMPERATURE OF PNIPAM/CNCS HYDROGEL

Yinghao Xu, Abdellah Ajji[†] and Marie-Claude Heuzey[†]

Submitted: Macromolecules, 2020

[†]Department of Chemical Engineering, Research Center for High Performance Polymer and Composite Systems (CREPEC), Polytechnique de Montréal, 2900 Boulevard Edouard-Montpetit, Montréal, Quebec, Canada

Corresponding Author E-mail: Abdellah.ajji@polymtl.ca and marie-claude.heuzey@polymtl.ca

KEYWORDS: PNIPAM, CNC, hydrogel, electrospinning, shape-change

6.1 Abstract

PNIPAM (poly(N-isopropylacrylamide)), a well-studied thermo-responsive polymer, undergoes conformational transition around 32 °C. On the other hand, cellulose nanocrystals (CNCs), as a promising and biocompatible material, is barely introduced into PNIPAM-based fibrous hydrogel system. CNCs' impact on hydrogels temperature responsive behaviors, either in single layer or bilayer hydrogel systems, is still awaiting to be investigated. In this work, stable well dispersed PNIPAM/CNCs suspensions (with various CNCs proportion) are prepared and electrospun into nanofiber membranes. Corresponding hydrogels are then obtained via UV-induced crosslinking. CNCs are found to exert significant constraint effect on hydrogels swelling when it exceeded 5 wt% but negligible effect for contraction. The difference between hydrogels with various CNCs proportion regarding their temperature responsive behaviors is utilized to fabricate bilayer hydrogels. These bilayer samples are capable of generating 3D geometries at first time contacting water via anisotropically swelling between two layers and changing their dimension reversibly in following swelling and contraction. In addition, these geometries are found to be highly tunable via finely tuned thickness ratio between two layers. This promising feature would significantly extend the application of these materials in tissue engineering where a controllable geometry of the culture substrate is of great importance.

6.2 Introduction

Smart materials, also called stimuli-responsive, are materials with at least one property that changes in response to at least one stimulus, including changes in temperature, light, mechanical stress, or environmental pH.^[228] Large number of smart materials are based on polymers, which derive their responsive character from the responsive molecular moieties and/or groups.^[229] Among all stimuli-responsive polymers, poly(N-isopropylacrylamide), known as PNIPAM, or PNIPAAm is a well-studied thermo-responsive polymer that has a lower critical solution temperature (LCST) of 32 °C.^[230] PNIPAM chains undergo a conformational transition from extended state below the LCST to dehydrated contracted state above the LCST.^[231] This critical feature allows its wide application on human cells or tissue engineering and drug delivery field.^[232]

Aiming at improving the functionality of these stimuli-responsive polymers, a strategic incorporation of nanomaterials has attracted increasing attention recently.^[230] For instance, biomacromolecules or proteins have been conjugated to smart polymers to achieve better bioactivity.^[170] Inorganic nanoparticles, like gold, have also been reported to be incorporated into smart polymer matrices, introducing tunable optical properties.^[171] Because most of the potential application of PNIPAM would be in the biological field, any nanomaterials to be introduced have to be biocompatible. Cellulose nanocrystals (CNCs) meet these requirements perfectly and can be easily surface modified with functional groups with specific functionality.^[172] They can be obtained from natural wood, agricultural waste, cotton, bacteria, and tunicate.^[233-235] Thus, they are naturally biocompatible and biodegradable. The morphologies of obtained CNCs were reported as rods, spheres, and network,^[236] depending not only on their origin but also on their extraction method, like acid hydrolysis, sonochemical fragmentation, microbial or enzymatic

digestion.^[174, 175] A few efforts have been made to incorporate CNCs into PNIPAM, either by grafting technique or by polymerization of NIPAM in CNCs suspensions. For example, Zubik et al. synthesized a CNC-g-PNIPAM thermo-responsive hydrogel, and the mechanical strength was improved by increasing amount of CNC.^[183] Zoppe et al. have synthesized PNIPAM brushes grafted from CNCs via living radical polymerization and applied this system as a switchable stabilizer for water-in-oil Pickering emulsions.^[180] Most of these efforts were about grafting CNC to PNIPAM or the reverse route where the CNC serve as a platform to introduce other functional groups or moieties.

However, CNC's other desirable feature as a reinforcement nanofiller, was neglected when incorporated into PNIPAM-based materials, even though it has been used in other nanocomposite systems.^[237] Specifically, how CNC would reinforce PNIPAM-based hydrogels, when introduced to a fibrous-structured system, was never investigated before. Especially, the influence of molecular interaction between PNIPAM and CNCs on temperature responsive behaviors of fibrous hydrogels is thus of our great interest. In addition, how the reinforced hydrogel would perform in a bilayer hydrogel system regarding temperature-induced deformation is missing in current studies.

Here, a stable well-dispersed CNC/PNIPAM suspension system was prepared and electrospun into nanofibers mats which were then crosslinked under UV to fabricate hydrogels. Materials consisting of PNIPAM and various CNC proportions were electrospun into collector sequentially to build bilayer structure samples. The hydrogels' fabrication steps are shown in **Figure 6.1**. The influence of CNC on electrospinnability and hydrogels temperature responsive properties was investigated. Subsequently, the reinforcement effect of CNC on hydrogels was also studied regarding 3D deformation of the CNC/PNIPAM hydrogels with bilayer structure. Finally, the

relationship between hydrogel geometries and thickness ratio between two layers was investigated in both swollen and contracted states.

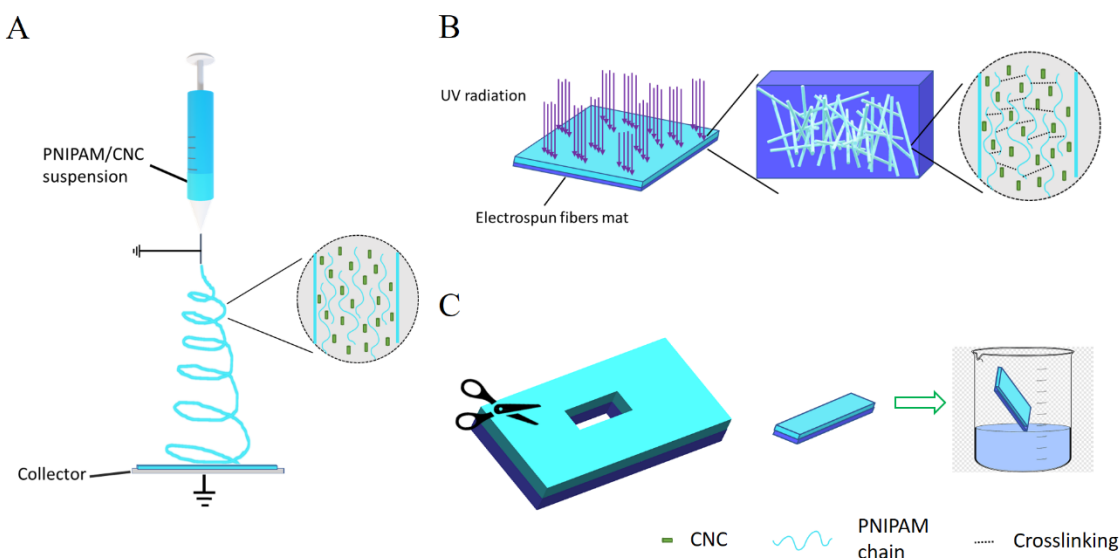


Figure 6.1 Schematics of building bilayer structured hydrogels using PNIPAM and CNC via electrospinning and UV-induced crosslinking. Specifically, A) the electrospinning of PNIPAM/CNC suspension, with insert illustrating PNIPAM and CNC molecules in single fiber; B) the obtained bilayer electrospun fibers mat were exposed under UV light for crosslinking, with insert showing that the crosslinking occurs between PNIPAM chains; c) cutting samples from fibers membrane (with length and width of 1 cm and 0.5 cm, respectively) and immersing in water to fabricate bilayer structured hydrogels.

6.3 Results and discussions

6.3.1 Fibers morphology

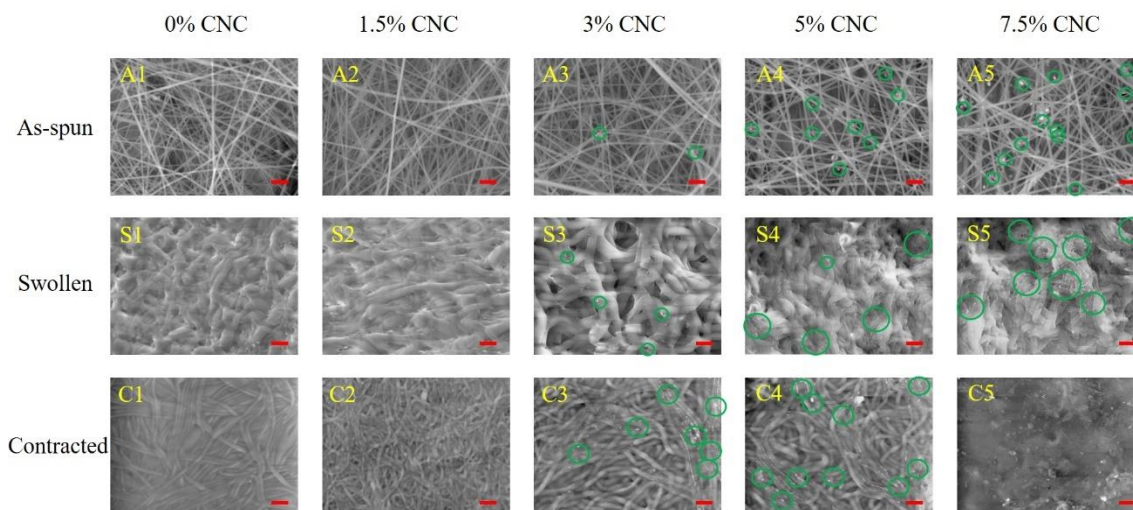


Figure 6.2 Electrospun fibers morphology in as-spun (A1~A5), swollen (S1-S5) and contracted (C1-C5) states with various CNC proportion (0%, 1.5%, 3%, 5% and 7.5%). Scale bars are 2 μm .

Table 6.1 Average fiber diameters for samples in as-spun, swollen and contracted states

	0% CNC	1.5% CNC	3% CNC	5% CNC	7.5% CNC
As-spun (μm)	0.16 ± 0.04	0.17 ± 0.07	0.14 ± 0.05	0.14 ± 0.06	0.15 ± 0.08
Swollen (μm)	1.74 ± 0.1	1.53 ± 0.14	1.47 ± 0.18	1.08 ± 0.14	0.74 ± 0.11
Contracted (μm)	0.34 ± 0.01	0.27 ± 0.01	0.33 ± 0.02	0.25 ± 0.01	X

CNCs' influence on fibers morphology was first investigated on 'single-layer' samples. The fibers morphology of all samples, either in as-spun state or dried from swollen/contracted hydrogels, was

observed under SEM (**Figure 6.2**) and the corresponding fibers diameters were measured and reported in **Table 6.1**. By the incorporation of 1.5 wt% of CNC, no significant morphological variation was observed in all three states (Figure 6.2. A2, S2 and C2). CNC exerted negligible influence on fibers morphology and average fibers diameters (Table. 1). However, starting from 3 wt%, the influence of CNCs was noticeable for samples in as-spun, swollen and contracted states. The ‘white dots’ highlighted by green circles could be the CNCs, which were located around fibers either independently or mixed with PNIPAM. Because these white dots only appear in SEM images for samples with CNC proportion above 3%. These particles could be detached from PNIPAM/CNCs suspension during electrospinning under electrical field. Thus, they had a different flight path, compared with ‘mainstream’ suspension, arriving on the collector. This could be the reason that more and more ‘white dots’ were seen at higher CNC content (Figure 6.2. A3-A5).

On the other hand, CNCs imposed their influence differently for swollen and contracted fibers, respectively, at temperature of 20 °C and 40 °C. When swelling, a trend of decline in terms of fibers diameters was shown for samples with 3 wt%, 5 wt% and 7.5 wt% CNCs (Figure 6.2. S3-S5). Apart from those ‘white dots’ present between fibers, other CNCs that were retained inside fibers showed great constraint effect for every fiber. In comparison with those fibers with 3 wt% CNCs, the ones with 7.5 wt% CNCs swelled much less, with average fibers diameter reduced ~55% with respect to those with 3 wt%. This interesting phenomenon could result from the following mechanisms: 1) inter-molecular interactions between PNIPAM and CNCs inside every fiber which are mostly hydrogen bonds; 2) intra-molecular effect among CNCs getting stronger with more CNCs content. Specifically, the hydrogen bond formed between CNCs and PNIPAM would occupy the reactive sites that were originally for water molecules.^[230] Therefore, less water content could be included in hydrogels domain. Another less significant factor would be the network

formed among CNCs which serves as a framework to hinder PNIPAM chains movement, including hydrogen bonds forming between PNIPAM and water molecules.^[230] However, this may not be a dominant factor as the CNCs were kept below 10 wt%. Unlike neat CNCs suspension where strong interaction can be generated with concentration as low as 5 wt%,^[238] the interaction among CNCs in this composite system would be much weaker as they are isolated by the main component PNIPAM. In our case, the impact of CNC' interaction was only observed at a concentration of 7.5wt%, which is discussed in the following paragraph.

For fibers contraction, CNCs showed much less impact than for swelling. Fibers contracted to almost the same level for samples with 0 wt%, 1.5 wt%, 3 wt% and 5 wt% CNCs. In theory, PNIPAM molecules undergo a conformational coil to globule transition around its LCST (32 °C) where the hydrophilic component in PNIPAM molecules turn from 'active' to 'inactive' states.^[231] This conformational transition leads to hydrogen bonds breaking not only between PNIPAM and water molecules but also between PNIPAM and CNCs. The actual situation illustrated in Figure 6.2 (C1-C4) confirmed the inference above, CNCs did not obstruct the conformational transition of PNIPAM when temperature increased to 40 °C. Almost all water molecules and CNCs were detached from PNIPAM chains. Otherwise, an increase in fibers diameters would be observed with higher CNCs weight percent because of the insufficient dehydration of the PNIPAM chains. On the other hand, the network formed by CNCs imposed significant influence morphologically on samples with 7.5 wt% CNC (Figure 6.2 C5). All fibers lost their boundary and no fibers were observed anymore, which could be explained by the network forming of CNCs among the sample. With sufficient CNCs content, the network could form among not only outside fibers but also between those located around the boundaries of some fibers. Thus, edges between fibers were eventually invisible.

We also tried suspensions with higher CNCs proportion (15 wt%) for electrospinning, but the strong effect brought by CNCs exerted negative impact on electrospinnability. Those samples underwent a combination of electrospinning and electrospray (Figure 6.1).

6.3.2 Hydrogel responsive behaviors

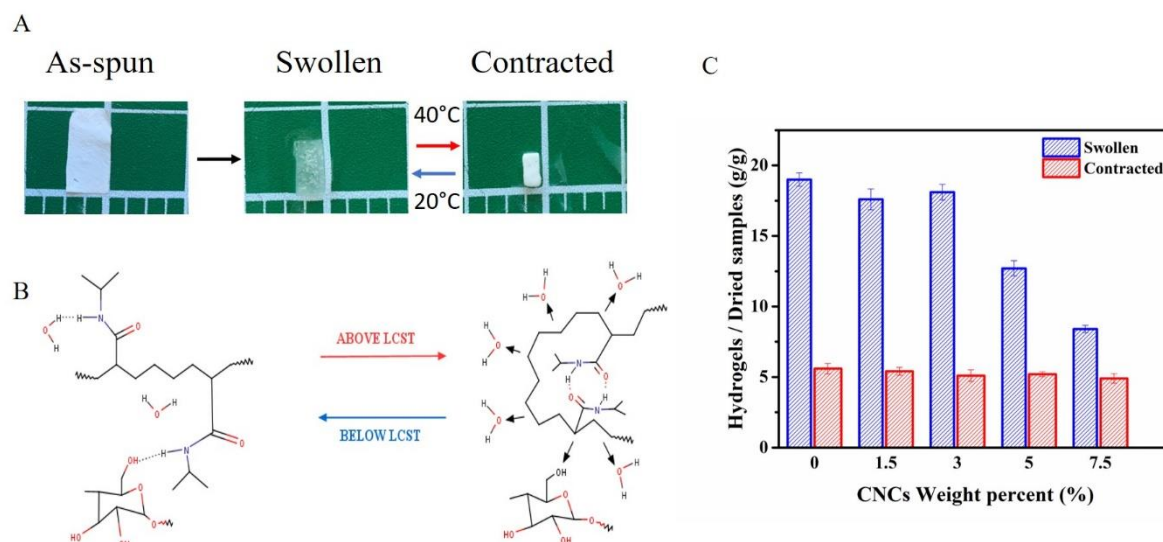


Figure 6.3 A) Schematic of ‘single layer’ hydrogels (with 1.5wt% CNCs) swelling and contraction; B) Conformational transition of PNIPAM in presence of CNCs and water molecules; C) Weights of hybrid hydrogels in swollen (blue bars) and contracted states (red bars).

The PNIPAM/CNCs hydrogel weights at swelling and contraction equilibrium were then checked.

Figure 6.3A shows how single-layer samples change from as-spun state to fully swollen and then fully contracted. Both hydrogels with and without CNCs showed similar behaviors: once these as-spun samples were immersed in water at 20 °C, all fibers contacted water and swell until equilibrium within seconds, then fully contracted when temperature increased above 32°C (LCST) within seconds. Interestingly, although the samples reached full swelling, their surface area reduced to 60% of the corresponding surface area of the original samples. This could result from the fibrous and porous structure of the electrospun membrane. When contacting water, all fibers swelled and were closer to each other to fill the hydrogel’s inner space, thus their surface area reduced even if

a swelling equilibrium was reached.^[239] The volume of hydrogel domain could only increase when all inner space was occupied and fibers continue to swell further. When temperature was higher than the LCST of PNIPAM, these hydrogels contracted and the surface area decreased further to 40% of the original samples, which was caused by the fiber's contraction. Thirty swelling/contraction cycles were carried out and no further swelling/contraction were observed for all hydrogels. The molecular effect and conformational transition are illustrated in Figure 6.3B. At temperatures below LCST, the hydrophilic amide ($-\text{CONH}-$) was exposed to water molecules and hydrogen bonds were established between them.^[240] However, with the presence of CNCs, hydrogen bonds could also form between the hydroxyl group ($-\text{OH}$) from CNC and amide ($-\text{CONH}-$) group from PNIPAM, thus reducing the number of hydrogen bonds with water molecules. Once temperature increased above LCST, the PNIPAM chains underwent a conformational change (coil-to-globule) where the amide groups were surrounded by its isopropyl domains and failed to expose to water molecules.^[241] The establishment of inner-molecular hydrogen bonds would result in hydrogen bonds breaking with water molecules and CNCs.

CNCs influence on hydrogels swelling and contraction regarding the hydrogel weights was investigated (Figure 6.3C). For hydrogels at swollen equilibrium, CNCs showed less significant effect when CNC weight percent was less than 3%, as these hydrogels were able to swell to approximately the same level (18 times weight to dried samples). When CNCs proportion continued to rise, their constraining effect eventually appeared. Specifically, with 5 wt% CNCs, these PNIPAM/CNCs hydrogels swelled to ~70% weight of those hydrogels containing less than 5 wt% CNCs. This value further dropped to ~50% for hydrogels with 7.5 wt% CNCs. This is consistent with our previous results of fibers average diameters. However, CNCs did not exert much influence on hydrogels when contraction, even for those with higher than 3 wt% CNCs

proportion. Considering CNCs proportion was below 10 wt% for all samples, CNCs chains are less likely to be bonded to PNIPAM chains to hinder the PNIPAM's conformational change around its LCST. Otherwise, the interaction between CNCs and PNIPAM chains would lead to insufficient conformational transition which means there will be a few hydrophilic amid group exposed to water molecules. In this case, some hydrogen bonds would be retained between PNIPAM and water/CNCs molecules. The hydrogel weights would rise with higher content of CNCs in hydrogels when contract at 40 °C.

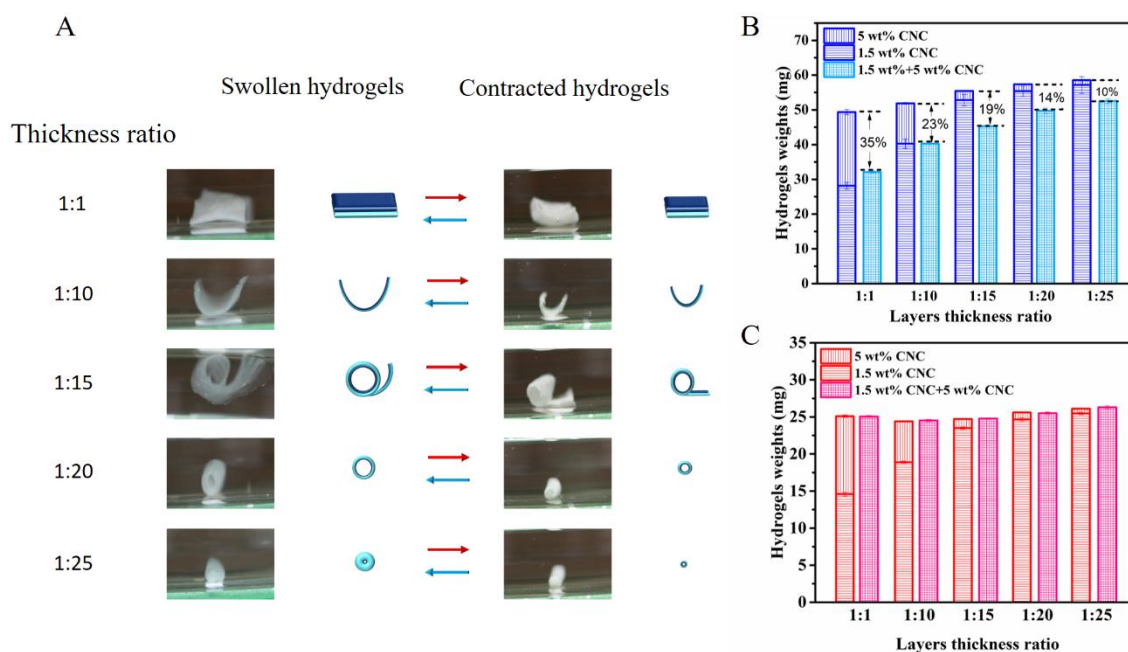


Figure 6.4 (A) geometry of bilayer hydrogels with thickness ratios in swollen and contracted states; weights comparison of swollen (B) and contraction (C) hydrogels among the bilayer hydrogels with thickness ratios and the sum of corresponding two separate layers.

Then the hydrogels with 1.5 wt% and 5 wt% CNCs were selected to fabricate bilayer samples with various thickness ratios. They were chosen because of the discrepancy between them is most significant in their temperature responsive behaviors, which is the most important factor to be considered when preparing bilayer hydrogels with the capability to complete complicated 3D

deformation.^[242] In all bilayer samples, the layer with 5 wt% CNCs would serve as the less ‘active’ layer and the one with 1.5 wt% CNCs acted as more ‘active’ layer, according to the above results. Thus, the thickness ratio of the less ‘active’ layer to that of the more ‘active’ layer was set as 1:1, 1:10, 1:15, 1:20 and 1:25. The geometries of these bilayer hydrogels are shown in Figure 6.4A. With the thickness of 1:1, no obvious 3D deformation was observed as these bilayer hydrogels formed a plate-like geometry. When the thickness of the layer with 1.5 wt% CNCs increased to 10 times to that of 5 wt% CNCs, the sample folded from its long-side and generate a ‘semi-tube’ shape. At thickness ratio of 1:20 (layer with 5 wt% CNCs: layer with 1.5 wt% CNCs), an integral tube was obtained by hydrogels’ continuous folding. These hydrogels folded further into a tighter tube at the thickness ratio of 1:25.

With the aim of verifying if either layer was constrained when swelling and contraction, the weights of the bilayer hydrogels were compared with the corresponding weights of the two separate layers at both swelling (Figure 6.4B) and contraction states (Figure 6.4C). For all swollen bilayer hydrogels (light blue bars), their weights were less than corresponding sum of two separate hydrogels (dark blue bars). These interesting results suggested either one of them or both layers were limited or constrained when hydrogels were swelling. Specifically, with thickness ratio of 1:1, the weight of bilayer hydrogels was reduced the most (~35% less) compared with the sum of the weights of the corresponding two single layer hydrogels. This drop suggested that the layer with better swelling capability (the one with 1.5 wt% CNCs) was constrained significantly, almost to the same level of what the layer with 5 wt% CNCs could reach. Thus, a cuboid shape without 3D deformation was obtained at this thickness ratio. However, these gaps were narrowed with increasing the thickness ratio of the layer with 1.5 wt% CNC, which means the constraint was overcome gradually to swell to higher degree. Because of this swelling difference between the two

layers, these hydrogels started to fold into 3D geometry,^[243] like semi-tube, tube, and double folded tube in our case. Here, for all these bilayer hydrogels, 3D geometries were generated by the anisotropic swelling of the two layers system for the first time the as-spun samples contacted water at 20 °C.

Interestingly, these 3D geometries formed by bilayer hydrogels were retained well after contraction instead of restoring to their original geometries which were bilayer films in as-spun states. The unfolding phenomenon did not occur as expected for these tubes or semi-tubes when contraction. In theory, all these 3D geometries brought by swelling should be reversible to their original film-like shape since CNCs did not exert significant influence on hydrogels' contraction regardless of their weight percent. However, these hydrogels with 3D geometry contracted isotropically. This may be explained by the weight comparison between bilayer hydrogels and the sum of the corresponding two layers hydrogels when they were contracted (Figure 6.4C). For hydrogels with either 1.5 wt% CNCs or 5 wt% CNCs, no matter they were combined into bilayer hydrogels or in single layers, they contracted to the same level. There was no expansion or enlargement force generated from either layer, as both layers contracted to alter their original geometry obtained in swollen states.^[244] Another factor that may also contribute to this interesting phenomenon was that all samples were more solid-like when contraction, which would be more difficult to alter their shape as compared with when they were in swollen state.

6.3.3 Deformation characterization

Thanks to the significant swelling difference between the hydrogels with 1.5 wt% and 5 wt% CNCs, the bilayer structured hydrogels fabricated from these two layers were able to illustrate 3D deformation.^[245] These geometries of bilayer hydrogels were highly reversible between swelling

and contraction states (**Figure 6.5**). In addition, the curvatures of these hydrogels' geometries were found to be tunable via the finely tailored thickness ratio between two layers.

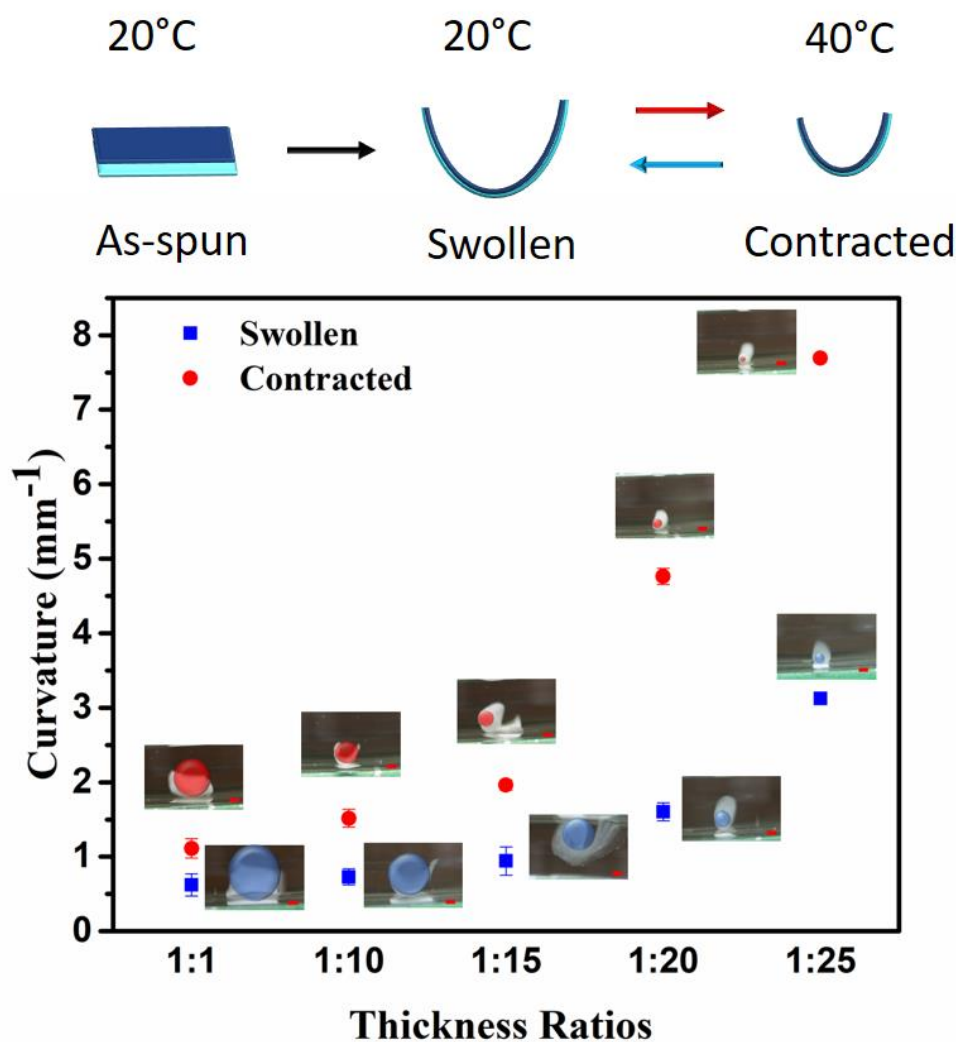


Figure 6.5 Curvatures of bilayer hydrogels in swollen (blue squares) and contracted (red circles) states with tunable thickness ratios. Inserts were pictures for corresponding hydrogels with scale bar of 1 mm.

First, curvatures for both swollen and contracted hydrogels illustrated exponential growth with increasing thickness ratio of layer with 1.5 wt% CNCs. Beginning from thickness ratio of 1:1, the curvatures of hydrogels geometry were 0.6 mm^{-1} for swollen state and 1.1 mm^{-1} for contracted

state. The difference was not significant as both geometries were almost cuboid with very little curvature. At the highest thickness ratio of 1:25, curvatures climbed to 3.1 and 7.7 mm⁻¹ for swollen and contracted tubes respectively. Specifically, significant jump occurred from the thickness ratio of 1:20, at which ratio hydrogels started forming integral tube geometry. Under this ratio, the internal space formed by these hydrogel tubes was relatively small when swelling but was reduced to almost zero when contracted. And curvatures raised further for thickness ratio of 1:25, in both swollen and contracted states, as tubes folded very tightly in both swollen and contracted states. On the other hand, the difference between tube curvatures in swollen and contracted states widen with the increasing ratio of the layer with 1.5 wt% CNCs. This illustrated that the layer with 1.5 wt% CNCs was capable of swelling more with increasing thickness ratio, which is consistent with our previous results. Thus, the corresponding bilayer hydrogels folded more tightly, which leads to higher curvatures when swelling.

In addition, these bilayer hydrogels' isotropic contraction and swelling enable highly reversible dimensional change at 40 °C and 20 °C respectively. Under our experimental conditions, 50 swelling/contraction cycles were conducted and both hydrogel geometries and corresponding curvature results were highly reproducible. We believe the geometry of hydrogels in swollen and contraction states will remain stable even after hundreds of cycles. Interestingly, all these bilayer samples fabricated with 1.5 wt% and 5 wt% CNCs, regardless of thickness ratio, presented anisotropic swelling at the first time contacting water at 20°C to form 3D geometries. Then these 3D geometries illustrated isotropic swelling and contraction behaviors between 20 °C and 40 °C, which was highly reversible. This irregular two-step temperature response behavior was caused by the interesting interaction between PNIPAM and CNCs. Specifically, small proportion of CNCs (5 wt% or less) exerted significant influence on PNIPAM's swelling but negligible impact for

contraction under the cooperation of PNIPAM's conformational transition and hydrogen bonds with CNCs.^[230]

6.4 Conclusions

Temperature responsive PNIPAM/CNCs hydrogels with fibrous structure were fabricated via electrospinning and UV-induced crosslinking. Up to 7.5 wt% of CNCs was successfully incorporated into hydrogels due to the limitation of suspension's electrospinnability and electrospun fibers morphology. CNCs' constraining effect was significant on hydrogels swelling but negligible on contraction. The large difference between hydrogels with 1.5 wt% and 5 wt% CNC when they swell (more swelling with 1.5 wt% CNC) was utilized to build bilayer structured hydrogels with various thickness ratios. 3D geometries were formed via anisotropic swelling when they were immersed in water at 20 °C. These geometries remained stable after 50 swelling/contraction cycles and underwent only reversible dimensional change via isotropic shape-change. The curvatures of these 3D geometries were compared among those in swollen and contracted states and were found to be tunable via finely tailored layer thickness ratios. To our best knowledge, this is the first time that CNCs was introduced into PNIPAM-based fibrous hydrogels and exerted its impact on hydrogels' temperature responsive behaviors. The interaction between CNCs and PNIPAM was utilized to design bilayer hydrogels with unique temperature responsive behaviors to form 3D geometries. The two steps temperature-dependent shape and dimensional change (anisotropic to isotropic) of these bilayer hydrogels also were never reported before. Unlike most studies about PNIPAM-based hydrogel actuators which mainly served as tunable manipulators or grippers, the PNIPAM/CNCs hydrogels with bilayer and fibrous structure are particularly suitable for applications in cell culture and tissue engineering because of their

biocompatibility and excellent mass exchange for water-based solution.^[246-248] The interesting feature of tunable hydrogel's geometries opens new perspective for designing bilayer and fibrous hydrogels with capability of shape and dimensional change. It would be extremely promising in tissue engineering field where geometry of the culture environment is of great importance, like cardiovascular cell culture.^[249]

6.5 Experimental

6.5.1 Materials

N, N'-dimethylformamide (DMF) (99.8%) and formamide were used as received from Sigma Aldrich (Canada). The UV-crosslinkable P(NIPAM-ABP) (NIPAM:ABP = 98:2 molar ratio) was prepared as in our previous report^[239]. The deionized water (DI) used for hydrogels' swelling and contraction tests was obtained from Barnstead Easypure II Purification System. The CNCs employed in this study were obtained from Cellulforce (Montreal, QC, Canada) as a spray-dried powder. They were prepared from Kraft wood pulp by a sulfuric acid hydrolysis treatment followed by neutralization with sodium hydroxide. Previous work from our group demonstrated that these particles are in average ~165 nm long and ~13 nm wide with a sulfur content equivalent of 3.4 sulfate half ester (O-SO₃H) per 100 anhydroglucose units^[250]. Their X-ray diffractogram showed typical I_β cellulose^[176] peaks and the crystallinity index was found to be of 81%.^[251]

6.5.2 Preparing PNIPAM/CNCs suspension

The CNC suspension was first prepared via the following protocol: 10 mL of DMF/formamide mixture (volume ratio of 9:1) were added to 0.25 g of CNCs in a glass vial. An ultrasonic probe (Cole-Parmer) was operated at a frequency of 20 kHz to disperse the CNCs with a power of ~34 W. The treatment was applied with a pulse cycle ON-OFF of 5–2 s for a total energy of 2000 J to 0.25

g CNCs in the 10 mL solvent mixture mentioned above.^[252] The vials were placed in an ice bath to avoid any overheating during the ultrasonication. Previous experimentation demonstrated that such a treatment does not result in any structure alteration of the CNCs.^[250] UV-crosslinkable P(NIPAM-ABP) was then added to CNCs suspension. By controlling the P(NIPAM-ABP) added, stable well dispersed suspension with various CNCs weight percent to P(NIPAM-ABP) (0.5%, 1%, 3%, 5%, 7.5% and 15%) were obtained.

6.5.3 Electrospinning

To produce nanofibers, P(NIPAM-ABP)/CNC suspensions were then used in electrospinning under the following conditions: the applied voltage on the needle (outer diameter: 0.6 mm) was 24 kV; the flow rate was fixed to 0.3 mL/h and the distance between the needle and collector was 20 cm. All fibers were collected on a grounded metal plate. The obtained fibers mats were dried under vacuum overnight at room temperature to remove any residual solvent. By controlling the volume of the suspensions to be electrospun, the thickness of electrospun membranes were finely tailored. PNIPAM/CNC suspensions with various CNC proportions were electrospun in sequence to fabricate bilayer structure samples and separately single layer for comparison purpose'. Small pieces were cut from the electrospun mats with length of 1 cm and width of 0.5 cm, respectively, for the subsequent responsive behaviour investigation. To fabricate bilayer structured hydrogels, two layers (containing 5wt% and 1.5 wt% CNCs respectively) with thickness ratio of 1:1, 1:10, 1:15, 1:20, 1:25 were prepared by controlling the suspension volume electrospun.

6.5.4 Fibers morphology

Fibers morphology was observed under a scanning electron microscope (SEM) (HITACHI TM3030Plus). All the samples were fully dried under vacuum until constant weight for SEM observation. To eliminate the influence of evaporation on fibers morphology, all hydrogels were dried under vacuum at 20 °C and 40 °C for swelling and contraction respectively, keeping the same temperature of which they reached swelling and contraction equilibrium. Because of the fibrous structure, the small size of samples and vacuum used, all samples were fully dried within seconds, which should minimize the impact of evaporation on fibers morphology. The microscopy images were analyzed by Image J software.

6.5.5 Swelling/contraction equilibrium

For single layer hydrogels, the gravimetric method^[220] was utilized to study the swelling and contraction equilibrium of PNIPAM/CNC hydrogels. The weights of hydrogels were obtained when they reached swollen and contracted equilibrium at temperatures of 20 °C and 40 °C, respectively.^[220] The excess water on the hydrogel surfaces was removed with filter paper. Then, the weights of the swollen hydrogels were compared using the sum of two separate layer hydrogels and the corresponding bilayer hydrogels, regardless of their geometries when swelling. The thicknesses of both layers, either in single layer or bilayer structure, were kept the same.

6.5.6 Deformation characterization

For bilayer structured hydrogels, pictures were taken from horizontal view of the samples at a fixed distance. Then all pictures were processed in Image J to characterize their swelling and contraction behaviors, the brightness and contrast were optimized for better visibility. Specifically, virtual balls were employed to fit the inner space of tubes diameters and curvatures formed by samples. The curvatures (reciprocal to the radii of these virtual balls) were employed to define the deformation of these hydrogels and to quantify their variation with environmental temperature change.

6.6 Acknowledgements

The authors acknowledge financial support from Postgraduate Scholarship Program of China Scholarship Council, Natural Sciences and Engineering Research Council of Canada (NSERC) and the Canada Foundation for Innovation (CFI). We also thank Charles Bruel, Chemical Engineering Department, Polytechnique Montreal, Canada, for the suggestions on preparation of CNCs suspensions.

References

- [1] A. S. Hoffman, *Artificial organs* 1995, 19, 458.
- [2] M. R. Aguilar, J. San Román, "Smart polymers and their applications", Woodhead publishing, 2019.

- [3] X. Sun, P. Tyagi, S. Agate, L. Lucia, M. McCord, L. Pal, Carbohydrate polymers 2019, 208, 495.
- [4] Y. Zhang, S. Furyk, D. E. Bergbreiter, P. S. Cremer, Journal of the American Chemical Society 2005, 127, 14505.
- [5] N. A. Cortez-Lemus, A. Licea-Claverie, Progress in Polymer Science 2016, 53, 1.
- [6] I. Cobo, M. Li, B. S. Sumerlin, S. Perrier, Nature materials 2015, 14, 143.
- [7] M. Karg, T. Hellweg, Journal of Materials Chemistry 2009, 19, 8714.
- [8] N. Grishkewich, N. Mohammed, J. Tang, K. C. Tam, Current Opinion in Colloid & Interface Science 2017, 29, 32.
- [9] J. Bras, S. Saini, "Nanocellulose in functional packaging", in Cellulose-Reinforced Nanofibre Composites, Elsevier, 2017, p. 175.
- [10] Y. Habibi, L. A. Lucia, O. J. Rojas, Chemical reviews 2010, 110, 3479.
- [11] H. Kargarzadeh, M. Mariano, D. Gopakumar, I. Ahmad, S. Thomas, A. Dufresne, J. Huang, N. Lin, Cellulose 2018, 25, 2151.
- [12] P. Lu, Y.-L. Hsieh, Carbohydrate polymers 2010, 82, 329.
- [13] I. A. Sacui, R. C. Nieuwendaal, D. J. Burnett, S. J. Stranick, M. Jorfi, C. Weder, E. J. Foster, R. T. Olsson, J. W. Gilman, ACS applied materials & interfaces 2014, 6, 6127.
- [14] P. B. Filson, B. E. Dawson-Andoh, Bioresource Technology 2009, 100, 2259.
- [15] K. Zubik, P. Singhsa, Y. Wang, H. Manuspiya, R. Narain, Polymers 2017, 9, 119.
- [16] J. O. Zoppe, Y. Habibi, O. J. Rojas, R. A. Venditti, L.-S. Johansson, K. Efimenko, M. Osterberg, J. Laine, Biomacromolecules 2010, 11, 2683.
- [17] H. Kargarzadeh, M. Mariano, J. Huang, N. Lin, I. Ahmad, A. Dufresne, S. Thomas, Polymer 2017, 132, 368.

- [18] J. P. F. Lagerwall, C. Schütz, M. Salajkova, J. Noh, J. Hyun Park, G. Scalia, L. Bergström, *NPG Asia Materials* 2014, 6, e80.
- [19] Y. Xu, A. Ajji, M.-C. Heuzey, *Polymer* 2019, 183, 121880.
- [20] M. Alavi, A. Nokhodchi.
- [21] H. Yim, M. Kent, S. Mendez, S. Balamurugan, S. Balamurugan, G. Lopez, S. Satija, *Macromolecules* 2004, 37, 1994.
- [22] S. Zakharchenko, E. Sperling, L. Ionov, *Biomacromolecules* 2011, 12, 2211.
- [23] L. Ionov, *Langmuir* 2015, 31, 5015.
- [24] L. Liu, S. Jiang, Y. Sun, S. Agarwal, *Advanced Functional Materials* 2016, 26, 1021.
- [25] S.-J. Jeon, A. W. Hauser, R. C. Hayward, *Accounts of chemical research* 2017, 50, 161.
- [26] J. Shang, P. Theato, *Soft Matter* 2018, 14, 8401.
- [27] J. Liu, W. Xu, Z. Kuang, P. Dong, Y. Yao, H. Wu, A. Liu, F. Ye, *Journal of Materials Chemistry C* 2020.
- [28] C. Yoon, *Nano convergence* 2019, 6, 1.
- [29] M. B. Chen, S. Srigunapalan, A. R. Wheeler, C. A. Simmons, *Lab on a Chip* 2013, 13, 2591.
- [30] Q. Beuguel, J. R. Tavares, P. J. Carreau, M.-C. Heuzey, *Journal of colloid and interface science* 2018, 516, 23.
- [31] S. Elazzouzi-Hafraoui, Y. Nishiyama, J.-L. Putaux, L. Heux, F. Dubreuil, C. Rochas, *Biomacromolecules* 2008, 9, 57.
- [32] C. Bruel, J. R. Tavares, P. J. Carreau, M.-C. Heuzey, *Carbohydrate polymers* 2019, 205, 184.
- [33] Q. Beuguel, J. R. Tavares, P. J. Carreau, M. C. Heuzey, *Journal of Colloid and Interface Science* 2018, 516, 23.

- [34] M. Liu, H. Su, T. Tan, *Carbohydrate Polymers* 2012, 87, 2425.

CHAPTER 7 GENERAL DISCUSSION

The general discussion presented in this chapter is divided into two sections. First, electrospinning of PNIPAM-based hydrogels is discussed in the scope of this work. Then, the second part is about the hydrogel platform to introduce other polymer or nanoparticles.

7.1 Electrospinning of PNIPAM-based hydrogel

Although PNIPAM has been reported to be electrospun successfully before, the main concerns were the processing parameters and fibers' morphology^[218], which is a common concern for polymer electrospinning. Very few researches have looked into the fabrication of PNIPAM-based hydrogels via electrospinning, which may involve many theoretical and experimental issues, for example, crosslinking protocol employed and the corresponding impact on electrospinnability and temperature responsive capability, etc. Inevitably, crosslinking would lead to slower response rate as it would limit the chain movement of PNIPAM.^[253] Thus, electrospun fibers in nanoscale is employed to reduce the side effect resulting from crosslinking. Once electrospinning technology is selected, some processing-related challenges need to be overcome in the fabrication of PNIPAM-based hydrogels. Specifically, post-crosslinked PNIPAM is impossible to be electrospun because of the high viscosity of the corresponding solution resulting from ultrahigh molecular weight.^[89] Therefore, PNIPAM has to be crosslinked after electrospinning. Another challenge is to maintain the fibrous structure during crosslinking because fibrous structure is the key factor to accelerate mass exchange. If the fibrous structure is damaged, the electrospinning would be meaningless. Most crosslinking agents work under solvent condition where fibers would swell to extremely high degree until they lose their structure.^[84] Hence, a non-solvent condition for crosslinking the electrospun fibers, such as UV-induced crosslinking, would be an ideal route to follow.

In this work, a UV-induced crosslinking agent ABP (4-acryloylbenzophenone) was synthesized and incorporated into PNIPAM chains via free radical polymerization. The obtained copolymer was dissolved in DMF with weight ratio of 40% for electrospinning. Under finely tailored electrospinning parameters, uniform fibers with average fiber diameters in the range of 150-250 nm were obtained. Although ABP did not alter fibers' morphology when crosslinking, it exerted significant influence on hydrogel's responsive capability and mechanical strength. Briefly, with

more ABP incorporated, the maximum swelling and contraction ratio of hydrogel were reduced; while it did not slow down the hydrogel's response rate. In theory, crosslinking should also impose a negative impact on hydrogel's response rate. But this was not observed under our experimental conditions, which could result from the efficient water molecules exchange accelerated by fibrous structure. All hydrogel samples, with original width and length of 1 cm and thickness up to 0.5 μm , could reach swelling and contraction equilibrium within 4 min. Although swelling/contraction equilibrium was reported to be reached within seconds, the dimension of samples has to be taken into consideration when making a comparison. Unlike application of drug or cells carrier, it was set to serve as a platform to incorporate other additives in our case, which requires a certain dimension.

It was reported the ABP is working more efficiently under UV irradiation of 254 nm.^[97] Under our UV light with no specific wavelength, all electrospun membranes have to be treated at least 2 hours to be crosslinked uniformly. On the other hand, ABP's influence on LCST of the copolymer was beyond our expectation. Because of the hydrophilicity difference between PNIPAM and ABP, a slight decrease of the LCST makes sense. But a significant drop of LCST on P(NIPAM-ABP) was detected in our case. The stress generated by hydrogel's contraction was measured the rheometer to illustrate the LCST of the material. Though the synthesis of the copolymer, electrospinning and crosslinking were successful, the drop of LCST ($\sim 4\text{ }^{\circ}\text{C}$) is still not favorable for material's biological applications, as this made the LCST slightly far from human body temperature. Thus, there is a need for more detailed work on: 1) more efficient UV light source; 2) designing and synthesis of a crosslinking agent that would impose less impact on the LCST of the material.

In terms of compression test, rheometer was employed in our work because of its sensitivity. Due to the very high degree of swelling, the swollen hydrogel was super soft, which was difficult to be fixed, especially in water. The specific experimental conditions made it hard to be compared with similar works. It was found to be a significant impediment for comparison among hydrogel's mechanical strength. Regardless the similarity of the materials, significant difference could be obtained with a slight divergence in measurement parameters. Thus, there is an urgent need for more generalized and standardized mechanical test protocols, especially for these super soft hydrogels.

7.2 Multifunctional PNIPAM-based fibrous hydrogel

To serve as a platform, the PNIPAM-based fibrous hydrogel fabricated was facing some challenges regarding introducing new functions or features by other materials. The first one would be the way the new material(s) are being incorporated. They can be introduced before electrospinning, which implies the preparation of a stable dual or multi-component system for electrospinning; or after electrospinning, which suggests the additives would be distributed in electrospun membrane or hydrogel domain. A few critical issues need to be addressed for both protocols.

In this work, PANI was introduced via “after electrospinning” route to introduce the electrical conductive feature to this hydrogel in Chapter 5. The PNIPAM-based fibrous hydrogel was obtained in the same way as described before. PANI was then incorporated to the hydrogel domain via in-situ polymerization of aniline. The synthesized PANI occupied all inner spaces in PNIPAM-based hydrogel domain, thus no fibrous structure was observed. The hybrid hydrogel was solid like and no temperature responsiveness was detected. At this stage, the best conductive property, with a resistance below 100 Ω , was obtained. However, the fibrous structure and hydrogel’s flexibility were both recovered after ~60% of PANI was washed from hydrogel domain. This interesting phenomenon suggests that the non-temperature responsive PANI synthesized in hydrogel domain play a role of a frame to block hydrogel volume change. Although this hybrid hydrogel was still with good conductive capability, the waste of PANI is still regrettable.

Another interesting phenomenon that beyond our expectation was the conductivity of hybrid hydrogel in swollen and contracted states. As the synthesis of PANI was conducted in hydrogel domain in swollen state, where the hydrogel was extended at highest degree, PANI should be formed and distributed among swollen hydrogel domain. In this case, the conductivity, contributed 100% by PANI, should be in same level for hydrogel in swollen and contracted states. This is consistent with our results for “before washing” hydrogels, but not for “after washing” hydrogels. The large conductive difference between “after washing” hydrogel’s swollen and contracted states was detected. This may suggest that the reduction of PANI not only leads to the recovery of fibrous structure and hydrogel’s temperature responsive capability, but also results in the significant decrease of electron-transfer path. Therefore, the conductivity of the hydrogel in swollen state was

much worse after washing, compared with those hydrogels right after PANI's polymerization. On the other hand, the conductivity of "after washing" hydrogel undergoes reversible increase and decrease along with its contraction and swelling. This may suggest a dynamic self-healing phenomenon for PANI with hydrogel's volume change, as electrons can only be transferred along with the covalent bonds among PANI chains. However, this is still in the speculation stage as it is difficult to observe the dynamic self-healing phenomenon of PANI, especially when it occurs in fibers at the nanoscale.

On the other hand, CNC, as a promising and biocompatible material, was also introduced into this hydrogel platform via "before electrospinning" route. The CNC suspension in DMF/formamide mixture with volume ratio of 9:1 was well dispersed by ultrasonication treatment. The incorporation of P(NPAM-ABP) would be in favor of stabilizing CNC suspension because of the viscosity. Nevertheless, all PNIPAM/CNC suspensions were employed in electrospinning right after ultrasonication treatment to avoid potential difference resulting from CNC's agglomeration. The constraint effect brought by CNC was then utilized to build bilayer hydrogel where two layers possess different CNC proportions. These bilayer electrospun samples generated 3D geometries irreversibly because of the anisotropic swelling when contacting water for the first time. The hydrogels with 3D geometries then underwent isotropic deformation with temperature which leads to reversible dimensional change. However, due to the limitation of the suspension's electrospinnability, CNC's weight ratio was kept below 10 wt% to PNIPAM. Although CNC's effect was significant to generate deformation difference between two hydrogel layers at this proportion, the optical property of this hydrogel would be non-detectable, which normally require more than 70 wt% of CNC to form chiral nematic structure.^[254] Another limitation is the total thickness of the bilayer hydrogel which was fabricated by sequential electrospinning of suspension with various CNC proportions. The interface area between two layers is difficult for UV irradiation to reach. Any thickness higher than 0.3 mm would result in insufficient crosslinking between the two layers, which leads to delamination when deformation occurs. This limitation would be the main reason that only tube or tubelike geometries were achieved in this work. The combination of other material processing technology, such as 3D-printing^[255], would be a feasible route to design and fabricate multi-layer structures to generate more complex deformations and geometries.

CHAPTER 8 CONCLUSION AND RECOMMENDATIONS

8.1 Conclusion

In this thesis, electrospinning is employed to fabricate PNIPAM-based hydrogel which then served as a platform for the incorporation of PANI and CNC. A UV-induced crosslinking agent ABP was synthesized and introduced into PNIPAM chain via free radical polymerization. The P(NIPAM-ABP) prepared was dissolved in DMF for electrospinning. After crosslinking of electrospun membrane, a fibrous structured hydrogel was obtained by UV-crosslinking. Its temperature responsive behaviors and mechanical strength were investigated under the influence of crosslinking agent. Then PANI and CNC were introduced into this hydrogel platform via “after electrospinning” and “before electrospinning” route respectively. New features brought by these two additives were characterized and correlated with original temperature responsive capability. The conclusions drawn from this work are presented below:

UV-induced crosslinking agent ABP was prepared and its chemical structure was characterized via ^1H NMR. Then it was incorporated to PNIPAM chains by free radical polymerization. The obtained copolymer was prepared in DMF for electrospinning. The morphology of electrospun fibers was reserved well after exposing to UV irradiation for crosslinking. When swelled in water at 20 °C, the water contained in hydrogel reached over 10 times in comparison material's weight. While the fully swollen hydrogel contracted around 40% when moved to water at 40 °C. Because of the fibrous structure, this hydrogel could response to temperature change very fast, both swelling and contraction equilibrium could reach within 4 mins. A higher ratio of crosslinker had a negligible impact on the response rate but significant influence on maximum swelling and de-swelling equilibrium ratios. In terms of mechanical strength, results from both compression tests and rheological characterization showed that a higher ratio of crosslinker led to higher strength for hydrogels in shrunk state but had less impact on the hydrogels in swollen state, which was due to their quite high swelling degree. A closer-to-solid behavior was observed in both swelling and de-swelling equilibrium states under Small amplitude oscillatory shear test.

Then this hydrogel served as a platform to incorporate PANI “after electrospinning” with the aim of building a conductive and temperature responsive hydrogel. The monomer aniline and dopant

phytic acid were introduced in PNIPAM fibrous hydrogel domain via in-situ polymerization in ice bath condition. The fibrous structure was able to be restored after 5 times washing and maintained well for further swelling and contraction. The resistance of hybrid hydrogels varied highly consistently with their corresponding swelling and contraction degree. The correlation between the conductive and thermal-responsive properties was further investigated to propose an evaluation system for this type of hydrogel. The establishment of this evaluation system would allow the prediction of potential applications for these hybrid hydrogels with various PANI proportions.

The “before electrospinning” route was then followed to introduce CNCs into this hydrogel. CNCs, as a promising nanofiller, exerted its impact on hydrogel’s temperature responsive behaviors but did not reduce its biocompatibility. A stable CNC suspension was prepared in DMF/formamide solvent with a ratio of 9:1 after ultrasonication treatment. This suspension was utilized to dissolve P(NIPAM-ABP) which could further stabilize the CNC in mixture solvent. Then this P(NIPAM-ABP)/CNC suspension was employed for electrospinning with same processing parameters as that for P(NIPAM-ABP) alone. Electrospun fibers were successfully fabricated and they were maintained well in following swelling and contraction cycles. CNCs’ constraining effect was significant on hydrogels swelling but negligible on contraction. The difference among hydrogels’ deformation with various CNC proportions was utilized to build bilayer structure hydrogel. It was observed that these bilayer hydrogels were able to generate 3D geometries via irreversible and anisotropic swelling at the first-time contacting water. Then they underwent reversible swelling/contraction, where geometries were maintained and only dimensional changes were observed. Finally, these geometries were found to be highly tunable by tailoring the thickness ratio between two layers hydrogel.

8.2 Recommendations

Recommendations for future work are as follows:

- 1) Many other polymer materials that are responsive to other stimuli could be investigated via the route developed in this thesis. For example, Polymethyl methacrylate (PMMA) for pH response, azobenzene-containing polymer for light response and poly(vinylidene fluoride)(PVDF) for electrical response, etc.

- 2) Other crosslinking agents that can work under non-solvent environment could be employed for producing polymer based fibrous hydrogel.
- 3) A more general characterization method on mechanical strength should be further designed and investigated.
- 4) Other conductive additives, such as carbon nanotubes (CNT) or graphene could be introduced together with PANI to achieve better conductive properties.
- 5) CNC's alignment inside electrospun fibers because of electrospinning is of great interest to study further.
- 6) Modeling and simulation could be carried out to analyze hydrogel's deformation, especially for bilayer hydrogel's 3D deformation.

REFERENCES

- [1] J. Doshi, D. H. Reneker, *Journal of electrostatics* **1995**, 35, 151.
- [2] W. E. Teo, S. Ramakrishna, *Nanotechnology* **2006**, 17, R89.
- [3] P. Van de Witte, P. Dijkstra, J. Van den Berg, J. Feijen, *Journal of membrane science* **1996**, 117, 1.
- [4] S. Chakarvarti, J. Vetter, *Radiation measurements* **1998**, 29, 149.
- [5] S. Ramakrishna, "*An introduction to electrospinning and nanofibers*", World Scientific, 2005.
- [6] Z.-M. Huang, Y. Zhang, S. Ramakrishna, C. Lim, *Polymer* **2004**, 45, 5361.
- [7] I. S. Chronakis, *Journal of materials processing technology* **2005**, 167, 283.
- [8] Y. K. Wang, T. Yong, S. Ramakrishna, *Australian journal of chemistry* **2005**, 58, 704.
- [9] W. J. Li, C. T. Laurencin, E. J. Caterson, R. S. Tuan, F. K. Ko, *Journal of Biomedical Materials Research: An Official Journal of The Society for Biomaterials, The Japanese Society for Biomaterials, and The Australian Society for Biomaterials and the Korean Society for Biomaterials* **2002**, 60, 613.
- [10] R. R. Kokardekar, V. K. Shah, H. R. Mody, *Internet Journal of Medical Update-EJOURNAL* **2012**, 7.
- [11] M. A. Haq, Y. Su, D. Wang, *Mater Sci Eng C Mater Biol Appl* **2017**, 70, 842.
- [12] P. Kujawa, V. Aseyev, H. Tenhu, F. M. Winnik, *Macromolecules* **2006**, 39, 7686.
- [13] Y. Okada, F. Tanaka, *Macromolecules* **2005**, 38, 4465.
- [14] G. Chen, A. S. Hoffman, *Nature* **1995**, 373, 49.
- [15] C. S. Brazel, N. A. Peppas, *Journal of controlled release* **1996**, 39, 57.
- [16] J. Wang, L. Li, Y. Feng, H. Yao, X. Wang, *Chinese medical journal* **1993**, 106, 441.
- [17] C. Yoon, R. Xiao, J. Park, J. Cha, T. D. Nguyen, D. H. Gracias, *Smart Materials and Structures* **2014**, 23, 094008.
- [18] A. Alexander, J. Khan, S. Saraf, S. Saraf, *European Journal of Pharmaceutics and Biopharmaceutics* **2014**, 88, 575.
- [19] E. A. Di Marzio, *Progress in Polymer Science* **1999**, 24, 329.
- [20] B. P. Tripathi, N. C. Dubey, F. Simon, M. Stamm, *RSC Advances* **2014**, 4, 34073.

- [21] J. Höpfner, C. Klein, M. Wilhelm, *Macromolecular rapid communications* **2010**, 31, 1337.
- [22] M. A. Haq, Y. Su, D. Wang, *Materials Science and Engineering: C* **2017**, 70, 842.
- [23] F. L. Buchholz, A. T. Graham, "*Modern superabsorbent polymer technology*", Wiley-vch New York, 1998.
- [24] L. Brannon-Peppas, R. S. Harland, "*Absorbent polymer technology*", Elsevier, 2012.
- [25] E. M. Ahmed, F. S. Aggor, A. M. Awad, A. T. El-Aref, *Carbohydrate polymers* **2013**, 91, 693.
- [26] Y. Li, G. Huang, X. Zhang, B. Li, Y. Chen, T. Lu, T. J. Lu, F. Xu, *Advanced Functional Materials* **2013**, 23, 660.
- [27] E. M. Ahmed, *Journal of advanced research* **2015**, 6, 105.
- [28] J. Maitra, V. K. Shukla, *Am. J. Polym. Sci* **2014**, 4, 25.
- [29] K. T. Nguyen, J. L. West, *Biomaterials* **2002**, 23, 4307.
- [30] S. Burkert, T. Schmidt, U. Gohs, H. Dorschner, K.-F. Arndt, *Radiation Physics and Chemistry* **2007**, 76, 1324.
- [31] O. Wichterle, D. Lim, *Nature* **1960**, 185, 117.
- [32] A. Singh, P. K. Sharma, V. K. Garg, G. Garg, *Int J Pharm Sci Rev Res* **2010**, 4, 97.
- [33] M. Hamidi, A. Azadi, P. Rafiei, *Advanced drug delivery reviews* **2008**, 60, 1638.
- [34] X. Chen, B. Martin, T. Neubauer, R. Linhardt, J. Dordick, D. Rethwisch, *Carbohydrate polymers* **1995**, 28, 15.
- [35] J. PACHIONI-VASCONCELOS, "Nanostructures for protein drug delivery", University of São Paulo, 2015.
- [36] S. Kaihara, S. Matsumura, J. P. Fisher, *European journal of pharmaceuticals and biopharmaceutics* **2008**, 68, 67.
- [37] L. Zhang, K. Li, W. Xiao, L. Zheng, Y. Xiao, H. Fan, X. Zhang, *Carbohydrate polymers* **2011**, 84, 118.
- [38] P. Sikareepaisan, U. Ruktanonchai, P. Supaphol, *Carbohydrate Polymers* **2011**, 83, 1457.
- [39] F. Wang, Z. Li, M. Khan, K. Tamama, P. Kuppasamy, W. R. Wagner, C. K. Sen, J. Guan, *Acta biomaterialia* **2010**, 6, 1978.
- [40] P. Krsko, T. E. McCann, T.-T. Thach, T. L. Laabs, H. M. Geller, M. R. Libera, *Biomaterials* **2009**, 30, 721.

- [41] G. Stoychev, N. Pureskiy, L. Ionov, *Soft Matter* **2011**, 7, 3277.
- [42] F. Ilmain, T. Tanaka, E. Kokufuta, *Nature* **1991**, 349, 400.
- [43] J. Ricka, T. Tanaka, *Macromolecules* **1984**, 17, 2916.
- [44] O. E. Philippova, D. Hourdet, R. Audebert, A. R. Khokhlov, *Macromolecules* **1997**, 30, 8278.
- [45] J. L. Thomas, H. You, D. A. Tirrell, *Journal of the American Chemical Society* **1995**, 117, 2949.
- [46] V. R. Babu, K. Rao, M. Sairam, B. V. K. Naidu, K. M. Hosamani, T. M. Aminabhavi, *Journal of Applied Polymer Science* **2006**, 99, 2671.
- [47] J. Zhang, N. A. Peppas, *Macromolecules* **2000**, 33, 102.
- [48] M. V. Risbud, A. A. Hardikar, S. V. Bhat, R. R. Bhonde, *Journal of Controlled Release* **2000**, 68, 23.
- [49] S. Chaterji, I. K. Kwon, K. Park, *Progress in Polymer Science* **2007**, 32, 1083.
- [50] S. A. Glynn, D. Albanes, *Nutrition and Cancer-an International Journal* **1994**, 22, 101.
- [51] Q. Garrett, B. Laycock, R. W. Garrett, *Investigative Ophthalmology & Visual Science* **2000**, 41, 1687.
- [52] A. K. Bajpai, S. K. Shukla, S. Bhanu, S. Kankane, *Progress in Polymer Science* **2008**, 33, 1088.
- [53] A. M. Schmidt, *Colloid and Polymer Science* **2007**, 285, 953.
- [54] H. Zareie, E. V. Bulmus, A. Gunning, A. Hoffman, E. Piskin, V. Morris, *Polymer* **2000**, 41, 6723.
- [55] Y. Hirokawa, H. Jinnai, Y. Nishikawa, T. Okamoto, T. Hashimoto, *Macromolecules* **1999**, 32, 7093.
- [56] K. Ishida, T. Uno, T. Itoh, M. Kubo, *Macromolecules* **2012**, 45, 6136.
- [57] A. Alexander, Ajazuddin, J. Khan, S. Saraf, S. Saraf, *European Journal of Pharmaceutics and Biopharmaceutics* **2014**, 88, 575.
- [58] M. R. Matanovic, J. Kristl, P. A. Grabnar, *International Journal of Pharmaceutics* **2014**, 472, 262.
- [59] Y. Zhang, S. Furyk, L. B. Sagle, Y. Cho, D. E. Bergbreiter, P. S. Cremer, *The Journal of Physical Chemistry C* **2007**, 111, 8916.
- [60] C. Wu, S. Zhou, *Macromolecules* **1995**, 28, 5388.

- [61] I. Ankareddi, C. S. Brazel, *International Journal of Pharmaceutics* **2007**, 336, 241.
- [62] J. Chen, Y. Pei, L. M. Yang, L. L. Shi, H. J. Luo, "Synthesis and Properties of Poly (N-isopropylacrylamide-co-acrylamide) Hydrogels", in *Macromolecular Symposia*, Wiley Online Library, 2005, p. 225/103.
- [63] A. S. Hoffman, P. S. Stayton, V. Bulmus, G. Chen, J. Chen, C. Cheung, A. Chilkoti, Z. Ding, L. Dong, R. Fong, *Journal of Biomedical Materials Research* **2000**, 52, 577.
- [64] M. A. Ward, T. K. Georgiou, *Polymers* **2011**, 3, 1215.
- [65] T. Serizawa, K. Wakita, M. Akashi, *Macromolecules* **2002**, 35, 10.
- [66] X. Z. Zhang, C. C. Chu, *Journal of Applied Polymer Science* **2003**, 89, 1935.
- [67] G. L. Puleo, F. Zulli, M. Piovaneli, M. Giordano, B. Mazzolai, L. Beccai, L. Andreozzi, *Reactive & Functional Polymers* **2013**, 73, 1306.
- [68] N. Gundogan, D. Melekaslan, O. Okay, *Macromolecules* **2002**, 35, 5616.
- [69] T. Takigawa, T. Yamawaki, K. Takahashi, T. Masuda, *Polymer Gels and Networks* **1997**, 5, 585.
- [70] T. R. Matzelle, G. Geuskens, N. Kruse, *Macromolecules* **2003**, 36, 2926.
- [71] K. Haraguchi, T. Takehisa, *Advanced Materials* **2002**, 14, 1120.
- [72] Z. Li, J. Shen, H. Ma, X. Lu, M. Shi, N. Li, M. Ye, *Materials Science & Engineering C-Materials for Biological Applications* **2013**, 33, 1951.
- [73] J. Wang, L. Lin, Q. Cheng, L. Jiang, *Angewandte Chemie-International Edition* **2012**, 51, 4676.
- [74] K. Van Durme, B. Van Mele, W. Loos, F. E. Du Prez, *Polymer* **2005**, 46, 9851.
- [75] Y. Tan, K. Xu, P. Wang, W. Li, S. Sun, L. Dong, *Soft Matter* **2010**, 6, 1467.
- [76] S. B. Campbell, M. Patenaude, T. Hoare, *Biomacromolecules* **2013**, 14, 644.
- [77] J.-T. Zhang, R. Bhat, K. D. Jandt, *Acta Biomaterialia* **2009**, 5, 488.
- [78] T. Kanai, K. Pandey, A. B. Samui, *Polymers for Advanced Technologies* **2012**, 23, 1234.
- [79] S. Ekici, *Journal of Materials Science* **2011**, 46, 2843.
- [80] C. Alvarez-Lorenzo, A. Concheiro, A. S. Dubovik, N. V. Grinberg, T. V. Burova, V. Y. Grinberg, *Journal of Controlled Release* **2005**, 102, 629.
- [81] G. V. N. Rathna, P. R. Chatterji, *Journal of Macromolecular Science-Pure and Applied Chemistry* **2001**, 38, 43.

- [82] J. Djonlagić, Z. S. Petrović, *Journal of Polymer Science Part B: Polymer Physics* **2004**, 42, 3987.
- [83] E. S. Gil, S. M. Hudson, *Biomacromolecules* **2007**, 8, 258.
- [84] S. Jiang, F. Liu, A. Lerch, L. Ionov, S. Agarwal, *Advanced materials* **2015**, 27, 4865.
- [85] J. Sahyoun, A. Crepet, F. Gouanve, L. Keromnes, E. Espuche, *Journal of Applied Polymer Science* **2017**, 134.
- [86] N. Abhari, A. Madadlou, A. Dini, *Food Chemistry* **2017**, 221, 147.
- [87] T. Akisawa, K. Yamada, F. Nagatsugi, *Bioorganic & Medicinal Chemistry Letters* **2016**, 26, 5902.
- [88] Y.-J. Kim, M. Ebara, T. Aoyagi, *Science and technology of advanced materials* **2012**, 13, 064203.
- [89] J. Wang, A. Sutti, X. Wang, T. Lin, *Soft Matter* **2011**, 7, 4364.
- [90] S. Lee, S. Lee, B. Kim, *Journal of Macromolecular Science, Part B* **2014**, 53, 254.
- [91] R. Liu, X. Yang, Y. Yuan, J. Liu, X. Liu, *Progress in Organic Coatings* **2016**, 101, 122.
- [92] I. Mironi-Harpaz, D. Y. Wang, S. Venkatraman, D. Seliktar, *Acta biomaterialia* **2012**, 8, 1838.
- [93] T. Corrales, F. Catalina, N. S. Allen, C. Peinado, *Journal of Photochemistry and Photobiology A: Chemistry* **2005**, 169, 95.
- [94] S. F. Yates, G. B. Schuster, *The Journal of Organic Chemistry* **1984**, 49, 3349.
- [95] J.-P. Fouassier, "Photoinitiation, photopolymerization, and photocuring: fundamentals and applications", Hanser, 1995.
- [96] N. S. Allen, "Photopolymerisation and photoimaging science and technology", Springer, 1989.
- [97] F. Natalia, G. Stoychev, N. Puretskiy, I. Leonid, V. Dmitry, *European Polymer Journal* **2015**, 68, 650.
- [98] L. Ionov, *Advanced Functional Materials* **2013**, 23, 4555.
- [99] X. He, M. Aizenberg, O. Kuksenok, L. D. Zarzar, A. Shastri, A. C. Balazs, J. Aizenberg, *Nature* **2012**, 487, 214.
- [100] C. Huang, S. J. Soenen, J. Rejman, B. Lucas, K. Braeckmans, J. Demeester, S. C. De Smedt, *Chemical Society Reviews* **2011**, 40, 2417.
- [101] C. Huang, S. J. Soenen, J. Rejman, B. Lucas, K. Braeckmans, J. Demeester, S. C. De Smedt, *Chem Soc Rev* **2011**, 40, 2417.

- [102] L. Weng, J. Xie, *Current pharmaceutical design* **2015**, *21*, 1944.
- [103] X. Jin, Y.-L. Hsieh, **2005**, - 46.
- [104] S. H. Kim, S.-H. Kim, S. Nair, E. Moore, **2005**, - 38.
- [105] M. Qi, X. Li, Y. Yang, S. Zhou, **2008**, - 70.
- [106] C.-C. Kuo, Y.-C. Tung, W.-C. Chen, *Macromolecular Rapid Communications* **2010**, *31*, 65.
- [107] D. N. Rockwood, D. B. Chase, R. E. Akins Jr, J. F. Rabolt, *Polymer* **2008**, *49*, 4025.
- [108] G. D. Fu, L. Q. Xu, F. Yao, K. Zhang, X. F. Wang, M. F. Zhu, S. Z. Nie, *ACS Applied Materials & Interfaces* **2009**, *1*, 239.
- [109] S. J. Soenen, M. Hodenius, M. De Cuyper, **2009**.
- [110] M. Li, J. Zhang, H. Zhang, Y. Liu, C. Wang, X. Xu, Y. Tang, B. Yang, *Advanced Functional Materials* **2007**, *17*, 3650.
- [111] J. Chen, C. Wang, J. Irudayaraj, *Journal of biomedical optics* **2009**, *14*, 040501.
- [112] I.-D. Kim, A. Rothschild, B. H. Lee, D. Y. Kim, S. M. Jo, H. L. Tuller, *Nano Letters* **2006**, *6*, 2009.
- [113] W.-Y. Wu, J.-M. Ting, P.-J. Huang, *Nanoscale research letters* **2009**, *4*, 513.
- [114] D. Aussawasathien, J.-H. Dong, L. Dai, *Synthetic Metals* **2005**, *154*, 37.
- [115] J. R. Capadona, K. Shanmuganathan, D. J. Tyler, S. J. Rowan, C. Weder, *science* **2008**, *319*, 1370.
- [116] K. Haraguchi, *Polymer journal* **2011**, *43*, 223.
- [117] K. Haraguchi, T. Takehisa, *Advanced materials* **2002**, *14*, 1120.
- [118] A. Eklund, H. Zhang, H. Zeng, A. Priimagi, O. Ikkala, *Advanced Functional Materials* **2020**, 2000754.
- [119] A. G. MacDiarmid, *Angewandte Chemie International Edition* **2001**, *40*, 2581.
- [120] C. K. Chiang, C. Fincher Jr, Y. W. Park, A. J. Heeger, H. Shirakawa, E. J. Louis, S. C. Gau, A. G. MacDiarmid, *Physical review letters* **1977**, *39*, 1098.
- [121] J. L. Reddinger, J. R. Reynolds, "Molecular engineering of π -conjugated polymers", in *Radical Polymerisation Polyelectrolytes*, Springer, 1999, p. 57.
- [122] V. Krinichnyi, *Applied Physics Reviews* **2014**, *1*, 021305.

- [123] A. MacDiarmid, J. Chiang, A. Richter, Epstein, AJ, *Synthetic Metals* **1987**, *18*, 285.
- [124] C. Borsoi, A. Zattera, C. Ferreira, *Applied Surface Science* **2016**, *364*, 124.
- [125] M. Shabani-Nooshabadi, S. M. Ghoreishi, Y. Jafari, N. Kashanizadeh, *Journal of Polymer Research* **2014**, *21*, 416.
- [126] P. Tsotra, K. Friedrich, *Composites science and technology* **2004**, *64*, 2385.
- [127] J. Stejskal, *Chemical Papers* **2017**, *71*, 269.
- [128] J.-O. You, M. Rafat, G. J. Ye, D. T. Auguste, *Nano letters* **2011**, *11*, 3643.
- [129] A. Mihic, Z. Cui, J. Wu, G. Vlacic, Y. Miyagi, S.-H. Li, S. Lu, H.-W. Sung, R. D. Weisel, R.-K. Li, *Circulation* **2015**, *132*, 772.
- [130] B. S. Spearman, A. J. Hodge, J. L. Porter, J. G. Hardy, Z. D. Davis, T. Xu, X. Zhang, C. E. Schmidt, M. C. Hamilton, E. A. Lipke, *Acta biomaterialia* **2015**, *28*, 109.
- [131] Z. Shi, H. Gao, J. Feng, B. Ding, X. Cao, S. Kuga, Y. Wang, L. Zhang, J. Cai, *Angewandte Chemie International Edition* **2014**, *53*, 5380.
- [132] H. Baniasadi, A. R. SA, S. Mashayekhan, *International journal of biological macromolecules* **2015**, *74*, 360.
- [133] B. C. Kim, J. Y. Hong, G. G. Wallace, H. S. Park, *Advanced Energy Materials* **2015**, *5*, 1500959.
- [134] Y. Shi, G. Yu, *Chemistry of Materials* **2016**, *28*, 2466.
- [135] K. Sharma, V. Kumar, B. Chaudhary, B. Kaith, S. Kalia, H. Swart, *Polymer degradation and stability* **2016**, *124*, 101.
- [136] N. V. Blinova, M. Trchová, J. Stejskal, *European polymer journal* **2009**, *45*, 668.
- [137] S. Fedorova, J. Stejskal, *Langmuir* **2002**, *18*, 5630.
- [138] K. Wang, X. Zhang, C. Li, X. Sun, Q. Meng, Y. Ma, Z. Wei, *Advanced materials* **2015**, *27*, 7451.
- [139] A. Srinivasan, J. Roche, V. Ravaine, A. Kuhn, *Soft Matter* **2015**, *11*, 3958.
- [140] J. Zheng, X. Yu, C. Wang, Z. Cao, H. Yang, D. Ma, X. Xu, *Journal of Materials Science: Materials in Electronics* **2016**, *27*, 4457.
- [141] C. Wan, J. Li, *Carbohydrate polymers* **2016**, *146*, 362.
- [142] S. J. Kim, M. S. Kim, S. I. Kim, G. M. Spinks, B. C. Kim, G. G. Wallace, *Chemistry of materials* **2006**, *18*, 5805.

- [143] Y. Wu, Y. X. Chen, J. Yan, D. Quinn, P. Dong, S. W. Sawyer, P. Soman, *Acta biomaterialia* **2016**, 33, 122.
- [144] D. Zhang, F. Di, Y. Zhu, Y. Xiao, J. Che, *Journal of Bioactive and Compatible Polymers* **2015**, 30, 600.
- [145] P.-Y. Chen, N.-M. D. Courchesne, M. N. Hyder, J. Qi, A. M. Belcher, P. T. Hammond, *RSC Advances* **2015**, 5, 37970.
- [146] Q. Tang, J. Wu, H. Sun, S. Fan, D. Hu, J. Lin, *Carbohydrate polymers* **2008**, 73, 473.
- [147] M. Moussa, Z. Zhao, M. F. El-Kady, H. Liu, A. Micheltmore, N. Kawashima, P. Majewski, J. Ma, *Journal of Materials Chemistry A* **2015**, 3, 15668.
- [148] R. E. Rivero, M. A. Molina, C. R. Rivarola, C. A. Barbero, *Sensors and Actuators B: Chemical* **2014**, 190, 270.
- [149] Y. Shi, C. Ma, L. Peng, G. Yu, *Advanced Functional Materials* **2015**, 25, 1219.
- [150] S. Adhikari, P. Banerji, *Synthetic metals* **2009**, 159, 2519.
- [151] A. Jayakumar, Y.-J. Yoon, R. Wang, J.-M. Lee, *RSC advances* **2015**, 5, 94388.
- [152] A. Guiseppi-Elie, *Biomaterials* **2010**, 31, 2701.
- [153] T. F. O'Connor, K. M. Rajan, A. D. Printz, D. J. Lipomi, *Journal of Materials Chemistry B* **2015**, 3, 4947.
- [154] K.-H. Sun, Z. Liu, C. Liu, T. Yu, T. Shang, C. Huang, M. Zhou, C. Liu, F. Ran, Y. Li, *Scientific reports* **2016**, 6, 1.
- [155] H.-B. Zhao, L. Yuan, Z.-B. Fu, C.-Y. Wang, X. Yang, J.-Y. Zhu, J. Qu, H.-B. Chen, D. A. Schiraldi, *ACS Applied Materials & Interfaces* **2016**, 8, 9917.
- [156] Y. Shi, L. Peng, G. Yu, *Nanoscale* **2015**, 7, 12796.
- [157] S. K. Siddhanta, R. Gangopadhyay, *Polymer* **2005**, 46, 2993.
- [158] X. Shi, Y. Hu, K. Tu, L. Zhang, H. Wang, J. Xu, H. Zhang, J. Li, X. Wang, M. Xu, *Soft Matter* **2013**, 9, 10129.
- [159] Z. Shi, Y. Li, X. Chen, H. Han, G. Yang, *Nanoscale* **2014**, 6, 970.
- [160] L. Li, J. Ge, B. Guo, P. X. Ma, *Polymer Chemistry* **2014**, 5, 2880.
- [161] P. Petrov, P. Mokreva, I. Kostov, V. Uzunova, R. Tzoneva, *Carbohydrate polymers* **2016**, 140, 349.
- [162] H. Guo, W. He, Y. Lu, X. Zhang, *Carbon* **2015**, 92, 133.

- [163] Z. Zhang, M. Liang, X. Liu, F. Zhao, B. Wang, W. Li, Q. Wang, *RSC advances* **2015**, *5*, 88419.
- [164] H. S. Oh, H. M. Jeong, J. H. Park, I.-W. Ock, J. K. Kang, *Journal of Materials Chemistry A* **2015**, *3*, 10238.
- [165] Q. Liu, J. Wu, Z. Lan, M. Zheng, G. Yue, J. Lin, M. Huang, *Polymer Engineering & Science* **2015**, *55*, 322.
- [166] L. B. J. da Silva, R. L. Oréfice, *Journal of Polymer Research* **2014**, *21*, 466.
- [167] M. Molina, C. Rivarola, M. Miras, D. Lescano, C. Barbero, *Nanotechnology* **2011**, *22*, 245504.
- [168] Z. Liu, A. Lu, Z. Yang, Y. Luo, *Macromolecular Research* **2013**, *21*, 376.
- [169] R. Nasser, C. Deutschman, L. Han, M. Pope, K. Tam, *Materials Today Advances* **2020**, *5*, 100055.
- [170] I. Cobo, M. Li, B. S. Sumerlin, S. Perrier, *Nature materials* **2015**, *14*, 143.
- [171] M. Karg, T. Hellweg, *Journal of Materials Chemistry* **2009**, *19*, 8714.
- [172] N. Grishkewich, N. Mohammed, J. Tang, K. C. Tam, *Current Opinion in Colloid & Interface Science* **2017**, *29*, 32.
- [173] M. Islam, L. Chen, J. Sisler, K. Tam, *Journal of Materials Chemistry B* **2018**, *6*, 864.
- [174] I. A. Sacui, R. C. Nieuwendaal, D. J. Burnett, S. J. Stranick, M. Jorfi, C. Weder, E. J. Foster, R. T. Olsson, J. W. Gilman, *ACS applied materials & interfaces* **2014**, *6*, 6127.
- [175] P. B. Filson, B. E. Dawson-Andoh, *Bioresource Technology* **2009**, *100*, 2259.
- [176] S. Elazzouzi-Hafraoui, Y. Nishiyama, J.-L. Putaux, L. Heux, F. Dubreuil, C. Rochas, *Biomacromolecules* **2008**, *9*, 57.
- [177] A. Šturcová, G. R. Davies, S. J. Eichhorn, *Biomacromolecules* **2005**, *6*, 1055.
- [178] E. Lam, K. B. Male, J. H. Chong, A. C. Leung, J. H. Luong, *Trends in biotechnology* **2012**, *30*, 283.
- [179] S. Minko, "Grafting on solid surfaces: "Grafting to" and "grafting from" methods", in *Polymer surfaces and interfaces*, Springer, 2008, p. 215.
- [180] J. O. Zoppe, Y. Habibi, O. J. Rojas, R. A. Venditti, L.-S. Johansson, K. Efimenko, M. Osterberg, J. Laine, *Biomacromolecules* **2010**, *11*, 2683.
- [181] N. Grishkewich, S. P. Akhlaghi, Y. Zhaoling, R. Berry, K. C. Tam, *Carbohydrate polymers* **2016**, *144*, 215.

- [182] E. Cudjoe, S. Khani, A. E. Way, M. J. Hore, J. Maia, S. J. Rowan, *ACS central science* **2017**, *3*, 886.
- [183] K. Zubik, P. Singhsa, Y. Wang, H. Manuspiya, R. Narain, *Polymers* **2017**, *9*, 119.
- [184] X. Zhang, J. Zhang, L. Dong, S. Ren, Q. Wu, T. Lei, *Cellulose* **2017**, *24*, 4189.
- [185] Y. R. Lee, D. Park, S. K. Choi, M. Kim, H. S. Baek, J. Nam, C. B. Chung, C. O. Osuji, J. W. Kim, *ACS applied materials & interfaces* **2017**, *9*, 31095.
- [186] F. Lin, F. Cousin, J.-L. Putaux, B. Jean, *ACS Macro Letters* **2019**, *8*, 345.
- [187] F. Azzam, L. Heux, J.-L. Putaux, B. Jean, *Biomacromolecules* **2010**, *11*, 3652.
- [188] Z. Zhang, G. Sèbe, X. Wang, K. C. Tam, *Carbohydrate polymers* **2018**, *182*, 61.
- [189] J. Tang, M. F. X. Lee, W. Zhang, B. Zhao, R. M. Berry, K. C. Tam, *Biomacromolecules* **2014**, *15*, 3052.
- [190] J. T. Orasugh, G. Sarkar, N. R. Saha, B. Das, A. Bhattacharyya, S. Das, R. Mishra, I. Roy, A. Chattoapadhyay, S. K. Ghosh, *International journal of biological macromolecules* **2019**, *124*, 235.
- [191] R. Nigmatullin, V. Gabrielli, J. C. Muñoz-García, A. E. Lewandowska, R. Harniman, Y. Z. Khimyak, J. Angulo, S. J. Eichhorn, *Cellulose* **2019**, *26*, 529.
- [192] E. Gicquel, C. Martin, Q. Gauthier, J. Engström, C. Abbattista, A. Carlmark, E. D. Cranston, B. Jean, J. Bras, *Biomacromolecules* **2019**, *20*, 2545.
- [193] J. Zhou, Y. Li, H. Li, H. Yao, *Colloids and Surfaces B: Biointerfaces* **2019**, *177*, 321.
- [194] K. H. Kan, J. Li, K. Wijesekera, E. D. Cranston, *Biomacromolecules* **2013**, *14*, 3130.
- [195] M. Rahimi, S. Shojaei, K. D. Safa, Z. Ghasemi, R. Salehi, B. Yousefi, V. Shafiei-Irannejad, *New Journal of Chemistry* **2017**, *41*, 2160.
- [196] L. E. Low, L. T.-H. Tan, B.-H. Goh, B. T. Tey, B. H. Ong, S. Y. Tang, *International journal of biological macromolecules* **2019**, *127*, 76.
- [197] T. Nypelö, C. Rodriguez-Abreu, J. Rivas, M. D. Dickey, O. J. Rojas, *Cellulose* **2014**, *21*, 2557.
- [198] S.-S. Kim, C.-D. Kee, *International journal of precision engineering and manufacturing* **2014**, *15*, 315.
- [199] M. Haqani, H. Roghani-Mamaqani, M. Salami-Kalajahi, *Cellulose* **2017**, *24*, 2241.
- [200] J.-M. Malho, J. Brand, G. Pecastaings, J. Ruokolainen, A. Gröschel, G. Sèbe, E. Garanger, S. Lecommandoux, *ACS Macro Letters* **2018**, *7*, 646.

- [201] J.-F. Revol, H. Bradford, J. Giasson, R. Marchessault, D. Gray, *International journal of biological macromolecules* **1992**, *14*, 170.
- [202] X. Mu, D. G. Gray, *Langmuir* **2014**, *30*, 9256.
- [203] D. Qu, H. Zheng, H. Jiang, Y. Xu, Z. Tang, *Advanced Optical Materials* **2019**, *7*, 1801395.
- [204] T. H. Zhao, R. M. Parker, C. A. Williams, K. T. Lim, B. Frka-Petesic, S. Vignolini, *Advanced Functional Materials* **2019**, *29*, 1804531.
- [205] T. Wu, J. Li, J. Li, S. Ye, J. Wei, J. Guo, *Journal of Materials Chemistry C* **2016**, *4*, 9687.
- [206] Y.-D. He, Z.-L. Zhang, J. Xue, X.-H. Wang, F. Song, X.-L. Wang, L.-L. Zhu, Y.-Z. Wang, *ACS applied materials & interfaces* **2018**, *10*, 5805.
- [207] K. Yao, Q. Meng, V. Bulone, Q. Zhou, *Advanced Materials* **2017**, *29*, 1701323.
- [208] H. Wan, X. Li, L. Zhang, X. Li, P. Liu, Z. Jiang, Z.-Z. Yu, *ACS applied materials & interfaces* **2018**, *10*, 5918.
- [209] Y. Cao, L. Lewis, W. Y. Hamad, M. J. MacLachlan, *Advanced Materials* **2019**, *31*, 1808186.
- [210] O. Kose, C. E. Boott, W. Y. Hamad, M. J. MacLachlan, *Macromolecules* **2019**, *52*, 5317.
- [211] T. Hiratani, O. Kose, W. Y. Hamad, M. J. MacLachlan, *Materials Horizons* **2018**, *5*, 1076.
- [212] C. Sun, D. Zhu, H. Jia, K. Lei, Z. Zheng, X. Wang, *ACS applied materials & interfaces* **2019**, *11*, 39192.
- [213] O. Kose, A. Tran, L. Lewis, W. Y. Hamad, M. J. MacLachlan, *Nature communications* **2019**, *10*, 1.
- [214] X. Z. Zhang, C. C. Chu, *Journal of applied polymer science* **2003**, *89*, 1935.
- [215] K. Ito, *Polymer journal* **2007**, *39*, 489.
- [216] P. Schexnailder, G. Schmidt, *Colloid and Polymer Science* **2009**, *287*, 1.
- [217] F. Song, X.-L. Wang, Y.-Z. Wang, *Colloids and Surfaces B: Biointerfaces* **2011**, *88*, 749.
- [218] D. N. Rockwood, D. B. Chase, R. E. Akins Jr, J. F. Rabolt, *Polymer* **2008**, *49*, 4025.
- [219] Y. J. Kim, M. Ebara, T. Aoyagi, *Advanced Functional Materials* **2013**, *23*, 5753.
- [220] M. Liu, H. Su, T. Tan, *Carbohydrate Polymers* **2012**, *87*, 2425.
- [221] R. Fei, J. T. George, J. Park, A. K. Means, M. A. Grunlan, *Soft Matter* **2013**, *9*, 2912.
- [222] C. S. Wang, N. Virgilio, P. M. Wood-Adams, M. C. Heuzey, *Macromolecular Chemistry and*

Physics **2018**.

- [223] S. Jiang, F. Liu, A. Lerch, L. Ionov, S. Agarwal, *Advanced Materials* **2015**, 27, 4865.
- [224] L. Li, Y. L. Hsieh, *Nanotechnology* **2005**, 16, 2852.
- [225] X. Jin, Y.-L. Hsieh, *Polymer* **2005**, 46, 5149.
- [226] C. Yao, Z. Liu, C. Yang, W. Wang, X.-J. Ju, R. Xie, L.-Y. Chu, *Advanced Functional Materials* **2015**, 25, 2980.
- [227] M. Liu, H. Su, T. Tan, *Carbohydrate polymers* **2012**, 87, 2425.
- [228] A. S. Hoffman, *Artificial organs* **1995**, 19, 458.
- [229] M. R. Aguilar, J. San Román, "Smart polymers and their applications", Woodhead publishing, 2019.
- [230] X. Sun, P. Tyagi, S. Agate, L. Lucia, M. McCord, L. Pal, *Carbohydrate polymers* **2019**, 208, 495.
- [231] Y. Zhang, S. Furyk, D. E. Bergbreiter, P. S. Cremer, *Journal of the American Chemical Society* **2005**, 127, 14505.
- [232] N. A. Cortez-Lemus, A. Licea-Claverie, *Progress in Polymer Science* **2016**, 53, 1.
- [233] J. Bras, S. Saini, "Nanocellulose in functional packaging", in *Cellulose-Reinforced Nanofibre Composites*, Elsevier, 2017, p. 175.
- [234] Y. Habibi, L. A. Lucia, O. J. Rojas, *Chemical reviews* **2010**, 110, 3479.
- [235] H. Kargarzadeh, M. Mariano, D. Gopakumar, I. Ahmad, S. Thomas, A. Dufresne, J. Huang, N. Lin, *Cellulose* **2018**, 25, 2151.
- [236] P. Lu, Y.-L. Hsieh, *Carbohydrate polymers* **2010**, 82, 329.
- [237] H. Kargarzadeh, M. Mariano, J. Huang, N. Lin, I. Ahmad, A. Dufresne, S. Thomas, *Polymer* **2017**, 132, 368.
- [238] J. P. F. Lagerwall, C. Schütz, M. Salajkova, J. Noh, J. Hyun Park, G. Scalia, L. Bergström, *NPG Asia Materials* **2014**, 6, e80.
- [239] Y. Xu, A. Ajji, M.-C. Heuzey, *Polymer* **2019**, 183, 121880.
- [240] M. Alavi, A. Nokhodchi.
- [241] H. Yim, M. Kent, S. Mendez, S. Balamurugan, S. Balamurugan, G. Lopez, S. Satija, *Macromolecules* **2004**, 37, 1994.

- [242] S. Zakharchenko, E. Sperling, L. Ionov, *Biomacromolecules* **2011**, *12*, 2211.
- [243] L. Ionov, *Langmuir* **2015**, *31*, 5015.
- [244] L. Liu, S. Jiang, Y. Sun, S. Agarwal, *Advanced Functional Materials* **2016**, *26*, 1021.
- [245] S.-J. Jeon, A. W. Hauser, R. C. Hayward, *Accounts of chemical research* **2017**, *50*, 161.
- [246] J. Shang, P. Theato, *Soft Matter* **2018**, *14*, 8401.
- [247] J. Liu, W. Xu, Z. Kuang, P. Dong, Y. Yao, H. Wu, A. Liu, F. Ye, *Journal of Materials Chemistry C* **2020**.
- [248] C. Yoon, *Nano convergence* **2019**, *6*, 1.
- [249] M. B. Chen, S. Srigunapalan, A. R. Wheeler, C. A. Simmons, *Lab on a Chip* **2013**, *13*, 2591.
- [250] Q. Beuguel, J. R. Tavares, P. J. Carreau, M.-C. Heuzey, *Journal of colloid and interface science* **2018**, *516*, 23.
- [251] C. Bruel, J. R. Tavares, P. J. Carreau, M.-C. Heuzey, *Carbohydrate polymers* **2019**, *205*, 184.
- [252] Q. Beuguel, J. R. Tavares, P. J. Carreau, M. C. Heuzey, *Journal of Colloid and Interface Science* **2018**, *516*, 23.
- [253] M. Wang, Y. Fang, D. Hu, *Reactive and Functional polymers* **2001**, *48*, 215.
- [254] R. Xiong, S. Yu, S. Kang, K. M. Adstedt, D. Nepal, T. J. Bunning, V. V. Tsukruk, *Advanced Materials* **2020**, *32*, 1905600.
- [255] T. Chen, H. Bakhshi, L. Liu, J. Ji, S. Agarwal, *Advanced Functional Materials* **2018**, *28*, 1800514.